Morphological diversity and quantitative genetics of the maize shoot apical meristem

A dissertation
Presented to the Faculty of the Graduate School
of Cornell University
in Partial Fulfillment of the Requirements for the Degree of
Doctor of Philosophy

by
Samuel Allen Leiboff

January, 2017

MORPHOLOGICAL DIVERSITY AND QUANTITATIVE GENETICS OF THE MAIZE SHOOT APICAL MERISTEM

Samuel Allen Leiboff, PhD

Cornell University, 2017

Abstract

The maize shoot apical meristem (SAM) comprises a small pool of stem cells that generate all the organs in the above ground plant. Mutational analyses have identified genetic networks regulating SAM function, although little is known about the genetic determinants of SAM morphological variation in natural populations. We utilized high-throughput image processing to capture rich variation in SAM size for a diverse panel of maize inbred varieties, wild teosinte isolates, and a domesticated maize x wild progenitor teosinte backcross population. Focusing on diverse maize inbred lines, we identified significant correlations between seedling SAM size and agronomically-important adult plant traits such as flowering time, stem size, and leaf node number. Combining SAM phenotype data with a 1.2-million-SNP dataset in a genome-wide association study (GWAS) revealed unexpected SAM morphology candidate genes. We further confirmed correlations between SAM morphology and trait-associated SNP (TAS) alleles of several GWAS-derived SAM candidate genes through *in situ* hybridization and cell number and size estimation via image segmentation. Our data illustrate that the microscopic seedling SAM is predictive of adult phenotypes and that

SAM morphometric variation is associated with genes that were not previously predicted to regulate SAM size. In further exploration of natural variation of SAM shape and size, we implemented rapid and complex morphometric modeling approaches to quantify SAM morphology. Quantitative trait loci (QTL) mapping results suggest that a majority of genetically-attributable SAM shape and size variation can be captured by estimating the SAM as a paraboloid, which has several advantages for high-throughput phenotyping methods. Further application of this model to a broad sampling of evolutionarily-distant plant species suggests that a parabolic SAM may be a universal trait of plant meristems. Future investigations into the mechanisms that orchestrate parabolic SAM parameters may reveal additional correlations between SAM architecture and adult plant morphology that transcend phylogenetic determinants.

Biographical Sketch

Sam Leiboff was born and raised in the San Fernando Valley, just adjacent to Los Angeles, California. His interest in plant science was sparked by a high school Environmental Sciences class taught by Mr. Scott Holloway. Under Mr. Holloway's direction he first learned to identify trees and quantify their lumber value. This initial interest in land use and forest ecology transitioned to plant genetics while he was an undergraduate at the University of California, Berkeley. Working closely with postdoctoral fellows, Drs. Monica Alanadete-Saiz and Mily Ron in the lab of Prof. Shiela McCormick on pollen tube guidance in *Arabidopsis*, he learned the basics of molecular biology and plant developmental genetics. Later, he worked in Prof. Peggy Lemaux's lab to develop a seniors' thesis tracking the kernel development of transgenic sorghum varieties under drought stress. Undeterred by long hours at the greenhouse transferring seedlings to pots and ever impressed by the elegance of genetic systems, it was clear that plant genetics would be a life-long passion. After graduating from the University of California, Berkeley in 2010 with a B.S. in Environmental Sciences with a minor in Forestry and Natural Resources, Sam sought out the lab of Prof. Michael J. Scanlon at Cornell University. Enthralled by a research proposal Mike and others from the NSF-funded Maize Shoot Apical Meristem (SAM) Grant group had submitted, Sam began a fruitful research project working on the shape and size of maize stem cells. He hopes to continue unravelling the ways that maize plants take their beautiful shape

Acknowledgements

This work was enabled by many kind and generous individuals. I am afraid I will not be able to list all of them here. To those of you who remain unnamed, thank you nonetheless; your help has meant the world to me.

I owe many sincere thanks to my advisor, Prof. Michael J. Scanlon. Mike's advice and leadership has led me to wonderful discoveries and enkindled a scientific passion that, I hope, will guide me for years to come. He is a true advocate for his students and mentees. And despite our disagreements (sometimes heated), he has never betrayed my faith in his goodwill as a leader. He once told me that, given time, all students come to appreciate their advisors. I hope I can save a couple years; thank you, Mike.

The official and unofficial members of the Scanlon Lab (alphabetical order: Joseph Cammarata, Phillip Conklin, Dezi Elzinga, Silvia Federici, Eric Fich, Margaret Frank, Robyn Johnston, Sammy Manniero, Pengfei Qiao, Natalie Ronning, Joshua Strable) have been my most trusted co-workers and most cherished friends. A few of us share publications, but we *all* share wonderful memories of Pandora radio stations, muddy hikes, summer ice creams, winter skis, and many, many, many Manndible Café treats. Thank you for teaching me about science, and more importantly, scientists.

This work was generously funded by the National Science Foundation (NSF) through the SAM Grant Group (IOS-1238142). It has been a pleasure to work with the other investigators, postdoctoral fellows, and students as a part of this grant. I am especially grateful to Prof. Jianming Yu and his lab members, Drs. Xianran Li and Xiaoqing Yu for their careful mentorship in biostatistics and quantitative genetics.

Table of Contents

1 Understanding the Shoot Apical Meristem through Quantitative Genetics

1.1 Overview

Shoot apical meristems (SAMs) are microscopic pools of plant stem cells with two essential functions: 1) maintenance of pluripotent cells and 2) assignment of initial cells to form lateral organs (Steeves and Sussex 1972). Through these two processes, plant stem cells in the SAM generate complex and diverse adult plant morphologies. Genetic analyses in various model organisms (*Arabidopsis*, rice, maize, tomato, petunia, moss, and others) have begun to elucidate the fascinating molecular mechanisms underlying these processes. Many genes identified as essential to plant stem cell maintenance have been shown to have profound effects on the SAM as well as the lateral organs it produces. Homeodomain genes from the *KNOX* and *WOX* family are known for their profound mutant phenotypes which dramatically affect SAM morphology as well as the overall architecture of the plant. This chapter will focus on KNOX and WOX proteins (Figure 1.1) as a method of reviewing processes that are related to SAM function and prerequisites to establishing the plant body plan.

As in other eukaryotes, stem cell activity in plants is marked by the expression of homeodomain proteins (Mukherjee *et al.* 2009; Holland 2013). These transcriptional regulators assign the various morphological identities that comprise the complex body plans of multicellular eukaryotes (Carroll 2000). Through their controlled expression and interactions with other regulatory proteins, homeobox genes nucleate gene modules,

which manage stem cell reservoirs during morphogenesis. In plants, transcription factors from the *KNOX* and *WOX* gene families are required to organize and maintain stem cell identity (Mukherjee *et al.* 2009). These proteins possess 'atypical' DNA-binding homeodomains of between 60 and 66 amino acids; recent research shows that additional protein domains found in KNOX and WOX proteins allow complex protein-protein interactions that define their specific functions as plant stem cell regulators.

Although a great deal is known about the master regulators of plant stem cell function and their interactions, much less is known about how plant stem cell function varies in natural populations or if, indeed, stem cell regulatory pathways discovered by mutagenesis are responsible for the evolution or domestication of plant varieties. In the studies that follow this introductory chapter, we aim to make use of quantitative genetics to explore natural variation in the SAM, its prevailing plant stem cell pathways, and its correlates with overall plant morphology.

1.2 KNOTTED1 (KN1) and KNOX

The KNOTTED1-like homeobox proteins (KNOXs) comprise two phylogenetic classes (Chan *et al.* 1998). Class I KNOX proteins possess two KNOX domains, an ELK domain, as well as a 63 amino acid (three amino acid loop extension, TALE) homeodomain and are required for the establishment and maintenance of stem cell identity (Mukherjee *et al.* 2009). Homologs of the well-studied Class I *KNOX* genes have been identified in most plant lineages (Cronk 2001). In contrast, Class II *KNOXs* are less studied. Recent work in the moss *Physcomitrella patens* demonstrates that Class II *KNOX* genes regulate the transition from diploid to haploid body plans during the alternation of generations (Sakakibara *et al.* 2013); more recent work in

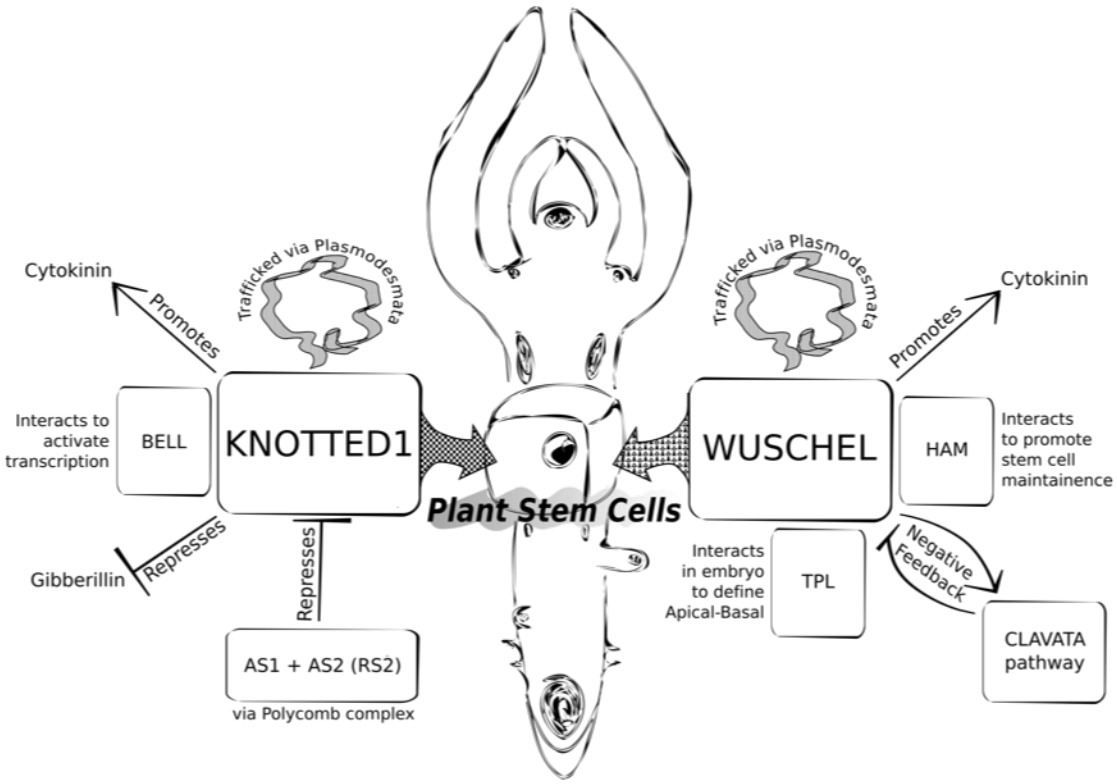

Figure 1.1 Plant stem cells are maintained by *KNOX* (ex. *KNOTTED1*) and *WOX* (ex. *WUSCHEL*) regulatory pathways. Reservoirs of plant stem cells can be found in shoot/branch apical meristems, the vascular cambium, and root apical meristems.

angiosperms suggests that that Class I and Class II KNOXs have antagonistic functions (Furumizu *et al.* 2015).

The classical dominant mutation of maize, *KNOTTED1* (*KN1*), causes ectopic 'knots' of cells to grow on the blade of mutant leaves and was cloned in 1989 by transposon tagging (Hake *et al.* 1989). The ectopic outgrowths found on gain-of-function *kn1-o* plants are believed to result from the projection of indeterminate stem cell identity onto a field of determinate leaf cells, ultimately forming organized clusters of rapidly-dividing tissues in the leaf blade (Vollbrecht *et al.* 1991; Smith *et al.* 1992). Loss of *KN1* in maize or *SHOOT MERISTEMLESS1* (*STM1*), its homolog in *Arabidopsis thaliana*, causes a lethal depletion of stem cells in some genetic backgrounds and environmental conditions (Long *et al.* 1996; Vollbrecht *et al.* 2000). In *kn1* or *stm1* loss-of-function mutants, stem cell identity is organized during embryogenesis, but is lost soon after germination. This failure in stem cell maintenance causes the shoot meristem to be depleted during the formation of lateral organs; ultimately the meristem is consumed, and organogenesis ceases (Vollbrecht *et al.* 2000).

1.2.1 KNOX expression domains and KN1 movement

In situ hybridization experiments show that *KNOX* transcript accumulation is restricted to the inner layers of the shoot meristem, and is conspicuously absent from the outer layers (Jackson *et al.* 1994; Long *et al.* 1996; Chuck *et al.* 1996). *KNOX* transcripts are downregulated in initiating leaf primordia**,** which correlates with the transition from indeterminate to determinate growth. Although *KNOTTED1* mRNA from is not found in the outermost, 'L1' meristem layer, immunohistolocalizations show that KN1 protein is found in all meristem layers (Jackson 2002). This discrepancy in the accumulation

pattern of *KN1* RNA and protein has led to exciting research supporting the hypothesis that KNOX proteins can traffic between cells via plasmodesmata, symplastic pores that connect the cytoplasm of adjacent plant cells (Jackson 2001). The first evidence for KNOX trafficking came from *in planta* assays of recombinant protein movement (Lucas *et al.* 1995; Kim *et al.* 2002, 2003). Starting with the full-length maize KNOTTED1, several recombinant alleles with mutated protein domains were tested for movement after microinjection into plant cells (Lucas *et al.* 1995). The full-length *KN1* sequence and several mutated recombinant alleles were successfully trafficked through the plant cell system. However, accumulation of the KN1-M6 protein, which contained a defective homeodomain, was restricted to injected cells. Transient expression assays have shown that full-length maize KN1 is able to transit between cells, with the efficiency observed in viral movement proteins. In contrast smaller proteins with no identified movement mechanisms are unable to traffic between cells (Kim *et al.* 2002). A genetic screen for interacting proteins that facilitate KN1 movement identified a chaperonin that is required for full function of trafficked KN1 in *Arabidopsis* (Xu *et al.* 2011). These data suggest that during trafficking to the Arabidopsis epidermis the KN1 protein is unfolded, transported through a plasmodesmatal pore, and then refolded within the destination cell (Xu *et al.* 2011).

1.2.2 KNOXs as transcription factors

Comparative RNAseq and ChIPseq analyses in *KN1* mutant and wild type backgrounds revealed that more than 600 maize genes are bound and regulated by KN1 (Bolduc *et al.* 2012). Interestingly, RNAseq read counts in KN1 loss-of-function and wild-type backgrounds suggest that KN1 can function as either a transcriptional activator, or as a

repressor of target genes. Subsequent *in vitro* assays of KN1 and other KNOX proteins showed that they are weak transcriptional activators (Smith *et al.* 2002). To provide transcriptional activation, KN1 and KNOX proteins interact with other TALE homeobox proteins, including members of the *BELL* family (Smith *et al.* 2002; Ragni *et al.* 2008). *In vitro* and *in planta*, KNOXs and BELLs interact as heterodimer complexes to activate target gene expression. This interaction is facilitated by two highly conserved MEINOX domains found on KNOX proteins, which interact with the MID domains (named SKY and BELL) of BELL proteins (Mukherjee *et al.* 2009).

The *Arabidopsis* gene, *KNATM*, encodes a truncated KNOX that lacks a functional homeodomain, and therefore cannot bind DNA (Magnani and Hake 2008; Mukherjee *et al.* 2009). Intriguingly, KNATM retains the ability to interact with BELL proteins, and the resulting heterodimer can act as a strong transcriptional activator *in vitro* (Magnani and Hake 2008). These studies suggest that interactions with other TALE homeobox proteins may be at least as important as autonomous KNOX/DNA binding during KNOX-mediated stem cell regulation (Hay and Tsiantis 2010).

1.2.3 KNOXs and plant hormones

KNOXs maintain stem cell identity in part by the regulation of plant hormone biosynthesis. In several species, KNOXs directly regulate gibberellin (GA) levels through the activation of gibberellin oxidases such as *GA2ox1*, which function in GA catabolism. Likewise, KNOXs repress the expression of the GA biosynthetic gene *GA20ox1* (Sakamoto *et al.* 2001; Hay *et al.* 2002; Shani *et al.* 2006; Bolduc and Hake 2009). Thus, KNOX-mediated repression of GA accumulation inhibits determinate growth by preventing cell expansion and maturation. In addition, KNOXs promote

cytokinin (CK) accumulation via activation of *ADENOSINE PHOSPHATE ISOPENTENYLTRANSFERASE* (*IPT*) CK-biosynthetic genes, and of the cytokinin activation gene *LONELY GUY* (*LOG*), which encodes a phosphoribohydrolase that converts inactive CK conjugates into biologically-active CK (Jasinski *et al.* 2005; Scofield *et al.* 2013). Although some of the stem cell organizing function of KNOXs is independent of cytokinin, high cytokinin levels repress endoreduplication and prevent cellular differentiation. Thus, KNOXs maintain an undifferentiated, pluripotent stem cell fate by direct upregulation of CK and downregulation of GA (Shani *et al.* 2006).

1.2.4 KNOXs are regulated by the POLYCOMB REPRESSIVE COMPLEX (PRC)

Whereas the expression of *KNOXs* is required for stem cell maintenance, the proper patterning of determinate lateral organs requires repression of stem cell identity (Micol et al. 2003). Multiple transcription factors act together to repress *KNOXs* during organogenesis (Hay and Tsiantis 2010). Whereas *KNOX* genes are expressed in stem cell niches and are absent from the differentiating cells of young leaf primordia, the MYB-domain transcription factor, *ASYMMETRIC LEAVES1* (*AS1*) and the lateral organ boundary domain (LBD) protein *AS2* both show KNOX-complimentary expression in differentiating cells of young leaf primorida (Theodoris *et al.* 2003). Loss of *AS1* in *Arabidopsis*, or its maize homologue *ROUGH SHEATH2* (*RS2*), leads to ectopic *KNOX* expression in developing leaf primordium, ultimately yielding dramatic mutant leaf phenotypes (Tsiantis *et al.* 1999; Phelps-Durr *et al.* 2005). AS1 and AS2 heterodimerize and recruit the POLYCOMB REPRESSIVE COMPLEX to epigenetically repress *KNOX* expression in determinate lateral organ primordia (Xu and Shen 2008).

1.2.5 KNOXs at the center of organogenesis

In the shoot meristem, stem cell identity is marked by KNOX accumulation, whereas developing leaf primordia do not accumulate KNOX proteins. The site of new leaf initiation is marked by local accumulation of the plant hormone auxin, (Reinhardt 2000; Deb *et al.* 2015) which results in downregulation of KNOX accumulation in the incipient leaf (Scanlon 2003; Hay *et al.* 2006). This localized auxin maxima is created by the convergence of polar auxin transporters from the *PIN-formed* (*PIN*) and *AUXIN-INSENSITIVE* / *LIKE AUXIN-INSENSITIVE* (*AUX*/*LAX*) families, and is followed by the expression of *LBD* genes such as *LATERAL ORGAN BOUNDARY* (*LOB*) and *AS2* (Hay and Tsiantis 2010; Johnston *et al.* 2014). AS2 and LBD proteins then repress KNOXs and stem cell identity in the developing leaf primordium, as described above. In this simple model for lateral organ specification, auxin-induced *LBD* gene expression plays a central role in repression of KNOX-mediated, stem cell identity (Hay and Tsiantis 2010; Johnston *et al.* 2014). This model has been successful extrapolated to multiple organ boundaries throughout plant development during the morphogenesis of leaves, branches, flowers, and ligules (Johnston *et al.* 2014).

Conserved *KNOX* function is required in several species for development of dissected (compound) leaves and lobed leaf margins (Chuck *et al.* 1996; Rupp *et al.* 1999; Bharathan *et al.* 2002; Scanlon 2003). In tomato, *KNOX* genes and auxin/*LBD* modules mark the location of pinnae in dissected leaves, similar to what is observed during initiation of lateral organ primordia from the shoot meristem (Kimura *et al.* 2008). Similarly, overexpression of the *Arabidopsis KNOX* genes *BREVIPEDICELLUS* (*BP*) or *KNAT2* yields a highly lobed leaf lamina covered with ectopic meristems, complete with

fully functional stem cells (Lincoln *et al.* 1994; Hake *et al.* 1995; Chuck *et al.* 1996). These data, and related studies, suggest that reactivation of stem cell regulatory networks in the marginal blastozones of otherwise determinate leaf primordia can activate a secondary stage of morphogenesis in plants with dissected or highly lobed leaves (Barkoulas *et al.* 2008; Blein *et al.* 2008; Koenig *et al.* 2009).

1.3 WUSCHEL (WUS) and WOXs

The WUSCHEL-like homeobox proteins (WOXs) comprise a large family of proteins with a single homeodomain and an 8 amino-acid WUS-box domain (Mukherjee *et al.* 2009; van der Graaff *et al.* 2009). There are three commonly accepted subfamilies of *WOXs*: the '*WUSCHEL*-like' subfamily that contains a two amino acid T-L motif at the beginning of the WUS-box, the ancient WOX subfamily with conserved members identified in algae and moss, and the intermediate WOX subfamily that establishes apical-basal auxin transport during embryogenesis (van der Graaff *et al.* 2009). The '*WUSCHEL*-like' subfamily is the most studied and best understood WOX clade. Within this subfamily of *WOXs* there are many members with tissue-specific expression domains, acting as organizers of stem cell identity throughout plant development (van der Graaff *et al.* 2009). Promoter fusion assays in *wox* mutant backgrounds show that the functions of several WOX proteins are cross-complementary, suggesting that WOX family evolution involved the subfunctionalization of conserved stem-cell organizing functions via adoption of distinct, tissue-specific promoters (Sarkar *et al.* 2007; Shimizu *et al.* 2009; Lin *et al.* 2013). Additionally, *WOXs* may act as persistent organizers of stem cell reservoirs such as *WUS* in the shoot apical meristem and *WOX5* in the root (Laux *et al.* 1996; Schoof *et al.* 2000; Zhang *et al.* 2013); other *WOXs* may act as

ephemeral founder cell recruitment factors for organogenesis such as *NARROW SHEATH1* (*NS1*) and *NS2* in maize and *PRESSED FLOWER1* (*PRS1*)/*WOX3* in *Arabidopsis* (Scanlon 2000; Matsumoto and Okada 2001; Shimizu *et al.* 2009; van der Graaff *et al.* 2009; Vandenbussche *et al.* 2009).

1.3.1 Antagonism with the CLAVATA pathway

WUS, the founding member of the *WOXs* is noted for its antagonistic interaction with the *CLAVATA* genes in *Arabidopsis thaliana* (Laux *et al.* 1996; Müller *et al.* 2006; Durbak and Tax 2011). Whereas mutations in *WUS* lead to the loss of stem cells in the vegetative or inflorescence meristem, mutations in *CLAVATA* (*CLV*) genes lead to stem cell over-proliferation, which distorts the morphology of the shoot meristem. Although the phenotypes of loss-of-function *CLV* mutants are similar, *CLV1*, *CLV2*, and *CLV3* encode proteins of distinctly dissimilar molecular function (Fletcher and Meyerowitz 2000). *CLV3* encodes a small, secreted peptide-ligand that moves between cells through the extracellular apoplast (Clark *et al.* 1996; Rojo 2002; Wong *et al.* 2013). Studies of meristem size mutants in tomato reveal that proper recognition of this peptide is enhanced by post-translational arabinosylation (Xu *et al.* 2015). The small CLV3 peptide is in turn recognized by the leucine-rich-repeat (LRR) receptor kinase, CLV1 (Clark *et al.* 1996; Nimchuk *et al.* 2011). CLV1 can from dimers with several other LRR proteins including CLV2, a LRR that lacks a functional kinase domain (Durbak and Tax 2011). While CLV1 has been shown to bind CLV3 and respond by an unknown kinase cascade, the mechanism underlying the *CLV2* phenotype is still contested (Deyoung and Clark 2008; Nimchuk *et al.* 2011; Durbak and Tax 2011). However, it is generally accepted that WUS activates *CLV3* expression, while the CLAVATA signaling pathway

in turn acts to repress *WUS*. This negative-feedback loop thereby preserves a steady-state level of stem cells in the shoot meristem (Yadav *et al.* 2010, 2011, 2013).

Regulatory loops consisting of *WOX* and *CLAVATA*-like (*CLE*) genes have been demonstrated in distinct processes during plant development as a widely-employed signaling module in plant morphogenesis (Wu *et al.* 2007). Notably, *WOX*/*CLE* stem cell regulation is found in root meristem maintenance (*WOX5*/*CLE40*) via the receptor kinase *CRINKLY4* (*CR4*) (Sarkar *et al.* 2007; Jun *et al.* 2010), and vascular differentiation employs *WOX4* in conjunction with *CLE41* and *CLE44* (Miyawaki *et al.* 2013). The conservation of *WOX*/*CLE* negative feedback loops in multiple plant species suggests that *WOX*/*CLE* interaction may be an ancestral, plant patterning tool-kit (Miyawaki *et al.* 2013).

There is strong evidence for dynamic evolution of the WOX gene family among the species examined to date (Nardmann and Werr 2013). Although maize and *Arabidopsis* have 14 and 15 WOX family genes, respectively, not all WOX genes are represented in both lineages (van der Graaff *et al.* 2009; Vandenbussche *et al.* 2009). It may come as no surprise then, that several plant lineages show unique elaboration of the ancestral *WOX*/*CLE* regulatory pathway. For example, although mutation of the maize *CLV1* homolog, *THICK TASSEL DWARF1* (*TD1*) generates an inflorescence phenotype similar to the stem cell over proliferation observed in *Arabidopsis,* no interacting *WOX* has yet been identified (Bommert *et al.* 2005; Lunde and Hake 2009). Similar investigations with rice *CLV1* and *CLV3* homologs *FLORAL ORGAN NUMBER1* (*FON1*) and *FON2*, still seek an interacting *WOX* (Miyawaki *et al.* 2013). Recent research in maize has identified previously unrelated genetic mechanisms involving G-

proteins, amongst others, that contribute to the stem cell maintenance and may indeed participate in *WOX*/*CLE* regulation (Bommert *et al.* 2013b).

1.3.2 WOX interactions

ChIP-microarray data demonstrate that WUS directly binds more than 100 targets in the *Arabidopsis* genome (Busch *et al.* 2010). Several studies reported that WOXs generally act as transcriptional repressors (Leibfried *et al.* 2005; van der Graaff *et al.* 2009; Lin *et al.* 2013), however WUS is a known activator of *AGAMOUS* (*AG*) expression in floral meristems (Lenhard *et al.* 2001; Lohmann *et al.* 2001). Moreover, combined ChIP-microarray and RNAseq analyses suggest that WUS may either activate or repress its direct targets, which indicates that WUS regulatory functions are complex and multivariate (Busch *et al.* 2010).

WOXs interact with a variety of other proteins (van der Graaff et al. 2009). In petunia and *Arabidopsis* WOXs interact with the *HAIRY MERISTEM* (*HAM*) genes, GRAS-family transcription factors (Engstrom *et al.* 2011; Zhou *et al.* 2014). HAMs dimerize with WOX proteins and are required for stem cell maintenance. *WOXs* additionally interact with the transcriptional corepressor *TOPLESS* (*TPL*) genes during specification of the apical-basal axis in Arabidopsis embryos (Long *et al.* 2002, 2006).

WOX proteins influence cytokinin signaling via direct transcriptional repression of the stem cell repressor *RESPONSE REGULATOR7* (*RR7*), a negative regulator of cytokinin signaling (Leibfried *et al.* 2005). Models of WUS homeostasis in the shoot meristem predict that WUS, CLV, and cytokinin response are all required to maintain a steady state number of stem cell initials in the growing shoot (Gordon *et al.* 2009; Chickarmane *et al.* 2012).

1.3.3 WUSCHEL moves

Exiting new research reveals that WUS, much like KN1, is capable of intercellular trafficking, which enables non-cell-autonomous function (Yadav *et al.* 2011; Daum *et al.* 2014). WUS fusion proteins migrate several cell layers, from the interior of the *Arabidopsis* shoot meristem to the outer layers of the meristem, wherein *CLV* genes are activated. Careful dissection of WUSCHEL protein domains shows that the *WUS*-box domain promotes widespread, plasmodesmata-dependent protein movement—to a higher degree than observed with the native, full-length protein (Daum *et al.* 2014). Interestingly, conserved sequences in the C-terminus act to restrict WUS cell-to-cell trafficking to levels seen in wild-type *Arabidopsis* plants. Fusion proteins created from WOX5, another *WUS*-like WOX*,* can also traffic through the shoot meristem (Daum *et al.* 2014). In contrast, constructs containing WOX13, from the ancient WOX clade, did not show significant cell-to-cell-movement.

Genetic evidence indicates that *WUS*, *WOX3*, and *WOX5* all exhibit non-cell autonomous function to maintain stem/initial cell homeostasis (Scanlon 2000; Reddy and Meyerowitz 2005; Sarkar *et al.* 2007; van der Graaff *et al.* 2009). These data, when considered together with the cross-complementarity of WOX function, suggest that movement may be a key feature of *WUS*-like WOX proteins. However, analysis of PRESSED FLOWER1 (PRS1/WOX3) function revealed no evidence of cell-to-cell trafficking in floral meristems (Shimizu *et al.* 2009). Thus, whether the WUS-like clade of WOX proteins shares ancestral mechanisms enabling non-cell autonomous function is an unresolved question.

1.4 KNOXs and WOXs underlie persistent and flexible plant forms

Plants are noted for their indeterminate growth pattern (Steeves and Sussex 1972). They comprise both the largest and oldest living things on our planet. Whereas animals undergo organogenesis only at key times during their lifecycle and most patterns are established in the embryo, plants continuously and reiteratively generate new organs across their lifetime (Walbot 1985). As sessile organisms, plants must additionally integrate information from dynamic aboveground and belowground environments to establish a favorable organ form and fitting overall morphology (Sultan 2000). It comes as no surprise then, that plants maintain several sources of pluripotent stem cells (Steeves and Sussex 1972). Marked by the expression of KNOX and WOX proteins, plant stem cells are tightly regulated by a suite of partially redundant and intricately connected molecular pathways, integrating hormone signaling, epigenetic regulation, and even mechanical forces (Mukherjee *et al.* 2009; van der Graaff *et al.* 2009; Hay and Tsiantis 2010; Hamant 2013).

The similarities of these two gene families are striking (Figure 1.1). Both families of proteins use homeobox domains to directly bind and regulate hundreds of genes (Busch *et al.* 2010; Bolduc *et al.* 2012). KNOX and WOX direct targets may either be activated or repressed. Gene regulatory modules involving KNOX/auxin/LBD and WOX/CLE interactions have been deployed in diverse plant tissues across distinct evolutionary clades (Hay *et al.* 2006; Johnston *et al.* 2014). KNOXs and WOXs participate in plasmodesmata-dependent cell-to-cell movement for proper function (Xu *et al.* 2011; Yadav *et al.* 2011; Daum *et al.* 2014). Both regulate key plant hormones, including CK to suppress cell differentiation (Shani *et al.* 2006). Localization assays find KNOXs and

WOXs in overlapping domains in the shoot meristem (Lucas *et al.* 1995; Long *et al.* 1996). Yet, *KNOX* and *WOX* genes act independently of each other (Lenhard *et al.* 2002).

Such exquisite complexity in stem cell regulation points to the necessity of proper activation and deactivation of indeterminate growth programs. Without indeterminate growth, the plant cannot generate new organs (Long *et al.* 1996; Mayer *et al.* 1998; Vollbrecht *et al.* 2000). This phenotype is seen in the seedling-lethal loss-of-function mutants of *kn1* and *wus*. On the other hand, without deactivation of indeterminate growth, cell division will continue and differentiation will not occur (Hake *et al.* 1989; Timmermans *et al.* 1999; Schoof *et al.* 2000; Brand 2000; Phelps-Durr *et al.* 2005). Animal cancers, where cells divide indefinitely without differentiation, may be an example of such a syndrome (Shah and Sukumar 2010). Despite the many reservoirs of indeterminate stem cells plants maintain, plants do not have a similar endogenous disease (Doonan and Sablowski 2010). Tumor-forming pathogens of plants must rely on reprogramming molecular machinery, by genetic transformation in some cases (Smith *et al.* 1912; Doonan and Sablowski 2010). By maintaining separate highly redundant and complex *KNOX* and *WOX* stem cell regulation pathways, plants protect themselves from disastrous adventitious cellular growth.

1.5 Quantitative genetics of developmental traits

Plant stem cell regulatory genes such as *KN1* were discovered through the analysis of mutations with large phenotypic effect that are easily studied using Mendelian principles. For example, an individual from a field sown with *KN1* mutant plants and their siblings can be separated into two phenotypic categories: with ectopic knots of leaf

tissue, or without ectopic knots (Smith *et al.* 1992). Using unlinked, independently inherited markers with known genomic positions, the presence or absence of ectopic knots allowed KN1 to be mapped to the genome (Hake *et al.* 1989). However in analyses of natural populations many phenotypes of interest are observed in a continuous distribution, and cannot be divided into simple categories. These phenotypes, such as height, weight, flowering time, etc. may be stably transmitted between generations, but they do not appear to be linked to one Mendelian gene but rather are caused by several loci throughout the genome (Tanksley 1993; Hill 2010). Quantitative genetic methods use correlations between genetic markers and a continuous distribution of phenotypic values to probe the genomic basis for such natural variation in an observable trait. Although the details of associative methods may differ, quantitative genetics uses high linkage disequilibrium between genetic markers near any causative genomic features to discriminate from genetic markers that flank loci that are unrelated to phenotype (Tanksley 1993; Nordborg and Weigel 2008). Recent work has applied quantitative genetic techniques to understand developmental traits, with potential application to understand the SAM and plant stem cell function.

1.5.1 Quantitative Trait Locus (QTL) mapping

Controlled mating of two dissimilar genotypes can be used to generate many recombinant lines in a mapping population. Quantitative trait loci (QTL) mapping then combines both genotype information and phenotype information for all recombinant progeny to correlate stretches of chromosomes with the measured phenotype (Tanksley 1993; Broman *et al.* 2003). Because both parental alleles are highly represented in their progeny, controlled mating methods, as typical for QTL mapping, are excellent at

detecting relatively rare alleles, but typical QLT mapping populations have a small number of generations, limiting in the total number of possible recombinations and the total resolution in discriminating causative from non-causative genomic regions (Nordborg and Weigel 2008).

Many researchers have used QTL mapping to identify chromosomal regions, and even candidate genes, controlling interesting developmental phenotypes. Studies in tomato and snapdragon have uncovered QTL that are associated with inter-species differences in leaf morphology (Langlade *et al.* 2005; Chitwood *et al.* 2013). Commonly-used maize inbred varieties possess several QTL associated with SAM shape and size, which do not implicate known regulators of plant stem cell function (Thompson *et al.* 2014, 2015). A QTL study of kernel row number, however, discovered that natural variation at FASCIATED EAR2 (FEA2), an ortholog of the CLAVATA pathway gene, CLV2 was responsible for inbred-specific differences in plant stem cell activity (Bommert *et al.* 2013a).

1.5.2 Genome-wide association studies (GWAS)

In genome-wide association studies (GWAS), the natural history of diverse lines is exploited to correlate genetic markers with phenotypes (Weigel and Nordborg 2005; Korte and Farlow 2013). Including many diverse varieties of the same species captures recombination between markers which may have occurred over hundreds of years of breeding history (Korte and Farlow 2013). The pedigree of lines selected for GWAS may include many closely related subpopulations of lines harboring systematic differences in allele frequencies, at times implicating alleles that are not in fact linked to the trait of interest (Nordborg and Weigel 2008). If uncorrected, these underlying

relationships between lines, formally termed kinship or population structure, may introduce confounding associations (Yu *et al.* 2006; Korte and Farlow 2013). Correcting for relatedness between lines using kinship and population structure estimates in mixed-model GWAS approaches reduces the appearance of such spurious associations (Yu *et al.* 2006; Zhang *et al.* 2010).

In maize, genome-wide association mapping studies (GWAS) have identified genetic loci associated with variation in kernel carotenoid qualities, leaf architecture, flowering time, plant height, and other high-throughput phenotypes (Buckler *et al.* 2009; Tian *et al.* 2011; Cook *et al.* 2012; Romay *et al.* 2013; Peiffer *et al.* 2014). Although a few studies in other systems have examined microscopic phenotypes, such as human retina morphology in a study of macular degeneration (Klein *et al.* 2005) or root meristem size in the model plant, *Arabidopsis thaliana* (Meijón *et al.* 2014), GWAS has not yet been applied to microscopic phenotypes of developmental significance in maize.

1.6 Purpose of study

Although a great deal is known about the genetic mechanisms of plant stem cell function in the SAM, little is known about natural variation in the SAM. The studies presented in this dissertation use quantitative genetic techniques to understand natural variation in maize SAM morphology with the ultimate goal of uncovering new information about the plant stem cells that comprise the SAM. Following additional molecular genetic analysis, the candidate genes and uncovered during these studies may reveal previously overlooked biological mechanisms with significant impacts on plant stem cell function. Selection in either the breeders' field, or in wild ecosystems is likely to act upon these natural variants to change plant form over time (Tanksley 1993;

Klingenberg 2010). The results of these studies may similarly provide a guide for breeding efforts aimed at modulating stem cell function, or in elucidating the natural history of the evolution of the SAM.

1.6.1 Research approach

Chapter 2 makes use of image processing to analyze 369 maize inbred varieties for a mixed-model GWAS of shoot meristem shape and size. We additionally pursue candidate genes using molecular developmental techniques to confirm correlations between quantitative genetic results and SAM function.

Chapter 3 describes a comparison of morphological models for quantitative genetics used to discriminate SAMs from wild teosinte varieties and domesticated maize. We use QTL mapping of a maize x teosinte intercross population to compare the genetic architecture of rapid estimation of SAM morphology as a paraboloid with comprehensive shape analysis conducted with Fourier transform related techniques. We further apply our findings to a broad survey of plant taxa, including species from all branches of the plant kingdom.

1.6.2 Chapter publication and author contributions

The contents of Chapters 1-3 and Appendix A are published, or are submitted for publication and are the product of collaborative research efforts. Text and figures have been reformatted to generate one continuous document. Supplementary Data files for Chapter 2 are available at ‘https://figshare.com/s/98384be7c50f19d1baaf’. Supplementary Data files for Chapter 3 are available at

‘https://figshare.com/s/620b5aa46891a934a471’. Supplementary Movie files for Appendix A are available at ‘https://figshare.com/s/ab6250250f2c12a6a323’.

Sections 1.2 – 1.4 of Chapter 1 (this chapter) are published in Leiboff S., Scanlon M., 2016. Plant Stem Cells. In: *Molecular Cell Biology of the Growth and Differentiation of Plant Cells*, CRC Press, pp. 284–297, reproduced here with permission from the publisher, Taylor and Francis Group LLC Books (license number: 3950250769000) provided by Copyright Clearance Center. I wrote the text and designed the figure with edits from MJ Scanlon. Additional sections on quantitative genetics and shoot apical meristems have been added to Chapter 1 of this thesis.

Chapter 2 is available as Leiboff S., Li X., Hu H.-C., Todt N., Yang J., Li X., Yu X., Muehlbauer G. J., Timmermans M. C. P., Yu J., Schnable P. S., Scanlon M. J., 2015 Genetic control of morphometric diversity in the maize shoot apical meristem. *Nat. Commun*. **6**: 8974, reproduced here with permission from the publisher as permitted by Nature Publishing group policy. I conducted the primary phenotypic measurements and morphometric modeling. N Todt (Ronning) assisted with tissue harvesting and solution changes. High-density genotyping was completed in the lab of co-author PS Schnable by co-authors H-C Hu and J Yang, with assistance from co-authors X Li and X Yu. X Li conducted GWAS and provided scripts that I modified to generate final GWAS figures. GJ Muehlbauer, MCP Timmermans, J Yu, PS Schnable and MJ Scanlon had critical influence on the initial design of the diversity panel and the core study. All further studies and figures were generated independently. I wrote the text with close edits from MJ Scanlon.

Chapter 3 is under review as Leiboff S., DeAllie, C.K., Scanlon M. J. Modeling the morphometric evolution of the maize shoot apical meristem. *Frontiers in Plant Science*, reproduced here with permission from the publisher. Plant growth, dissection, imaging, and quantification of wild teosinte isolates was carried out by undergraduate researcher CK DeAllie, with my guidance. I completed other work independently. I wrote the text and designed the figures with edits from MJ Scanlon.

Appendix A includes work published in Johnston R., Leiboff S., Scanlon M. J., 2015 Ontogeny of the sheathing leaf base in maize (Zea mays). *New Phytol.* **205**: 306–315, reproduced here with permission from the publisher as accorded through John Wiley and Sons policy. An introductory section (5.1) has been added for this format. I prepared the samples for imaging by nano-scale computed tomography (CT) and processed image datasets to generate the images and text reported here. Co-authors R Johnston and MJ Scanlon edited contributions listed here and are primary contributors for the remainder of the publication listed.

1.7 Works Cited

Barkoulas M., Hay A., Kougioumoutzi E., Tsiantis M., 2008 A developmental framework for dissected leaf formation in the Arabidopsis relative Cardamine hirsuta. Nat. Genet. **40**: 1136–1141.

Bharathan G., Goliber T. E., Moore C., Kessler S., Pham T., Sinha N. R., 2002 Homologies in leaf form inferred from KNOXI gene expression during development. Science **296**: 1858–1860.

Blein T., Pulido A., Vialette-Guiraud A., Nikovics K., Morin H., Hay A., Johansen I. E., Tsiantis M., Laufs P., 2008 A conserved molecular framework for compound leaf development. Science **322**: 1835–1839.

Bolduc N., Hake S., 2009 The maize transcription factor KNOTTED1 directly regulates the

gibberellin catabolism gene ga2ox1. Plant Cell **21**: 1647–58.

Bolduc N., Yilmaz A., Mejia-Guerra M. K., Morohashi K., O'Connor D., Grotewold E., Hake S., 2012 Unraveling the KNOTTED1 regulatory network in maize meristems. Genes Dev. **26**: 1685–90.

Bommert P., Lunde C., Nardmann J., Vollbrecht E., Running M., Jackson D., Hake S., Werr W., 2005 thick tassel dwarf1 encodes a putative maize ortholog of the Arabidopsis CLAVATA1 leucine-rich repeat receptor-like kinase. Development **132**: 1235–45.

Bommert P., Nagasawa N. S., Jackson D., 2013a Quantitative variation in maize kernel row number is controlled by the FASCIATED EAR2 locus. Nat. Genet. **45**: 334–7.

Bommert P., Je B. Il, Goldshmidt A., Jackson D., 2013b The maize Gα gene COMPACT PLANT2 functions in CLAVATA signalling to control shoot meristem size. Nature **502**: 555–8.

Brand U., 2000 Dependence of Stem Cell Fate in Arabidopsis on a Feedback Loop Regulated by CLV3 Activity. Science **289**: 617–619.

Broman K. W., Wu H., Sen ??aunak, Churchill G. A., 2003 R/qtl: QTL mapping in experimental crosses. Bioinformatics **19**: 889–890.

Buckler E. S., Holland J. B., Bradbury P. J., Acharya C. B., Brown P. J., Browne C., Ersoz E., Flint-Garcia S. A., Garcia A., Glaubitz J. C., Goodman M. M., Harjes C., Guill K., Kroon D. E., Larsson S., Lepak N. K., Li H., Mitchell S. E., Pressoir G., Peiffer J. a, Rosas M. O., Rocheford T. R., Romay M. C., Romero S., Salvo S., Sanchez Villeda H., Silva H. S. da, Sun Q., Tian F., Upadyayula N., Ware D., Yates H., Yu J., Zhang Z., Kresovich S., McMullen M. D., 2009 The genetic architecture of maize flowering time. Science **325**: 714–8.

Busch W., Miotk A., Ariel F. D., Zhao Z., Forner J., Daum G., Suzaki T., Schuster C., Schultheiss S. J., Leibfried A., Haubeiss S., Ha N., Chan R. L., Lohmann J. U., 2010 Transcriptional control of a plant stem cell niche. Dev. Cell **18**: 849–61.

Carroll S. B., 2000 Endless Forms: The Evolution of Gene Regulation and Morphological Diversity. Cell **101**: 577–580.

Chan R. L., Gago G. M., Palena C. M., Gonzalez D. H., 1998 Homeoboxes in plant

development. Biochim. Biophys. Acta **1442**: 1–19.

Chickarmane V. S., Gordon S. P., Tarr P. T., Heisler M. G., Meyerowitz E. M., 2012 Cytokinin signaling as a positional cue for patterning the apical-basal axis of the growing Arabidopsis shoot meristem. Proc. Natl. Acad. Sci. **109**: 4002–4007.

Chitwood D. H., Kumar R., Headland L. R., Ranjan A., Covington M. F., Ichihashi Y., Fulop D., Jiménez-Gómez J. M., Peng J., Maloof J. N., Sinha N. R., 2013 A quantitative genetic basis for leaf morphology in a set of precisely defined tomato introgression lines. Plant Cell **25**: 2465–81.

Chuck G., Lincoln C., Hake S., 1996 KNAT1 induces lobed leaves with ectopic meristems when overexpressed in Arabidopsis. Plant Cell **8**: 1277–89.

Clark S. E., Jacobsen S. E., Levin J. Z., Meyerowitz E. M., 1996 The CLAVATA and SHOOT MERISTEMLESS loci competitively regulate meristem activity in Arabidopsis. Development **122**: 1567–75.

Cook J. P., McMullen M. D., Holland J. B., Tian F., Bradbury P., Ross-Ibarra J., Buckler E. S., Flint-Garcia S. A., 2012 Genetic architecture of maize kernel composition in the nested association mapping and inbred association panels. Plant Physiol. **158**: 824–34.

Cronk Q. C., 2001 Plant evolution and development in a post-genomic context. Nat. Rev. Genet. **2**: 607–619.

Daum G., Medzihradszky A., Suzaki T., Lohmann J. U., 2014 A mechanistic framework for noncell autonomous stem cell induction in Arabidopsis. Proc. Natl. Acad. Sci. **111**: 14619–14624.

Deb Y., Marti D., Frenz M., Kuhlemeier C., Reinhardt D., 2015 Phyllotaxis involves auxin drainage through leaf primordia. Development: 1–10.

Deyoung B. J., Clark S. E., 2008 BAM receptors regulate stem cell specification and organ development through complex interactions with CLAVATA signaling. Genetics **180**: 895–904.

Doonan J. H., Sablowski R., 2010 Walls around tumours - why plants do not develop cancer. Nat. Rev. Cancer **10**: 794–802.

Durbak A. R., Tax F. E., 2011 CLAVATA signaling pathway receptors of Arabidopsis regulate cell proliferation in fruit organ formation as well as in meristems. Genetics **189**: 177–94.

Engstrom E. M., Andersen C. M., Gumulak-Smith J., Hu J., Orlova E., Sozzani R., Bowman J. L., 2011 Arabidopsis homologs of the petunia hairy meristem gene are required for maintenance of shoot and root indeterminacy. Plant Physiol. **155**: 735–50.

Fletcher J. C., Meyerowitz E. M., 2000 Cell signaling within the shoot meristem. Curr. Opin. Plant Biol. **3**: 23–30.

Furumizu C., Alvarez J. P., Sakakibara K., Bowman J. L., 2015 Antagonistic Roles for KNOX1 and KNOX2 Genes in Patterning the Land Plant Body Plan Following an Ancient Gene Duplication. PLOS Genet. **11**: e1004980.

Gordon S. P., Chickarmane V. S., Ohno C., Meyerowitz E. M., 2009 Multiple feedback loops through cytokinin signaling control stem cell number within the Arabidopsis shoot meristem. Proc. Natl. Acad. Sci. U. S. A. **106**: 16529–16534.

Graaff E. van der, Laux T., Rensing S. a, 2009 The WUS homeobox-containing (WOX) protein family. Genome Biol. **10**: 248.

Hake S., Vollbrecht E., Freeling M., 1989 Cloning Knotted, the dominant morphological mutant in maize using Ds2 as a transposon tag. EMBO J. **8**: 15–22.

Hake S., Char B. R., Chuck G., Foster T., Long J. A., Jackson D. P., 1995 Homeobox genes in the functioning of plant meristems. Philos. Trans. R. Soc. Lond. B. Biol. Sci. **350**: 45–51.

Hamant O., 2013 Widespread mechanosensing controls the structure behind the architecture in plants. Curr. Opin. Plant Biol. **16**: 654–60.

Hay A., Kaur H., Phillips A., Hedden P., Hake S., Tsiantis M., 2002 The gibberellin pathway mediates KNOTTED1-type homeobox function in plants with different body plans. Curr. Biol. **12**: 1557–65.

Hay A., Barkoulas M., Tsiantis M., 2006 ASYMMETRIC LEAVES1 and auxin activities converge to repress BREVIPEDICELLUS expression and promote leaf development in Arabidopsis. Development **133**: 3955–3961.

Hay A., Tsiantis M., 2010 KNOX genes: versatile regulators of plant development and diversity. Development **137**: 3153–65.

Holland P. W. H., 2013 Evolution of homeobox genes. Wiley Interdiscip. Rev. Dev. Biol. 2: 31–45.

Jackson D. P., Veit B., Hake S., 1994 Expression of maize KNOTTED1 related homeobox genes in the shoot apical meristem predicts patterns of morphogenesis in the vegetative shoot. Development **413**: 405–413.

Jackson D. P., 2001 The long and the short of it: signaling development through plasmodesmata. Plant Cell **13**: 2569–2572.

Jackson D. P., 2002 Double labeling of KNOTTED1 mRNA and protein reveals multiple potential sites of protein trafficking in the shoot apex. Plant Physiol. **129**: 1423–1429.

Jasinski S., Piazza P., Craft J., Hay A., Woolley L., Rieu I., Phillips A., Hedden P., Tsiantis M., 2005 KNOX action in Arabidopsis is mediated by coordinate regulation of cytokinin and gibberellin activities. Curr. Biol. **15**: 1560–5.

Johnston R., Wang M., Sun Q., Sylvester A. W., Hake S., Scanlon M. J., 2014 Transcriptomic Analyses Indicate That Maize Ligule Development Recapitulates Gene Expression Patterns That Occur during Lateral Organ Initiation. Plant Cell Online **26**: 4718–4732.

Jun J., Fiume E., Roeder A. H. K., Meng L., Sharma V. K., Osmont K. S., Baker C., Ha C. M., Meyerowitz E. M., Feldman L. J., Fletcher J. C., 2010 Comprehensive analysis of CLE polypeptide signaling gene expression and overexpression activity in Arabidopsis. Plant Physiol. **154**: 1721–1736.

Kim J. Y., Yuan Z., Cilia M., Khalfan-Jagani Z., Jackson D., 2002 Intercellular trafficking of a KNOTTED1 green fluorescent protein fusion in the leaf and shoot meristem of Arabidopsis. Proc. Natl. Acad. Sci. U. S. A. **99**: 4103–8.

Kim J. Y., Yuan Z., Jackson D., 2003 Developmental regulation and significance of KNOX protein trafficking in Arabidopsis. Development **130**: 4351–4362.

Kimura S., Koenig D., Kang J., Yoong F. Y., Sinha N. R., 2008 Natural Variation in Leaf Morphology Results from Mutation of a Novel KNOX Gene. Curr. Biol. **18**: 672–677.

Klein R. J., Zeiss C., Chew E. Y., Tsai J.-Y., Sackler R. S., Haynes C., Henning A. K., SanGiovanni J. P., Mane S. M., Mayne S. T., Bracken M. B., Ferris F. L., Ott J., Barnstable C., Hoh J., 2005 Complement factor H polymorphism in age-related macular degeneration. Science **308**: 385–9.

Klingenberg C. P., 2010 Evolution and development of shape: integrating quantitative approaches. Nat. Rev. Genet. **11**: 623–635.

Koenig D., Bayer E., Kang J., Kuhlemeier C., Sinha N. R., 2009 Auxin patterns Solanum lycopersicum leaf morphogenesis. Development **136**: 2997–3006.

Korte A., Farlow A., 2013 The advantages and limitations of trait analysis with GWAS: a review. Plant Methods **9**: 29.

Langlade N. B., Feng X., Dransfield T., Copsey L., Hanna A. I., Thébaud C., Bangham A., Hudson A., Coen E., 2005 Evolution through genetically controlled allometry space. Proc. Natl. Acad. Sci. U. S. A. **102**: 10221–6.

Laux T., Mayer K. F., Berger J., Jürgens G., 1996 The WUSCHEL gene is required for shoot and floral meristem integrity in Arabidopsis. Development **122**: 87–96.

Leibfried A., To J. P. C., Busch W., Stehling S., Kehle A., Demar M., Kieber J. J., Lohmann J. U., 2005 WUSCHEL controls meristem function by direct regulation of cytokinin-inducible response regulators. Nature **438**: 1172–5.

Lenhard M., Bohnert A., Jürgens G., Laux T., 2001 Termination of stem cell maintenance in Arabidopsis floral meristems by interactions between WUSCHEL and AGAMOUS. Cell **105**: 805–14.

Lenhard M., Jürgens G., Laux T., 2002 The WUSCHEL and SHOOTMERISTEMLESS genes fulfil complementary roles in Arabidopsis shoot meristem regulation. Development **129**: 3195–3206.

Lin H., Niu L., McHale N. a, Ohme-Takagi M., Mysore K. S., Tadege M., 2013 Evolutionarily conserved repressive activity of WOX proteins mediates leaf blade outgrowth and floral organ development in plants. Proc. Natl. Acad. Sci. U. S. A. **110**: 366–71.

Lincoln C., Long J. A., Yamaguchi J., Serikawa K., Hake S., 1994 A knotted1-like homeobox gene in Arabidopsis is expressed in the vegetative meristem and dramatically alters leaf

morphology when overexpressed in transgenic plants. Plant Cell **6**: 1859–76.

Lohmann J. U., Hong R. L., Hobe M., Busch M. a, Parcy F., Simon R., Weigel D., 2001 A molecular link between stem cell regulation and floral patterning in Arabidopsis. Cell **105**: 793–803.

Long J. A., Moan E., Medford J., Barton M., 1996 A member of the KNOTTED class of homeodomain proteins encoded by the STM gene of Arabidopsis. Nature **379**: 66–69.

Long J. A., Woody S., Poethig S., Meyerowitz E. M., Barton M. K., 2002 Transformation of shoots into roots in Arabidopsis embryos mutant at the TOPLESS locus. Development **129**: 2797–806.

Long J. A., Ohno C., Smith Z. R., Meyerowitz E. M., 2006 TOPLESS Regulates Apical Embryonic Fate in Arabidopsis. Science **312**: 1520–1522.

Lucas W. J., Bouché-Pillon S., Jackson D. P., Nguyen L., Baker L., Ding B., Hake S., 1995 Selective trafficking of KNOTTED1 homeodomain protein and its mRNA through plasmodesmata. Science **270**: 1980–1983.

Lunde C., Hake S., 2009 The interaction of knotted1 and thick tassel dwarf1 in vegetative and reproductive meristems of maize. Genetics **181**: 1693–7.

Magnani E., Hake S., 2008 KNOX lost the OX: the Arabidopsis KNATM gene defines a novel class of KNOX transcriptional regulators missing the homeodomain. Plant Cell **20**: 875–887.

Matsumoto N., Okada K., 2001 A homeobox gene, PRESSED FLOWER, regulates lateral axis-dependent development of Arabidopsis flowers. Genes Dev. **15**: 3355–3364.

Mayer K. F., Schoof H., Haecker A., Lenhard M., Jürgens G., Laux T., 1998 Role of WUSCHEL in regulating stem cell fate in the Arabidopsis shoot meristem. Cell **95**: 805–15.

Meijón M., Satbhai S. B., Tsuchimatsu T., Busch W., 2014 Genome-wide association study using cellular traits identifies a new regulator of root development in Arabidopsis. Nat. Genet. **46**: 77–81.

Miyawaki K., Tabata R., Sawa S., 2013 Evolutionarily conserved CLE peptide signaling in plant development, symbiosis, and parasitism. Curr. Opin. Plant Biol. **16**: 598–606.

Mukherjee K., Brocchieri L., Bürglin T. R., 2009 A comprehensive classification and evolutionary analysis of plant homeobox genes. Mol. Biol. Evol. **26**: 2775–2794.

Müller R., Borghi L., Kwiatkowska D., Laufs P., Simon R., 2006 Dynamic and compensatory responses of Arabidopsis shoot and floral meristems to CLV3 signaling. Plant Cell **18**: 1188–98.

Nardmann J., Werr W., 2013 Symplesiomorphies in the WUSCHEL clade suggest that the last common ancestor of seed plants contained at least four independent stem cell niches. New Phytol. **199**: 1081–92.

Nimchuk Z. L., Tarr P. T., Ohno C., Qu X., Meyerowitz E. M., 2011 Plant stem cell signaling involves ligand-dependent trafficking of the CLAVATA1 receptor kinase. Curr. Biol. **21**: 345–52.

Nordborg M., Weigel D., 2008 Next-generation genetics in plants. Nature **456**: 720–723.

Peiffer J. A., Romay M. C., Gore M. A., Flint-Garcia S. A., Zhang Z., Millard M. J., Gardner C. A. C., McMullen M. D., Holland J. B., Bradbury P. J., Buckler E. S., 2014 The genetic architecture of maize height. Genetics **196**: 1337–56.

Phelps-Durr T. L., Thomas J., Vahab P., Timmermans M. C. P., 2005 Maize rough sheath2 and its Arabidopsis orthologue ASYMMETRIC LEAVES1 interact with HIRA, a predicted histone chaperone, to maintain knox gene silencing and determinacy during organogenesis. Plant Cell **17**: 2886–2898.

Ragni L., Belles-Boix E., Günl M., Pautot V., 2008 Interaction of KNAT6 and KNAT2 with BREVIPEDICELLUS and PENNYWISE in Arabidopsis inflorescences. Plant Cell **20**: 888–900.

Reddy G. V., Meyerowitz E. M., 2005 Stem-cell homeostasis and growth dynamics can be uncoupled in the Arabidopsis shoot apex. Science **310**: 663–7.

Reinhardt D., 2000 Auxin Regulates the Initiation and Radial Position of Plant Lateral Organs. Plant Cell Online **12**: 507–518.

Rojo E., 2002 CLV3 Is Localized to the Extracellular Space, Where It Activates the Arabidopsis CLAVATA Stem Cell Signaling Pathway. Plant Cell Online **14**: 969–977.

Romay M. C., Millard M. J., Glaubitz J. C., Peiffer J. a, Swarts K. L., Casstevens T. M., Elshire R. J., Acharya C. B., Mitchell S. E., Flint-Garcia S. A., McMullen M. D., Holland J. B., Buckler E. S., Gardner C. A. C., 2013 Comprehensive genotyping of the USA national maize inbred seed bank. Genome Biol. **14**: R55.

Rupp H. M., Frank M., Werner T., Strnad M., Schmülling T., 1999 Increased steady state mRNA levels of the STM and KNAT1 homeobox genes in cytokinin overproducing Arabidopsis thaliana indicate a role for cytokinins in the shoot apical meristem. Plant J. **18**: 557–63.

Sakakibara K., Ando S., Yip H. K., Tamada Y., Hiwatashi Y., Murata T., Deguchi H., Hasebe M., Bowman J. L., 2013 KNOX2 genes regulate the haploid-to-diploid morphological transition in land plants. Science **339**: 1067–70.

Sakamoto T., Kamiya N., Ueguchi-Tanaka M., Iwahori S., Matsuoka M., 2001 KNOX homeodomain protein directly suppresses the expression of a gibberellin biosynthetic gene in the tobacco shoot apical meristem. Genes Dev. **15**: 581–90.

Sarkar A. K., Luijten M., Miyashima S., Lenhard M., Hashimoto T., Nakajima K., Scheres B., Heidstra R., Laux T., 2007 Conserved factors regulate signalling in Arabidopsis thaliana shoot and root stem cell organizers. Nature **446**: 811–814.

Scanlon M. J., 2000 NARROW SHEATH1 functions from two meristematic foci during founder-cell recruitment in maize leaf development. Development **127**: 4573–85.

Scanlon M. J., 2003 The polar auxin transport inhibitor N-1-naphthylphthalamic acid disrupts leaf initiation, KNOX protein regulation, and formation of leaf margins in maize. Plant Physiol. **133**: 597–605.

Schoof H., Lenhard M., Haecker A., Mayer K. F., Jürgens G., Laux T., 2000 The stem cell population of Arabidopsis shoot meristems in maintained by a regulatory loop between the CLAVATA and WUSCHEL genes. Cell **100**: 635–44.

Scofield S., Dewitte W., Nieuwland J., Murray J. a H., 2013 The Arabidopsis homeobox gene SHOOT MERISTEMLESS has cellular and meristem-organisational roles with differential requirements for cytokinin and CYCD3 activity. Plant J. **75**: 53–66.

Shah N., Sukumar S., 2010 The Hox genes and their roles in oncogenesis. Nat. Rev. Cancer **10**: 361–371.

Shani E., Yanai O., Ori N., 2006 The role of hormones in shoot apical meristem function. Curr. Opin. Plant Biol. **9**: 484–9.

Shimizu R., Ji J., Kelsey E., Ohtsu K., Schnable P. S., Scanlon M. J., 2009 Tissue specificity and evolution of meristematic WOX3 function. Plant Physiol. **149**: 841–850.

Smith E. F., Brown N. A., McCulloch L., 1912 *The structure and development of crown gall: A plant cancer*. US Government Printing Office.

Smith L. G., Greene B., Veit B., Hake S., 1992 A dominant mutation in the maize homeobox gene, Knotted-1, causes its ectopic expression in leaf cells with altered fates. Development **116**: 21–30.

Smith H. M. S., Boschke I., Hake S., 2002 Selective interaction of plant homeodomain proteins mediates high DNA-binding affinity. Proc. Natl. Acad. Sci. U. S. A. **99**: 9579–84.

Steeves T. A., Sussex I. M., 1972 *Patterns in plant development*. Prentice-Hall, Englewood Cliffs, N.J.

Sultan S. E., 2000 Phenotypic plasticity for plant development, function and life history. Trends Plant Sci. **5**: 537–542.

Tanksley S. D., 1993 Mapping Polygenes. Annu. Rev. Genet. **27**: 205–233.

Theodoris G., Inada N., Freeling M., 2003 Conservation and molecular dissection of ROUGH SHEATH2 and ASYMMETRIC LEAVES1 function in leaf development. Proc. Natl. Acad. Sci. U. S. A. **100**: 6837–6842.

Thompson A. M., Crants J., Schnable P. S., Yu J., Timmermans M. C. P., Springer N. M., Scanlon M. J., Muehlbauer G. J., 2014 Genetic control of maize shoot apical meristem architecture. G3 (Bethesda). **4**: 1327–37.

Thompson A. M., Yu J., Timmermans M. C. P., Schnable P., Crants J. C., Scanlon M. J., Muehlbauer G. J., 2015 Diversity of Maize Shoot Apical Meristem Architecture and Its Relationship to Plant Morphology. G3!; Genes|Genomes|Genetics: 1–14.

Tian F., Bradbury P. J., Brown P. J., Hung H., Sun Q., Flint-Garcia S. A., Rocheford T. R., McMullen M. D., Holland J. B., Buckler E. S., 2011 Genome-wide association study of leaf architecture in the maize nested association mapping population. Nat. Genet. **43**: 159–62.

Timmermans M. C. P., Hudson A., Becraft P. W., Nelson T., 1999 ROUGH SHEATH2: A Myb Protein That Represses knox Homeobox Genes in Maize Lateral Organ Primordia. Science **284**: 151–153.

Tsiantis M., Schneeberger R., Golz J. F., Freeling M., Langdale J. a, 1999 The maize rough sheath2 gene and leaf development programs in monocot and dicot plants. Science **284**: 154–6.

Vandenbussche M., Horstman A., Zethof J., Koes R., Rijpkema A. S., Gerats T., 2009 Differential recruitment of WOX transcription factors for lateral development and organ fusion in Petunia and Arabidopsis. Plant Cell **21**: 2269–2283.

Vollbrecht E., Veit B., Sinha N. R., Hake S., 1991 The developmental gene Knotted-1 is a member of a maize homeobox gene family. Nature **350**: 241–243.

Vollbrecht E., Reiser L., Hake S., 2000 Shoot meristem size is dependent on inbred background and presence of the maize homeobox gene, knotted1. Development **127**: 3161–72.

Walbot V., 1985 On the life strategies of plants and animals. Trends Genet. **1**: 165–169.

Weigel D., Nordborg M., 2005 Natural variation in Arabidopsis. How do we find the causal genes? Plant Physiol. **138**: 567–8.

Wong C. E., Singh M. B., Bhalla P. L., 2013 Spatial expression of CLAVATA3 in the shoot apical meristem suggests it is not a stem cell marker in soybean. J. Exp. Bot.

Wu X., Chory J., Weigel D., 2007 Combinations of WOX activities regulate tissue proliferation during Arabidopsis embryonic development. Dev. Biol. **309**: 306–316.

Xu L., Shen W.-H., 2008 Polycomb silencing of KNOX genes confines shoot stem cell niches in Arabidopsis. Curr. Biol. **18**: 1966–71.

Xu X. M., Wang J., Xuan Z., Goldshmidt A., Borrill P. G. M., Hariharan N., Kim J. Y., Jackson

D., 2011 Chaperonins facilitate KNOTTED1 cell-to-cell trafficking and stem cell function. Science **333**: 1141–1144.

Xu C., Liberatore K. L., MacAlister C. a, Huang Z., Chu Y.-H., Jiang K., Brooks C., Ogawa-Ohnishi M., Xiong G., Pauly M., Eck J. Van, Matsubayashi Y., Knaap E. van der, Lippman Z. B., 2015 A cascade of arabinosyltransferases controls shoot meristem size in tomato. Nat. Genet.

Yadav R. K., Tavakkoli M., Reddy G. V., 2010 WUSCHEL mediates stem cell homeostasis by regulating stem cell number and patterns of cell division and differentiation of stem cell progenitors. Development **137**: 3581–9.

Yadav R. K., Perales M., Gruel J., Girke T., Jönsson H., Reddy G. V., 2011 WUSCHEL protein movement mediates stem cell homeostasis in the Arabidopsis shoot apex. Genes Dev. **25**: 2025–30.

Yadav R. K., Perales M., Gruel J., Ohno C., Heisler M. G., Girke T., Jönsson H., Reddy G. V., 2013 Plant stem cell maintenance involves direct transcriptional repression of differentiation program. Mol. Syst. Biol. **9**: 654.

Yu J., Pressoir G., Briggs W. H., Vroh Bi I., Yamasaki M., Doebley J. F., McMullen M. D., Gaut B. S., Nielsen D. M., Holland J. B., Kresovich S., Buckler E. S., 2006 A unified mixed-model method for association mapping that accounts for multiple levels of relatedness. Nat. Genet. **38**: 203–8.

Zhang Z., Ersoz E., Lai C.-Q., Todhunter R. J., Tiwari H. K., Gore M. a, Bradbury P. J., Yu J., Arnett D. K., Ordovas J. M., Buckler E. S., 2010 Mixed linear model approach adapted for genome-wide association studies. Nat. Genet. **42**: 355–60.

Zhang W., Swarup R., Bennett M., Schaller G. E., Kieber J. J., 2013 Cytokinin induces cell division in the quiescent center of the Arabidopsis root apical meristem. Curr. Biol. **23**: 1979–89.

Zhou Y., Liu X., Engstrom E. M., Nimchuk Z. L., Pruneda-Paz J. L., Tarr P. T., Yan A., Kay S. a., Meyerowitz E. M., 2014 Control of plant stem cell function by conserved interacting transcriptional regulators. Nature **517**: 377–380.

2 Genetic control of morphometric diversity in the maize shoot apical meristem

2.1 Abstract

The maize shoot apical meristem (SAM) comprises a small pool of stem cells that generate all above-ground organs. Although mutational studies have identified genetic networks regulating SAM function, little is known about SAM morphological variation in natural populations. Here we report the use of high-throughput image processing to capture rich SAM size variation within a diverse maize inbred panel. We demonstrate correlations between seedling SAM size and agronomically-important adult traits such as flowering time, stem size, and leaf node number. Combining SAM phenotypes with 1.2 million SNPs via genome-wide association study (GWAS) reveals unexpected SAM morphology candidate genes. Analyses of candidate genes implicated in hormone transport, cell division, and cell size confirm correlations between SAM morphology and trait-associated SNP (TAS) alleles. Our data illustrate that the microscopic seedling SAM is predictive of adult phenotypes and that SAM morphometric variation is associated with genes not previously predicted to regulate SAM size.

2.2 Introduction

Plants maintain populations of pluripotent stem cells called shoot apical meristems (SAMs) throughout their lifetime. Shoot meristems function to generate morphologically complex body plans by the coordinated activities of stem cell maintenance to sustain the SAM, and organogenesis of leaves and branches in a phyllotactic pattern (Steeves

and Sussex 1972). These dual SAM functions determine the number and position of all lateral organs that make up the plant shoot. Although microscopic in size, correlations of seedling SAM morphology and adult plant phenotypes may render the vegetative SAM predictive of agronomically-important plant traits (Thompson *et al.* 2015).

Decades of genetic research have delineated a complex, interactive network of transcription factors, hormonal signals, epigenetic marks, metabolites, and biophysical forces that contribute to the regulation of SAM function (Sussex and Kerk 2001; Francis and Halford 2006; Shani *et al.* 2006; Ha *et al.* 2010; Pautler *et al.* 2013; Hamant 2013). Single-gene mutations within these SAM genetic networks can alter the morphology of both the shoot meristem and the plant (Jackson and Hake 1999; Fujita and Kawaguchi 2011), revealing that SAM structure and function are intimately linked. Although these studies identified a number of genes required for SAM function, little is known about the genetic control of SAM morphological variation in large natural populations or in diverse breeding stocks. QTL analyses of bi-parental populations have shown that differences in SAM morphology may involve loci not previously identified via single gene mutations (Thompson *et al.* 2014, 2015).

In contrast to QTL analyses, genome-wide association studies (GWAS) exploit historical recombination events and linkage disequilibrium (LD) to dissect the genetic architecture of quantitative traits. The abundant polymorphism and relatively low LD present in the model crop plant maize (*Zea mays* subsp. *mays* L.), when coupled with exhaustive genotypic surveys and innovative statistical analyses, have increased the precision and power to identify genic associations for multiple maize traits (Wallace *et al.* 2014). Thus, further interrogation of the genetic architecture of SAM morphology amongst many

diverse genetic stocks may reveal novel regulators of SAM function, which have not been highlighted by single gene mutations or QTL analyses of bi-parental populations.

To date, the majority of maize GWAS have analyzed the genetic basis of macroscopic or biochemical phenotypes in adult plants (Buckler *et al.* 2009; Tian *et al.* 2011; Wallace *et al.* 2014). Although a few studies in other systems have examined microscopic phenotypes (Klein *et al.* 2005; Meijón *et al.* 2014), no GWAS in maize has utilized phenotypes collected at a microscopic scale. Here we report the first application of GWAS to study the genetic architecture of maize SAM morphology, a microscopic phenotype that poses unique challenges for quantitative analysis. Applying a high-throughput imaging pipeline to a diverse panel of 369 maize inbred lines, we detect extensive SAM morphometric variation. Significant correlations are identified between the microscopic SAM and several adult phenotypes, including flowering time, stem width, and leaf node number. These findings demonstrate that the morphology of the seedling SAM is predictive of agronomically-important adult plant traits. Utilizing a 1.2-million-SNP dataset that combined RNAseq-generated and previously published available genotypes, we identify candidate genes associated with SAM morphological variation. Although the majority of these GWAS-derived SAM candidate genes have not been previously implicated in studies of SAM structure, subsequent analyses of candidate genes with putative functions in hormone transport, cell division, and cell expansion support their predicted contributions to maize SAM morphological diversity.

2.3 Results

2.3.1 The maize SAM morphospace correlates with adult plant traits

Although several groups have documented differences in SAM morphology among common maize inbred varieties (Vollbrecht *et al.* 2000; Thompson *et al.* 2014, 2015), to date no studies have summarized the diversity of shapes and sizes that populate the maize SAM morphospace. We adapted a high-throughput histological clearing technique (Thompson *et al.* 2014; Yang *et al.* 2015) to image a panel of 369 diverse inbred maize inbred that represents more than 80% of the genetic diversity within *Zea mays* subsp. *mays* L. (Liu *et al.* 2003; Flint-Garcia *et al.* 2005). We hypothesized that this panel would likewise capture much of the natural variation in SAM microphenotypes.

We modeled the SAM as a paraboloid, a geometric shape that facilitates estimations of multiple measures such as volume, surface area, arc length and curvature, all of which can be calculated from just two discrete measurements, SAM height and SAM radius (Niklas and Mauseth 1980; Green 1999). To test the efficacy of this parabolic model, we analyzed two maize inbred lines (B73 and W22) with demonstrated differences in SAM size (Figure 2.1) (Vollbrecht *et al.* 2000). Modeling the SAM as a paraboloid identified statistically significant differences between inbreds in shape-determining model coefficients (Figure 2.1a- c). In a comparison of direct image processing and parabolic modeling of SAM microphenotypes, we found no statistical difference between measurement methods, yet the ability to differentiate genotypes was maintained (Figure 2.1d). We incorporated this parabolic model into our image-processing pipeline to

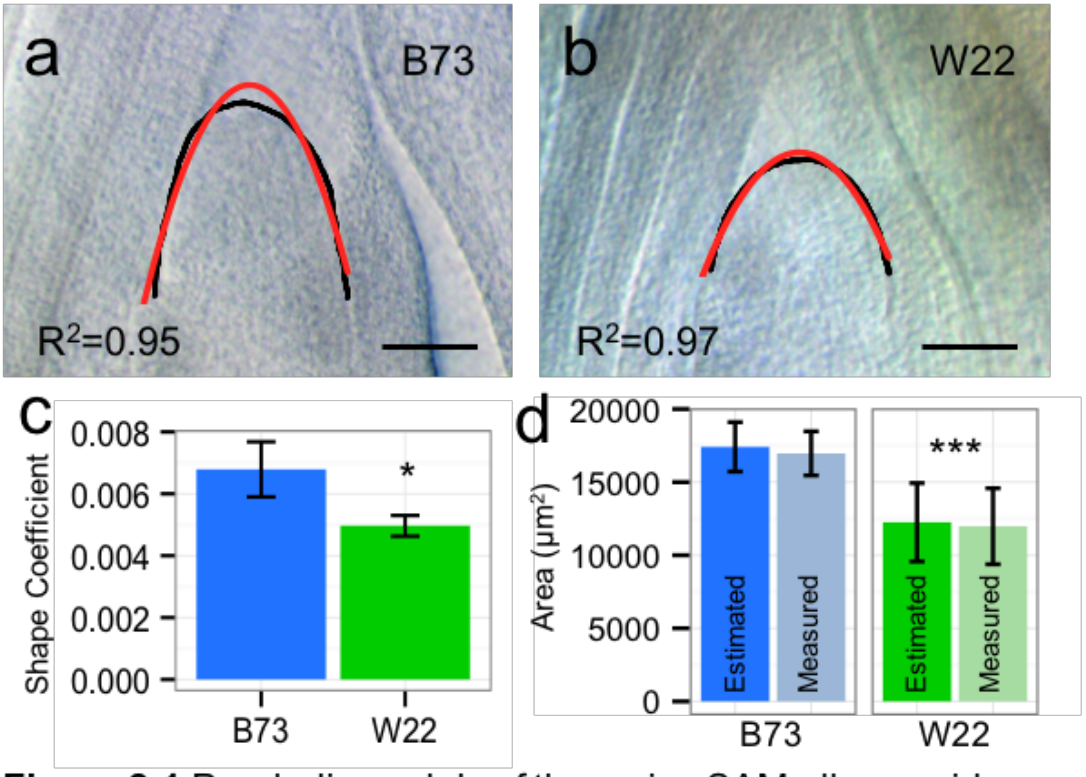

Figure 2.1 Parabolic models of the maize SAM allow rapid assessment of morphology. (a-b) Inbreds B73 and W22 have SAM morphology (black) closely approximated by a parabolic model (red). (c) Parabolic SAM model coefficients between inbreds are significantly distinct, Student's t-test, p=0.013 (d) SAM area calculations from model-derived estimates, "Estimated" and direct image-processed measures, "Measured" are not significantly different within a genotype, but significantly different between genotypes. Two-way ANOVA – Factor, genotype: p= 0.000325; Factor, measurement technique: p = 0.750547; Interaction, genotype and technique: p = 0.939353. Scale bars, 100 μm. Error bars, 95% CI.

quickly generate many SAM microphenotypes from rudimentary primary measurements (Supplementary Data 2.1).

Across four biological replicates we identified rich diversity in SAM morphology within our panel of 369 maize inbreds (Figure 2.2, Supplementary Data 2.2). Figure 2.2d portrays the maize SAM morphospace, plotted as SAM radius versus height; small, intermediate, and large size categories of maize SAMs were identified. The SAM from the inbred line B73, from which the reference maize genome was obtained(Schnable *et al.* 2009), occupies the center of our morphospace (Figure 2.2a-d). Modeling the SAM as a paraboloid enabled facile estimations of SAM volume (Figure 2.2e).

In comparisons of microscopic SAM seedling phenotypes to agronomically-important adult plant traits (Supplementary Data 3), we identified modest but significant correlations between seedling SAM volume and height to primary ear (Pearson's r = -0.18, Fisher transformation p = 9.871e-04), days to anthesis (Pearson's r = -0.33, Fisher transformation p = 6.743e-10), leaf node number (Peasrson's r = -0.21, Fisher transformation p = 8.922e-05) and stem diameter above the primary ear (Pearson's r = -0.13, Fisher transformation p = 0.01238) (Figure 2.3) (Peiffer *et al.* 2014).

2.3.2 GWAS of maize SAM volume

To better understand the genetic architecture controlling maize SAM morphology, we used GWAS to identify loci correlated with SAM microphenotypes within our diverse maize inbred panel. SAM volume was found to have a favorable entry mean heritability, or repeatability of 0.84, and its calculation captures variation contributed by multiple SAM microphenotypes (Figure 2.4, Methods). We therefore focused our analyses on SAM volume.

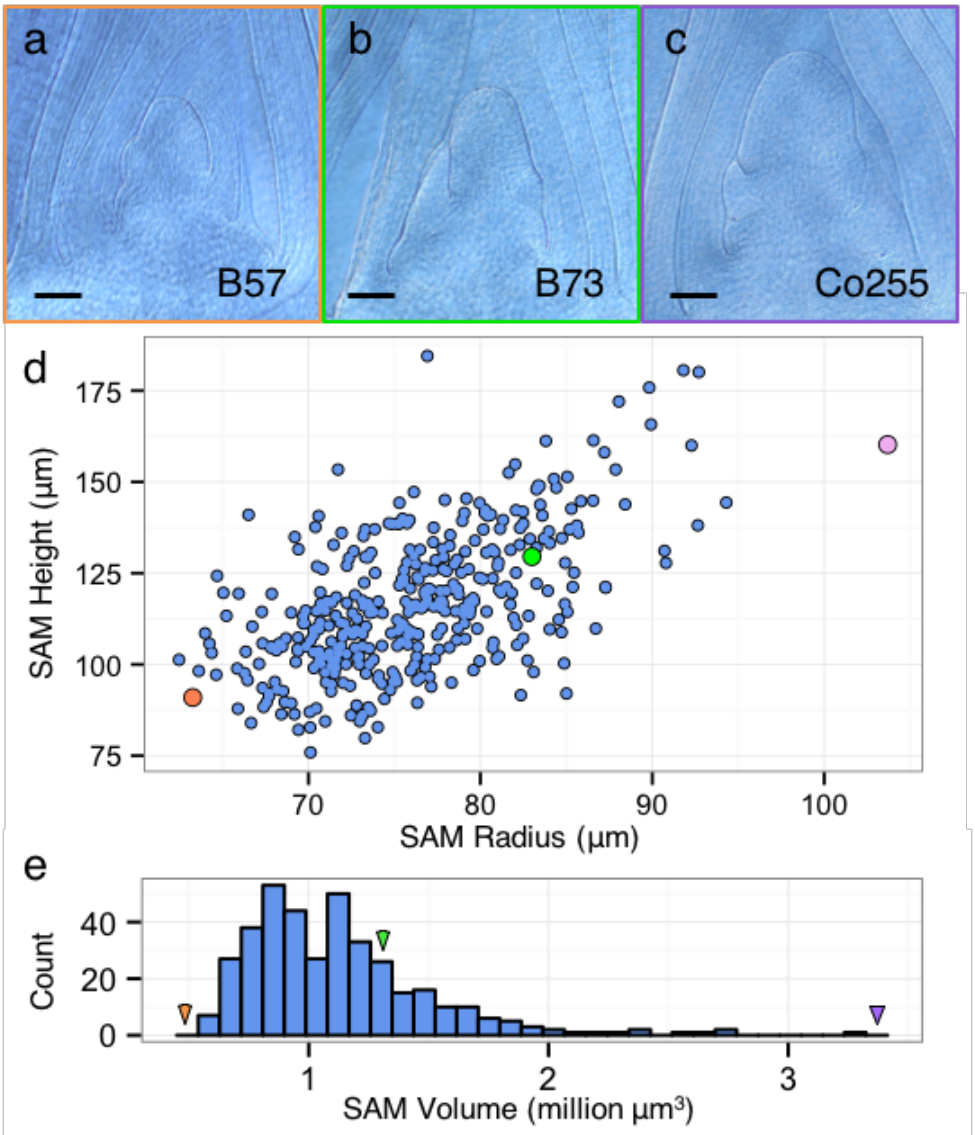

Figure 2.2 Extreme variation in maize SAM morphology. (a-c) Examples of small (a), intermediate (b), and large (c) SAM lines. (d) BLUPs calculated for SAM height and radius. (e) SAM volume estimated by parabolic model of SAM shape. Points/arrows highlight small, intermediate, and large accessions, B57 (orange), B73 (green), and Co255 (purple) respectively. Scale bar, 100µm.

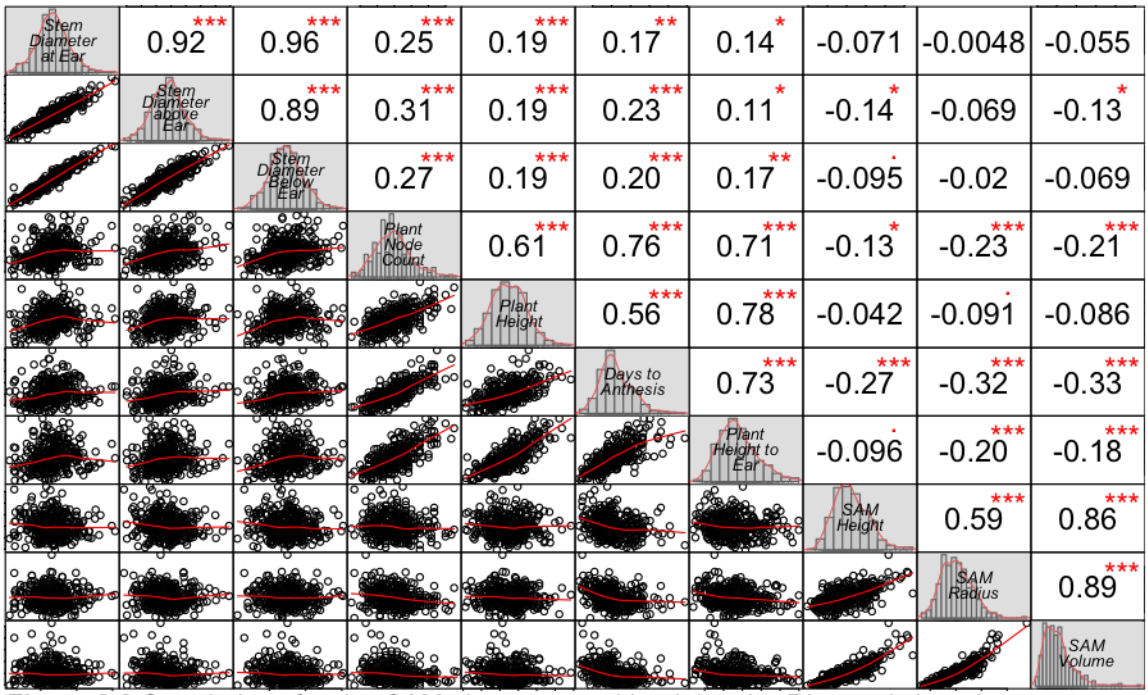

Figure 2.3 Correlation of maize SAM phenotypes with adult traits. Diagonal plots show histogram of each variable with density kernel in red. Numbers above diagonal show Pearson's r between variables. Scatterplots below diagonal show XY relationship between variables with loess curves fit in red. P-value: *** 0.001, ** 0.01, * 0.05, . 0.1, ' ' 1.

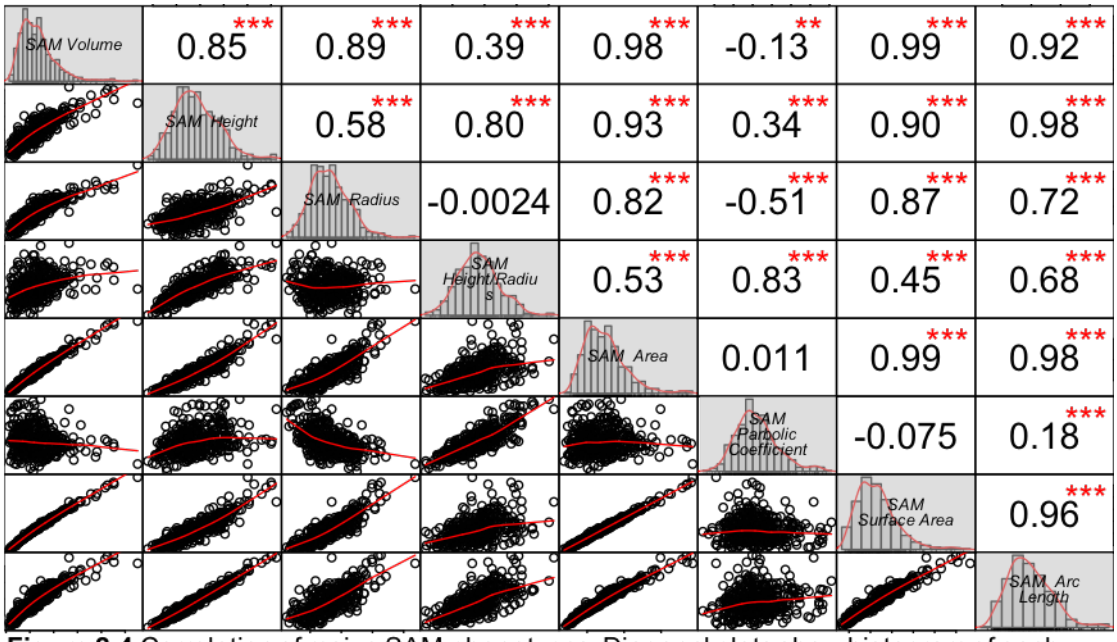

Figure 2.4 Correlation of maize SAM phenotypes. Diagonal plots show histogram of each variable with density kernel in red. Numbers above diagonal show Pearson's r between variables. Scatterplots below diagonal show XY relationship between variables with loess curves fit in red. P-value: *** 0.001, ** 0.01, * 0.05, . 0.1, ' ' 1.

Using RNAseq data obtained from SAM-enriched apex tissue, we generated 923,000 novel SNPs from our maize inbred panel. An additional 358,000 SNPs called from the Ames US Inbreds public dataset generated a combined genotyping matrix of more than 1.2 million high quality SNPs (Figure 2.5a) (Li *et al.* 2012; Romay *et al.* 2013). We used a unified mixed-model approach to associate SAM volume with SNPs from our genotyping matrix, accounting for kinship and population structure within the panel (Yu *et al.* 2006). Fifty-one trait-associated SNPs (TAS) that surpassed a stringent ($\alpha = 0.01$) Bonferroni-correction threshold of $-\log P > 8.11$ were detected. Thirty-four TAS were unique to RNAseq-generated SNPs, while only seven TAS were found in both SNP datasets (Figure 2.5b). Forty-eight TAS were within 100 kb of 23 unique candidate genes, with the majority of TAS (44/48) in predicted coding regions themselves (Figure 2.5c-o, Supplementary Data 2.4). This bias towards coding regions is in accordance with a previous report of GWAS conducted using SNPs generated from RNAseq data (Li *et al.* 2012).

In each of the 51 TAS, the common allele (COM) had a frequency above 91% (Supplementary Data 2.5). For all but one TAS, the B73 reference sequence was the COM. The total number of TAS alternate alleles (ALT) identified in an individual was moderately correlated with SAM volume (Pearson's $r = 0.50$, Fisher transformation $p < 2.22e\text{-}16$); inbreds with the largest SAMs were more frequently ALT at multiple TAS (Figure 2.5p). we selected four candidate genes with especially interesting predicted developmental functions for analyses of the contribution of ALT alleles to SAM shape and size.

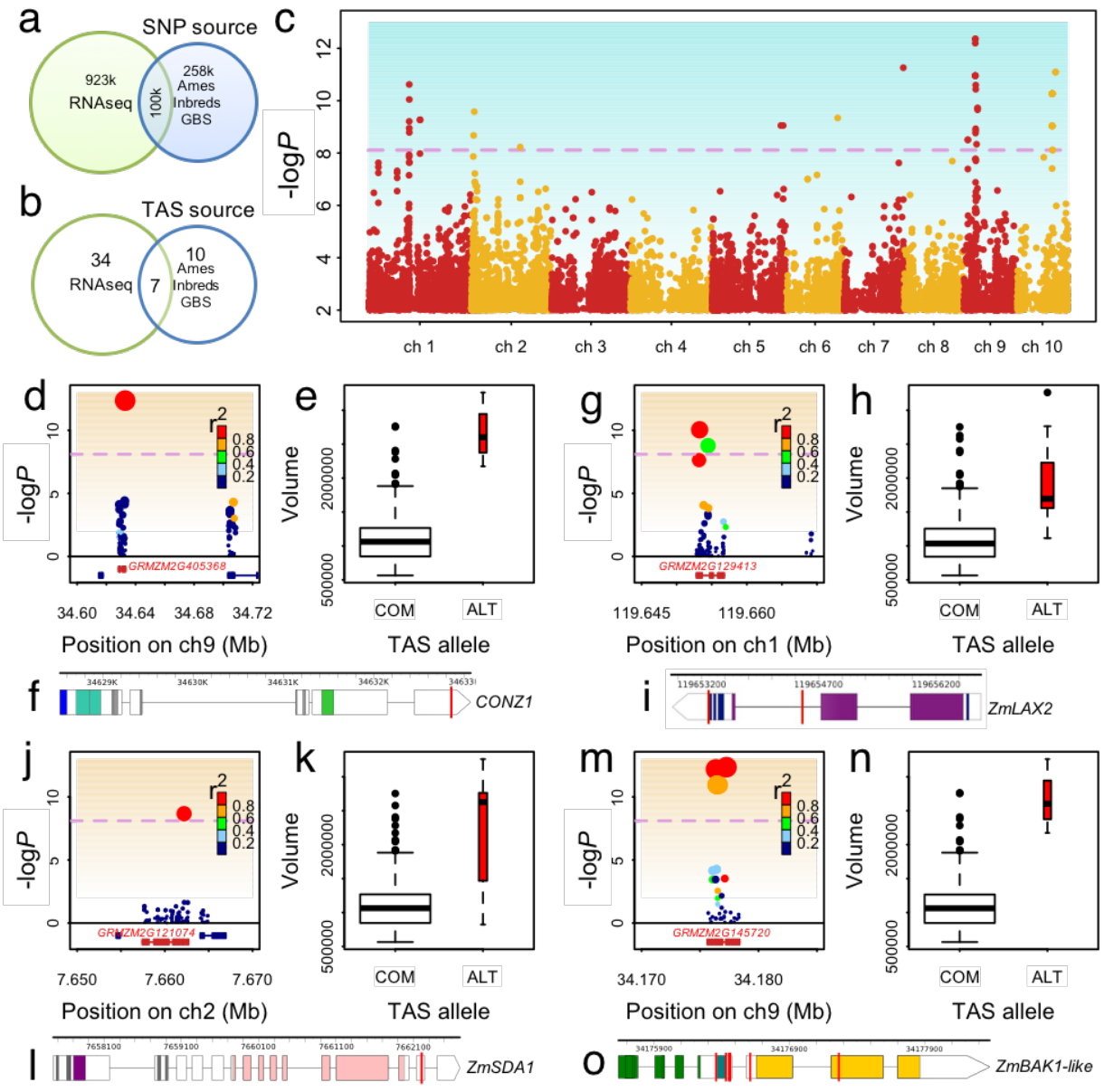

Figure 2.5 GWAS of maize SAM volume. (a) SNP genotyping matrix generated by RNAseq-analysis and Ames inbreds GBS SNPs. (b) Trait associated SNPs (TASs) from both SNP sources. (c) Manhattan plot of GWAS showing 51 TASs with -log*P* > 8.11, dotted line. Candidate genes with predicted developmental functions (d-o). (d,g,j,m) Regional plots show significant SNPs and LD (color scale) around candidate genes (red). (e,h,k,n) SAM volume for common (COM) and alternative (ALT) TAS alleles. Width scales with number of inbreds. (f,i,l,o) Gene models, colored rectangles indicate predicted protein domains. Location of TAS, red line. (d-f) GRMZM2G405368, *Constans-like 1* (*CONZ1*). (g-i) GRMZM2G129413, *Like Auxin-Resistant 2* (*ZmLAX2*). (j-l) GRMZM2G121074, *severe depolymerization of actin1* (*ZmSDA1*). (m-o) GRMZM2G145720, *BRASSINOSTEROID INSENSITIVE 1-associated receptor kinase 1 like* (*ZmBAK1-like*). (p) Number of ALT TAS alleles for inbred lines of different SAM volume.

2.3.3 SAM Morphology-Associated Genes

We detected one TAS within the 3'UTR of GRMZM2G405368, *Constans-like 1* (*CONZ1*) (Figure 2.5c). *CONZ1* exhibits diurnal transcript fluctuations and is associated with flowering time (Miller *et al.* 2008). Within our maize inbred panel, we found a significant, moderate/weak negative correlation between SAM volume and days to anthesis (DTA; Pearson's r = -0.33, Fisher transformation p = 6.743e-10) (Peiffer *et al.* 2014). Although flowering time data is available for just one of the four *CONZ1-ALT* lines, the DTA value for Co255 falls within the upper quartile of this inbred panel. Morphological examination of sampled SAMs revealed active production of leaf primordia (Figure 2.1ab, 2.2a-c), verifying that the SAMs assayed in our dataset had not undergone the transition from vegetative to inflorescence-staged shoot meristems (Pautler *et al.* 2013). Furthermore, neither CONZ1 nor any SAM morphology-associated candidate genes identified in our study have been implicated in prior GWAS of maize flowering time (Buckler *et al.* 2009; Peiffer *et al.* 2014).

We detected two TASs within the 2nd intron and 3rd exon of GRMZM2G129413, which appear as one allele in our panel (Figure 2.5d). The ALT form of the 3rd exon TAS is expected to render an amino acid change from histidine to asparagine near a predicted low-complexity protein domain. The closest *Arabidopsis thaliana* homolog to GRMZM2G129413 is *LIKE-AUXIN RESISTANT 2* (*LAX2*), a predicted auxin influx protein that is expressed within developing vasculature and may modulate auxin flow dynamics (Hochholdinger *et al.* 2000; Lawrence *et al.* 2008; Bainbridge *et al.* 2008).

In situ hybridization of B73 maize seedling apices (n = 20) with a probe specific to *ZmLAX2* shows a strong provascular expression pattern within leaf primordia and in the

developing stem (Figure 2.6a-c). Expression is not detected in differentiated xylem or phloem cells, but is restricted to the procambium, undifferentiated cells located between the xylem and phloem poles (Figure 2.6de). Due to the 3-dimensional arrangement of plant vasculature, single longitudinal sections do not capture entire vascular traces. To address this issue, we aligned and compiled our *ZmLAX2 in situ* hybridization data from several serial sections from ten additional inbred lines selected to reflect various SAM sizes and *ZmLAX2* genotypes to reconstruct the native expression pattern.

We detected spatiotemporal variation in *ZmLAX2* transcripts correlated with the *ZmLAX2* TAS genotype (Figure 2.7). Leaves are designated according to plastochron number, which specifies the relative time elapsed since initiation from the SAM, such that the newly-initiated leaf is termed P1 and the next incipient primordium is designated P0 (Sharman 1942). In four large SAM *ZmLAX2-COM* lines, transcript accumulation was detected in the P0 and in older leaf primordia (Figure 2.7a). Similarly, four small SAM *ZmLAX2-COM* lines examined exhibited *ZmLAX2* transcript accumulation in the P0 and older primordia (Figure 2.7b). In contrast, the large SAM *ZmLAX2-ALT* lines ND246 and Co255 displayed transcript accumulation in the P0 and older leaf primordia, as well as on the flank of the SAM opposite the P0 (Figure 2.7cd). This unique expression pattern extends into the SAM towards the predicted location of the yet-to-be-specified incipient primordium, designated P-1. Note that the accumulation of *ZmLAX2* transcript in P-1 primordia can been seen in apices with relatively larger, flanking P1 and P2 primordia (Figure 2.7c), as well as shoot apices with smaller P1 and P2 primordia (Figure 2.7d). Thus, the observed accumulation of *ZmLAX2* transcript in P-1 primordia in large SAMs containing the *ZmLAX2-ALT* allele is *not* correlated with

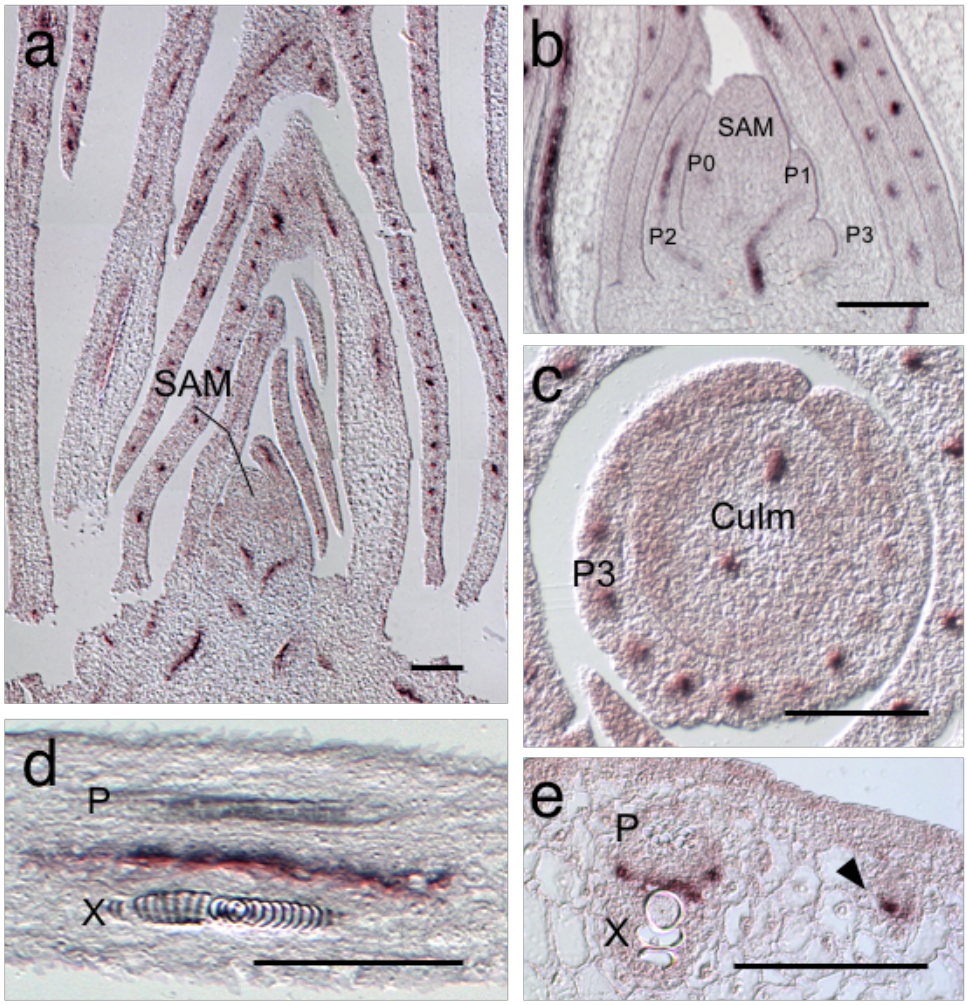

Figure 2.6 Transcript accumulation pattern of *ZmLAX2*. (a-b) in situ hybridization of 14-day-old maize seedlings (inbred B73) reveals *ZmLAX2* transcript localization in the vascular traces of leaf primordia. (c) Punctate provascular accumulation found in transverse of culm below the SAM. (d-e) Procambial cells between mature phloem, "P" and xylem, "X" show accumulation in longitudinal and transverse of P7 primordium. (e) Arrow denotes procambial expression in minor vein prior to xylem and phloem differentiation. Scale bar, 100µm.

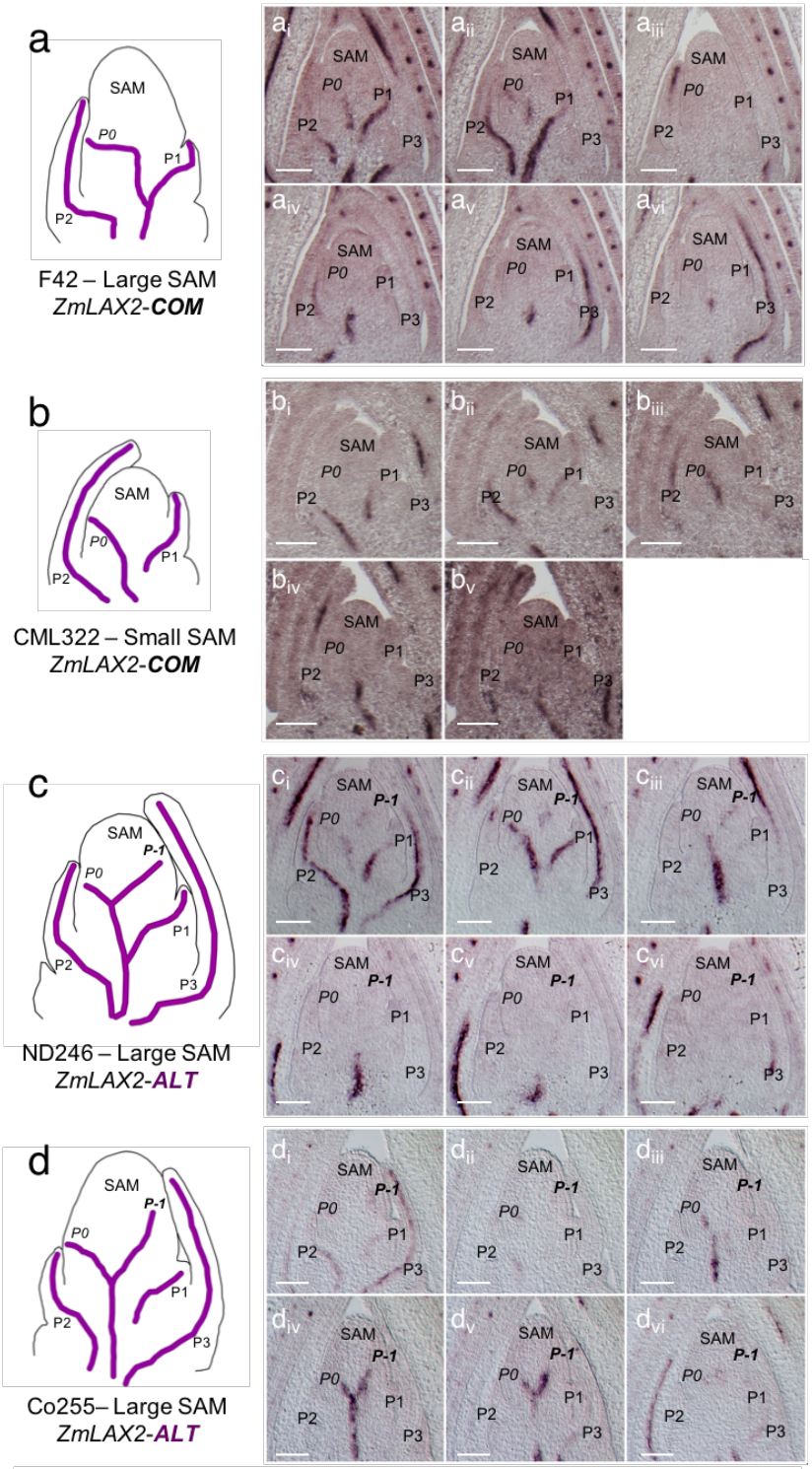

Figure 2.7 Differing spatiotemporal patterns of *ZmLAX2* transcript accumulation based on *ZmLAX2* TAS genotype, common (COM) or alternate (ALT). Serial section compilations from large (a) and small (b) SAM *ZmLAX2-COM* lines show transcript accumulation in P0 and later primordia, P1-P3. Serial sections (ai-avi, bi-bv) Large SAM *ZmLAX2-ALT* lines (c, d) exhibit additional transcript accumulation above the P0, in the position of the next anticipated primoridium, P-1. Serial sections (ci-cvi, di-dvi). Scale bars, 100 µm.

plastochron index and this expression pattern is not an artifact of relative developmental staging between plastochrons.

We detected one TAS within the 14th exon of GRMZM2G121074 that is predicted to cause a synonymous codon change in the *ZmSDA1-ALT* allele. GRMZM2G121074 is the closest maize homolog of *severe depolymerization of actin* (*SDA1*), a highly conserved gene required for cellular G1 phase transition and mitotic timing in *Saccharomyces cerevisiae* (Buscemi *et al.* 2000; Monaco *et al.* 2014).

We processed images from a subset of inbred lines treated with a Kasten's fluorescent Feulgen stain to test whether *ZmSDA1* genotype is correlated with differences in cell number (Figure 2.8) (Kasten 1958; Ruzin 1999; Bray *et al.* 2015). Images from three *ZmSDA1-ALT* lines and eleven randomly chosen *ZmSDA1-COM* lines with small, intermediate, and large maize SAMs were examined in three biological replicates (Figure 2.8a-h). *ZmSDA1-ALT* lines exhibited a statistically significant increase in SAM cell number (SCN) compared to *ZmSDA1-COM* lines (Figure 2.8i). Modeling SCN as the product of *ZmSDA1* genotype and SAM volume in a two-way ANOVA showed that *ZmSDA1* genotype and SAM volume are both significant predictive factors of SCN, and predictions of SCN are independent of the interaction between *ZmSDA1* genotype and SAM volume.

We detected four TASs within the 4th exon, one TAS within the 5th exon, and one TAS within the 6th exon of GRMZM2G145720, which appear as one allele in our panel. GRMZM2G145720 is a leucine-rich repeat receptor-like protein kinase gene homologous to the *Oryza sativa* gene *BRASSINOSTEROID INSENSITIVE 1-associated receptor kinase 1* (*OsBAK1*) (maizegdb.org). The ALT allele of *ZmBAK1-like* encodes

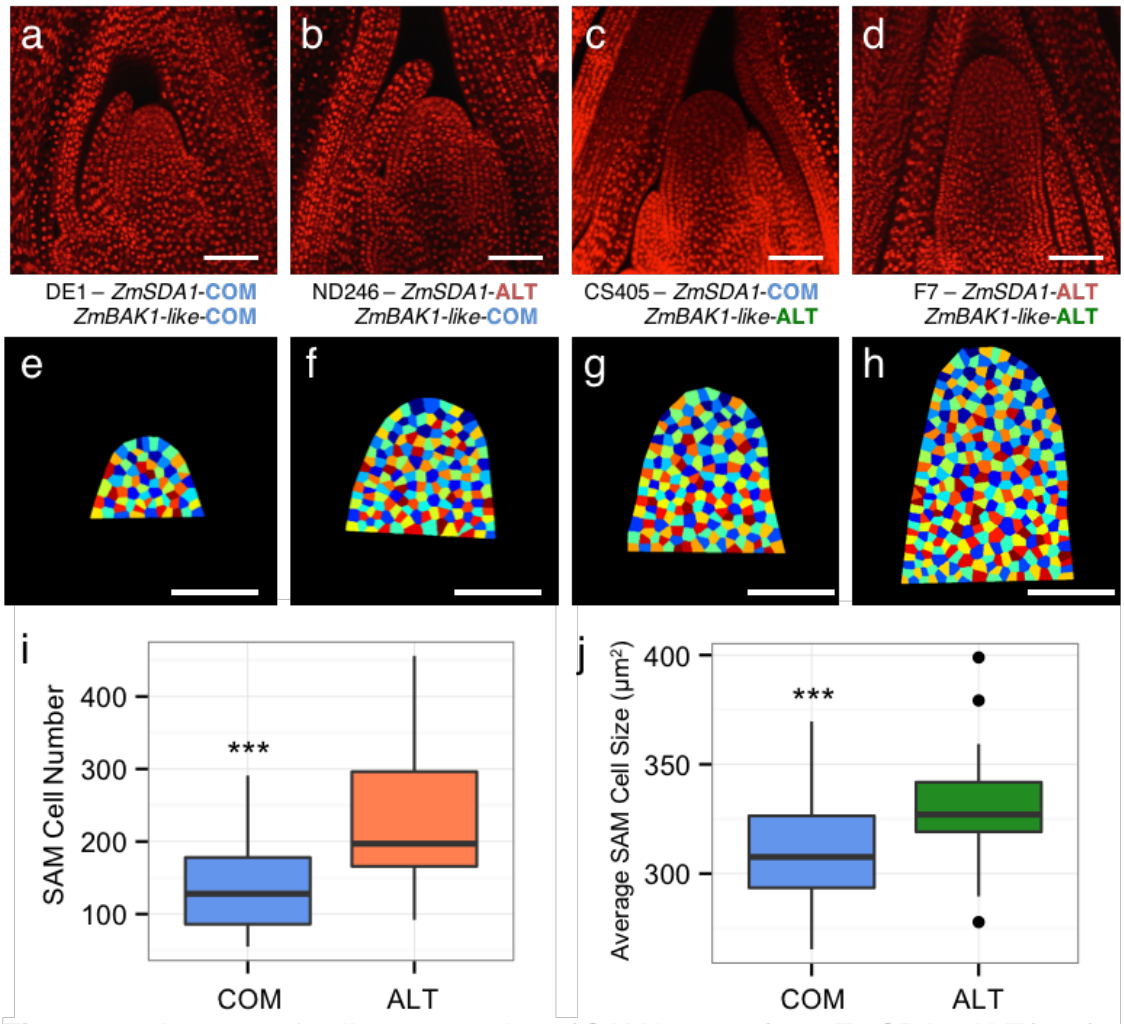

Figure 2.8 Automated cell segmentation of SAM images from *ZmSDA1-ALT* (n=3) and *ZmBAK1-like-ALT* (n=5) lines compared to large (n=3), intermediate (n=3) and small (n=3) common (COM) TAS allele lines. (a-d) SAM images collected by confocal microscopy. (e-h) Cell segmentation of SAM images identifies nuclei and divides space between them into a lattice of cells, used to determine cell number and cell size. (i) *ZmSDA1-ALT* lines (b,f) have increased SAM cell number, compared to *ZmSDA1-COM* lines (a,e), independent from SAM volume effects: two-way ANOVA – Factor, *ZmSDA1*: p= 4.37e-14; Factor, SAM volume: p = 2.98e-15; Interaction, *ZmSDA1* and SAM volume: p = 0.731. (j) *ZmBAK1-like-ALT* lines (c,g) have increased average SAM cell size, compared to *ZmBAK1-like-COM* lines (a,e), while SAM volume does not have a significant effect: two-way ANOVA – Factor, ZmBAK1-like: p= 0.000137; Factor, SAM volume: p = 0.516722; Interaction, ZmBAK1-like and SAM volume: p = 0.141583. Scale bars, 100 µm.

two expected amino acid changes flanking a predicted transmembrane domain, lysine to arginine and arginine to threonine, respectively. In *Oryza sativa*, *BAK1* participates in brassinosteroid-dependent cell expansion (Li *et al.* 2009). We therefore tested if cell size is affected in *ZmBAK1-like-ALT* lines.

As above, we processed SAM images from a subset of inbred lines to test the correlation of *ZmBAK1-like-ALT* and cell size (Figure 2.8) (Kasten 1958; Ruzin 1999; Bray *et al.* 2015). Images from five *ZmBAK1-like-ALT* lines, and nine *ZmBAK1-like-COM* inbred lines representing small, intermediate, and large SAM size categories, were examined in three biological replicates (Figure 2.8a-h). *ZmBAK1-like-ALT* lines exhibit a statistically significant increase in average SAM cell size (ASCS) compared to *ZmBAK1-like-COM* lines (Figure 2.8j). Modeling ASCS as the product of genotype and SAM volume in a two-way ANOVA showed that SAM volume was insignificant in predicting ASCS, however the *ZmBAK1-like-ALT* allele was a significant predictive factor for ASCS.

2.4 Discussion

2.4.1 GWAS of maize microphenotypes

Previous studies of maize seedling SAM shape and size diversity have been limited to a small number of inbred varieties(Vollbrecht *et al.* 2000; Thompson *et al.* 2014, 2015). By approximating SAM shape with parabolic models we were able to survey morphometric diversity in 369 maize inbred lines. GWAS of microscopic phenotypes such as macular degeneration in the human eye and root meristem size in the model plant, *Arabidopsis thaliana* identified a small number of statistically-significant genotype-phenotype

associations(Klein *et al.* 2005; Meijón *et al.* 2014). The high repeatability, or entry mean heritability, of SAM volume combined with our dense genotyping matrix of 1.2 million SNPs in a mixed-model approach allowed us to identify 51 TAS with a high stringency Bonferroni-correction, $\alpha = 0.01$. Previous reports of microphenotype GWAS used molecular developmental strategies to support candidate loci(Klein *et al.* 2005; Meijón *et al.* 2014). Likewise, we used a variety of molecular developmental techniques to characterize a small number of SAM morphology candidate genes.

2.4.2 Genic versus non-genic variation

Using a high-throughput image-processing pipeline to generate SAM morphological data for GWAS of 369 maize inbred lines, we identified candidate genes involved in intraspecific SAM morphological variation. Studies of natural variation in plants and animals have found that biologically significant changes are often linked to polymorphisms in non-genic regulatory regions that may contribute to the evolution of novel expression patterns (Hoekstra and Coyne 2007; Carroll 2008; Hung *et al.* 2012; Yang *et al.* 2013). In contrast with this trend, the majority of our GWAS-identified TASs are found within predicted gene coding regions. However, because 77% of SNPs from our genotyping matrix were generated by RNAseq analysis, we expect a bias towards the identification of genic polymorphisms by GWAS (Figure 2.5b) (Li *et al.* 2012). Although several of our gene candidates have TASs within coding regions, and some ALT alleles encode for predicted amino acid changes that may alter protein function, further validation involving reverse genetics or fine-mapping of advanced introgression lines is required to confirm any potentially functional nucleotide polymorphisms. TASs identified in our analysis may be markers of causative changes in flanking regulatory regions, for which we have not identified polymorphic SNPs (Li *et al.* 2012; Yang *et al.*

2013). Nevertheless our data provides additional evidence that SNPs generated by RNAseq analysis can be used to generate a dense genotyping matrix for GWAS, allowing for high-resolution, single-gene associations (Li *et al.* 2012).

2.4.3 The microscopic seedling SAM is predictive of agronomically-important adult maize traits

Our data agree with previous reports that correlate large SAM size with early flowering (decreased days-to-anthesis) phenotypes (Thompson *et al.* 2015), and our data expand this correlation to a markedly larger panel of inbred maize varieties. Previous research has shown that SAM size increases throughout vegetative development (Abbe *et al.* 1951; Bassiri *et al.* 1992; Thompson *et al.* 2015), whereafter the SAM transforms into the male inflorescence meristem. Morphological evidence showing P1 and P0 leaf primordia arising from the periphery of all the samples examined in this study (Figure 2.1ab, 2.2a-c) confirm that these SAMs are indeed vegetative shoot meristems and have not transformed into male inflorescences (Pautler *et al.* 2013). The significant correlation between large SAM size and early flowering suggests that large SAM lines undergo reproductive phase change earlier than small SAM lines. However, our SAM size GWAS did not detect genes previously implicated in regulation of flowering time (Buckler *et al.* 2009); in contrast, we find that natural variation in SAM size and flowering time are regulated by separate genes.

Significant negative correlations between large SAM volume and plant height at the primary ear are likely to reflect the early flowering time of large SAM lines simply because large SAM lines terminate vegetative growth earlier in the season. We also detected a negative correlation between SAM size and leaf node number, a proxy for

total leaf number, which would likewise be expected for plants that flower earlier in the growing season and therefore produce fewer leaves and stems. Significant correlations were likewise discovered between SAM size and stem diameter, which is an important factor in lodging resistance and damage from stem boring insects (Sétamou *et al.* 1995; Kashiwagi *et al.* 2008). Such a correlation in seedling SAM size and adult stem size is quite remarkable, considering there is an approximately 800-fold increase in size between the average SAM radius and the average stem diameter for the 369 lines in our study. Internode stem diameter and length are inversely correlated in maize and other grasses (Bonnett 1953; Forster *et al.* 2007), such that internode width decreases markedly in upper (younger) nodes as internode length increases. Our data suggest that the relationship between SAM size and stem diameter is driven by SAM height, whereas SAM radius is insignificant in explaining the correlation (Figure 2.3). Conversely, the relationship between SAM size and plant height to the primary ear is driven by SAM radius, and not SAM height (Figure 2.3). We expect that these two relationships represent an allometric trade-off between plant height and stem diameter, separated into discrete internodes, that is established within the SAM. At the same internode, increased SAM height leads to decreased stem diameter and increased SAM radius leads to decreased plant height.

Although statistically significant, these correlations are moderate. Nonetheless, the data suggest that the stem cell population housed in the diminutive, microscopic maize seedling SAM is predictive of several impactful adult agricultural traits, despite substantial intervening development and growth.

2.4.4 Known SAM function genes and SAM variation

This study uncovered 23 candidate genes associated with SAM size and shape. Notably, our GWAS did not detect any SAM master regulatory genes previously identified by mutational analyses, corroborating the results of previous QTL analyses of maize SAM morphology (Thompson *et al.* 2014, 2015). A successful GWAS ultimately links phenotypic variation with allelic polymorphisms. As such, our GWAS would fail to identify SAM master regulators if these genes were fixed in our population, perhaps due to strong purifying selective pressure for SAM function as observed in some species (Bauchet *et al.* 2014). However, our genotyping matrix includes ample polymorphisms within the coding sequences of multiple SAM master regulatory genes (Supplementary Data 6). For example, after filtering and quality control, 118 SNPs were identified in the SAM maintenance gene, *knotted1* (*kn1*) (Kerstetter *et al.* 1997) and 12 SNPs were found in the SAM size regulator, *aberrant phyllotaxy1* (*abph1*) (Jackson and Hake 1999), although SNPs in neither gene were significantly associated with SAM volume. Likewise, although 23 SNPs were identified in the leucine-rich repeat receptor-like, *faciated ear2* (*fea2*) (Taguchi-Shiobara *et al.* 2001), significant associations were not detected between SAM volume and *fea2* SNPs by GWAS. Loss of *fea2*, a putative CLAVATA2 ortholog, dramatically affects the shape and size of the maize inflorescence meristem (IM) (Taguchi-Shiobara *et al.* 2001), and natural variation in the regulation of *fea2* was shown to underlie ear morphological variation between maize inbreds B73 and Mo17 (Bommert *et al.* 2013a).

Notably, our data suggest that either known SAM master regulatory genes do not make major contributions to natural SAM morphometric variation, or else these contributions

are not detectable in our experiment. Instead, our data suggest SAM morphometric variation in natural populations and diverse breeding stocks, is more likely attributed to allelic variation in genes regulating cell expansion and cell division (Figure 2.8) as opposed to genes required for shoot meristem maintenance, stem cell indeterminacy, or organ initiation. With additional investigation into potential developmental molecular mechanisms, the gene candidates identified in this study may provide novel insights into the regulation of SAM function.

2.4.5 Auxin influx in leaf ontogeny and SAM morphology

This study revealed that allelic variants of *ZmLAX2*, a predicted member of the AUX/LAX family of auxin influx proteins (Bainbridge *et al.* 2008), are associated with SAM morphometric variation. Auxin canalization within the SAM is required for phyllotactic patterning and lateral organogenesis (Reinhardt *et al.* 2003; Jönsson *et al.* 2006; Smith *et al.* 2006). Canalization is established by the combined cellular efflux of PIN family proteins and auxin influx of AUX/LAX family proteins(Heisler *et al.* 2005; Jönsson *et al.* 2006; Swarup and Péret 2012). Cellular localization experiments and models of auxin flux dynamics both suggest that the mutually antagonistic functions of AUX/LAX and PIN proteins are localized to provascular traces that mark the developing leaf primordium (P0) (Jönsson *et al.* 2006; Bayer *et al.* 2009; Swarup and Péret 2012).

In situ hybridization reveals that *ZmLAX2* transcript accumulation coincides with previously described patterns of PIN localization in the developing leaf primordium (P0) (Carraro *et al.* 2006), suggesting that AUX/LAX protein family function has been conserved in maize. Interestingly, *ZmLAX2-ALT* inbred lines with large SAM phenotypes exhibit transcript accumulation in the developing leaf primordium (P0) as

well as the yet-to-be-elaborated leaf primordium (P-1). This unique spatiotemporal expression pattern suggests that *ZmLAX2* transcript accumulation occurs prior to previously documented markers of vascular trace formation in *ZmLAX2-ALT* lines (Carraro *et al.* 2006; Johnston *et al.* 2015). Because AUX/LAX influx functions are known antagonists of auxin canalization (Jönsson *et al.* 2006) and NPA-mediated inhibition of auxin transport/canalization dramatically increases SAM size (Scanlon 2003), increased SAM size identified in *ZmLAX2-ALT* inbred lines may result from expanded or developmentally hastened expression of AUX/LAX family genes in the maize SAM.

2.5 Methods

2.5.1 Plant Growth and Tissue Harvest

Plants for all experiments were grown in 10hr-day standard conditions in Percival A100 growth chambers (Percival Scientific, Perry, IA) planted in 98-well trays with all edge positions filled with inbred B73. Soil media was a 1:1 mixture of Turface MVP (PROFILE Products LLC, Buffalo Grove, IL) and LM111 (Lambert Peat Moss, Qc, Canada). All plants were harvested 14 days after planting and quickly trimmed to small SAM-containing tissue cassettes and fixed in FAA (3.7% formalin, 5% acetic acid, 50% ethanol in water) on ice, overnight.

For initial modeling ten kernels from inbred B73 and ten kernels from inbred W22 were planted as above. To map the maize SAM morphospace, kernels from 384 inbred varieties (Supplementary Data 2.1) were planted in randomized positions in four biological replicates. For RNA *in situ* hybridization, ten kernels from select lines were

grown as above in two biological replicates. To estimate SAM cell count and average SAM cell size, four kernels from 14 inbred varieties were planted with three biological replicates: three ZmSDA1 alternative allele (ALT) lines and five ZmBAK1-like1 ALT lines with remaining lines randomly chosen to equally represent the lower quartile (small), middle quartiles (intermediate), and upper quartile (large) of SAM volume with common alleles (COM) from *ZmSDA1* and *ZmBAK1-like1*.

2.5.2 SAM Tissue Preparation and Imaging

DIC of SAMs: For differential internal contrast (DIC) images, FAA-fixed 14-day-old seedling tissue was dehydrated in an ethanol solution series and cleared overnight with methyl salicylate as used in Vollbrecht et al. (2000) and Thompson et al. (2015). Cleared tissue was imaged with Nomarski optics on an Axio Imager.Z10 (Carl Zeiss Microscopy, LLC, Thornwood, NY) with an AxioCam MRc5 camera. We captured near-median longitudinal optical sections using primordia appearance and SAM apex contours as morphological cues. Images are available at MaizeGDB (maizegdb.org).

Fluorecent SAM nuclei: FAA-fixed 14-day-old seedling tissue was treated with Kasten's Feuglen stain as described in Ruzin (1999) and Kasten (1958): fully hydrated tissue was digested with 1N hydrochloric acid overnight then reacted with a solution of safranin-O (safO) incubated with potassium metabisulfite and hydrochloric acid. After a brief destain, samples were dehydrated and cleared with methyl salicylate. Images were collected with a Leica TCS-SP5 (Leica Microsystems Exton, PA, USA) using an argon ion laser (488 nm). SafO stained samples had a broad, low background emission spectrum (580-650nm). Single optical sections were selected at near median

longitudinal planes. Images were processed using Leica LAS-AF software (version 2.6.0) prior to analysis.

2.5.3 Image Processing

Parabolic modeling of SAMs: DIC images from 14-day-old seedlings of inbred B73 (n=5) and inbred W22 (n=5) were processed using ImageJ (Schneider *et al.* 2012). To test the efficacy of a parabolic model of SAM curvature, custom macros were used to collect and export a traced SAM contour. Splines were interpolated from raw contours and used to define points along the SAM surface in the XY plane. SAM surface points were passed to the statistical software R (http://www.r-project.org/) and analyzed by polynomial regression to the standard form of the parabolic equation:

$$Y = ax^2 + bx + c$$

The coefficient a was taken as the shape-defining model factor and area was estimated by the equation: $area = 4/3(height \times radius)$, where height and radius were collected as below. Estimated area was compared to measured area collected by the ImageJ freehand selection tool.

High-throughput analysis of SAM morphology: Custom ImageJ macros and python scripts were used to process 1186 DIC images of 14-day-old seedling SAMs from 369 inbred maize varieties. Using the point selection tool in ImageJ we collected height (*h*) from the SAM apex and parabola radius (*r*) from the P1 notch from each image. From these primary measures we calculated the following: height/radius = $\left(\frac{h}{r}\right)$, diameter = $(2\,r)$, area = $\left(\frac{4}{3}\right)(h \times r)$, volume = $\left(\frac{\pi}{2}\right)(h \times r^2)$, parabolic standard form coefficient *a* =

$\left(\frac{h}{r^2}\right)$, SAM surface area = $\left(\frac{\pi\, r}{6\, h^2}\left[(r^2 + 4\, h^2)^{3/2} - r^3\right]\right)$, and arc length = $\sqrt{(r^2 + 4h^2)} + \left(\frac{r^2}{2h}\right)\sinh^{-1}(\frac{2h}{r})$. To account for germination differences in some inbred lines, best linear unbiased predictors (BLUPs) were calculated for all measures using SAS (http://www.sas.com/) and the nlme R package. BLUPs were used for GWAS, and phenotypes were reported in BLUP + intercept form.

Alignment of in situ *hybridization serial sections:* DIC images of RNA *in situ* hybridization slides were imported into ImageJ, placed in sequential order by morphological cues, and aligned using the TrakEM2 package (http://fiji.sc/TrakEM2).

Cell count and size estimation: Images of fluorescent SAM nuclei were preprocessed in ImageJ using the freehand selection tool to remove cells outside the SAM. SAM images were analyzed with a standard pipeline in CellProfiler (Bray *et al.* 2015).

2.5.4 SNP Matrix Generation

RNAseq Analysis: RNA was extracted from SAM-enriched apices of 14 day-old seedlings and sequenced using Illumina HiSeq2000 instruments. The nucleotides of each raw read were scanned for low quality bases (Li *et al.* 2013). Bases with PHRED quality values <15 (out of 40)64, i.e., error rates of ≤3%, were removed. Each read was examined in two phases. In the first phase reads were scanned starting at each end and nucleotides with quality values lower than the threshold were removed. The remaining nucleotides were then scanned using overlapping windows of 10 bp and sequences beyond the last window with average quality value less than the specified threshold were truncated. Trimmed reads were aligned to the Maize B73 RefGen_v2 genome using GSNAP (Barbazuk *et al.* 2007; Li *et al.* 2012). To obtain confidently mapped

reads, reads were retained if they mapped uniquely in the genome, allowing ≤2 mismatches every 36 bp and fewer than 5 bases for every 75 bp in read length as unaligned “tails”. The coordinates of confident and single (unique) alignments that passed our filtering criteria were used for SNP discovery. Polymorphisms at each potential SNP site were examined and putative homozygous SNPs were identified using the following criteria after ignoring the first and last 3 aligned bases of each read. Before being used to call a SNP, a polymorphic base was required to have a PHRED base quality value of at least 20 (<1% error rate), and at least five unique reads must support the SNP call. The transcriptomic data for this project are available at the National Center for Biotechnology Information Short Reads Archive (NCBI SRA), accession number SRP055871.

Genomic SNP calling: 2,815 US Inbreds, including our 369 inbreds, have been genotyped at ~700,000 SNP sites by sequencing (Romay *et al.* 2013). The original dataset was downloaded from Panzea (panzea.org). For accessions that were sequenced multiple times, we scored the consensus allele for each site. Alleles with conflicting records were scored as missing.

SNP quality control: After merging RNASeq and genomic SNPs, polymorphisms with minor allele frequency less than 1% or missing in over 60% of inbreds were excluded from further GWAS analysis.

2.5.5 Mixed-model GWAS

The analysis was performed on SAM volume BLUP data with a compressed mixed linear model[67] implemented in the GAPIT R package (Version 3.55) by selecting the best model from PCA covariates and Kinship matrix (Lipka *et al.* 2012).

2.5.6 In situ RNA Hybridization

RNA *in situ* hybridization analyses were carried out as described in Jackson (1991) with modifications as in Johnston et al. (2015): FAA-fixed tissue was dehydrated and transferred to paraffin wax in preparation for sectioning. Longitudinal sections through the SAM were adhered to slides overnight, stripped of paraffin, rehydrated, and treated by with Proteinase K in preparation for incubation with a DIG-labeled RNA probe. After overnight incubation at 50°C with the *ZmLAX2*-specific probe, slides were rinsed several times in SSC, treated with RNase H to remove excess probe, and incubated with an anti-DIG alkaline phosphatase (AP) conjugated Fab-fragment serum at 4°C overnight (Roche Diagnostics, IN, USA). Transcript accumulation was visualized by incubating overnight at room temperature in a BCIP/NPT AP substrate (Roche Diagnostics, IN, USA).

SAM Tissue from the following genotypes was examined: Small SAM *ZmLAX2-COM* genotypes-- CML322, B104, B57, NC314; Large SAM *ZmLAX2-COM* genotypes-- F42, CS405, NC324, LP5; Large SAM *ZmLAX2-ALT* genotypes-- ND246, Co255. We constructed an antisense probe to GRMZM2G129413 (*ZmLAX2*) using 1kb of sequence from the last exon and 3'UTR of inbred B73 cDNA, using primers oSL33 (5'TCTATATCATCCCGGCGCTC) and oSL38 (5'TAACTTGCACCTTTGCTGCG).

2.5.7 Gene model annotation

Candidate genes model entries were queried on MaizeGDB (www.maizegdb.org) for classical names and best sequence homologs in *Arabidopsis thaliana* and *Oryza sativa***.** Genes without classical names were queried against a maximum likelihood protein

sequence tree (ensembl.gramene.org). Protein domains were determined by SMART (http://smart.embl-heidelberg.de/).

2.5.8 Field measurements

Stem diameter and node count measurements were collected in Summer 2014 at the Musgrave Research Farm (Aurora, NY). Measurements were gathered from three post-anthesis individuals from ten-kernel families of the 369 inbred varieties used above. The highest ear on the maize plant was designated the “primary ear.” The primary ear is clonally related to the node, internode, and leaf on the opposite side of the stem, above its own point of insertion at maturity (Poethig and Szymkowiak 1995). Stem diameter was collected from the widest diameter measured at the midpoint between nodes for: the clonally-related internode above the primary ear, the internode at the point of insertion of the primary ear, and internode below the point of insertion of the primary ear using a Fowler-Sylvac Digital Caliper Kit (Serialio.com, Cedar Park, TX). Above ground nodes were scored and counted as a proxy for total leaf count.

2.5.9 Statistical analysis and plotting

Descriptive statistical analysis, t-tests, one-way ANOVA, and two-way ANOVA were carried out using core R packages. Correlation analyses were carried out using the PerformanceAnalytics R package. All correlations report Pearson’s product-moment, r and were evaluated for statistical significance with the Fisher transformation. Additional adult phenotype data for correlation analyses were collected from published datasets (Peiffer *et al.* 2014).

2.6 Works Cited

Abbe E. C., Phinney B. O., Baer D. F., 1951 The Growth of the Shoot Apex in Maize: Internal Features. Am. J. Bot. **38**: 744.

Bainbridge K., Guyomarc'h S., Bayer E., Swarup R., Bennett M., Mandel T., Kuhlemeier C., 2008 Auxin influx carriers stabilize phyllotactic patterning. Genes Dev. **22**: 810–23.

Barbazuk W. B., Emrich S. J., Chen H. D., Li L., Schnable P. S., 2007 SNP discovery via 454 transcriptome sequencing. Plant J. **51**: 910–918.

Bassiri a, Irish E., Poethig R., 1992 Heterochronic Effects of Teopod 2 on the Growth and Photosensitivity of the Maize Shoot. Plant Cell **4**: 497–504.

Bauchet G., Munos S., Sauvage C., Bonnet J., Grivet L., Causse M., 2014 Genes involved in floral meristem in tomato exhibit drastically reduced genetic diversity and signature of selection. BMC Plant Biol. **14**: 279.

Bayer E. M., Smith R. S., Mandel T., Nakayama N., Sauer M., Prusinkiewicz P., Kuhlemeier C., 2009 Integration of transport-based models for phyllotaxis and midvein formation. Genes Dev. **23**: 373–84.

Bommert P., Nagasawa N. S., Jackson D., 2013 Quantitative variation in maize kernel row number is controlled by the FASCIATED EAR2 locus. Nat. Genet. **45**: 334–7.

Bonnett O. T., 1953 *Developmental morphology of the vegetative and floral shoots of maize*. University of Illinois Agricultural Experiment Station, Urbana, Ill.

Bray M.-A., Vokes M. S., Carpenter A. E., 2015 Using CellProfiler for Automatic Identification and Measurement of Biological Objects in Images. Curr. Protoc. Mol. Biol. **109**: 14.17.1–14.17.13.

Buckler E. S., Holland J. B., Bradbury P. J., Acharya C. B., Brown P. J., Browne C., Ersoz E., Flint-Garcia S. A., Garcia A., Glaubitz J. C., Goodman M. M., Harjes C., Guill K., Kroon D. E., Larsson S., Lepak N. K., Li H., Mitchell S. E., Pressoir G., Peiffer J. a, Rosas M. O., Rocheford T. R., Romay M. C., Romero S., Salvo S., Sanchez Villeda H., Silva H. S. da, Sun Q., Tian F., Upadyayula N., Ware D., Yates

H., Yu J., Zhang Z., Kresovich S., McMullen M. D., 2009 The genetic architecture of maize flowering time. Science **325**: 714–8.

Buscemi G., Saracino F., Masnada D., Carbone M., 2000 The Saccharomyces cerevisiae SDA1 gene is required for actin cytoskeleton organization and cell cycle progression. J. Cell Sci. **113**: 1199–1211.

Carraro N., Peaucelle A., Laufs P., Traas J., 2006 Cell differentiation and organ initiation at the shoot apical meristem. Plant Mol. Biol. **60**: 811–26.

Carroll S. B., 2008 Evo-devo and an expanding evolutionary synthesis: a genetic theory of morphological evolution. Cell **134**: 25–36.

Flint-Garcia S. A., Thuillet A.-C., Yu J., Pressoir G., Romero S. M., Mitchell S. E., Doebley J., Kresovich S., Goodman M. M., Buckler E. S., 2005 Maize association population: a high-resolution platform for quantitative trait locus dissection. Plant J. **44**: 1054–64.

Forster B. P., Franckowiak J. D., Lundqvist U., Lyon J., Pitkethly I., Thomas W. T. B., 2007 The barley phytomer. Ann. Bot. **100**: 725–733.

Francis D., Halford N. G., 2006 Nutrient sensing in plant meristems. Plant Mol. Biol. **60**: 981–93.

Fujita H., Kawaguchi M., 2011 Strategy for shoot meristem proliferation in plants. Plant Signal. Behav.: 1851–1854.

Green P., 1999 Expression of pattern in plants: combining molecular and calculus-based biophysical paradigms. Am. J. Bot. **86**: 1059–1076.

Ha C. M., Jun J. H., Fletcher J. C., 2010 Shoot apical meristem form and function. Curr. Top. Dev. Biol. **91**: 103–40.

Hamant O., 2013 Widespread mechanosensing controls the structure behind the architecture in plants. Curr. Opin. Plant Biol. **16**: 654–60.

Heisler M. G., Ohno C., Das P., Sieber P., Reddy G. V, Long J. a, Meyerowitz E. M., 2005 Patterns of auxin transport and gene expression during primordium

development revealed by live imaging of the Arabidopsis inflorescence meristem. Curr. Biol. **15**: 1899–911.

Hochholdinger F., Wulff D., Reuter K., Park W. J., Feix G., 2000 Tissue-specific expression of AUX1 in maize roots. J. Plant Physiol. **157**: 315–319.

Hoekstra H. E., Coyne J. A., 2007 The locus of evolution: evo devo and the genetics of adaptation. Evolution **61**: 995–1016.

Hung H.-Y., Shannon L. M., Tian F., Bradbury P. J., Chen C., Flint-Garcia S. A., McMullen M. D., Ware D., Buckler E. S., Doebley J. F., Holland J. B., 2012 *ZmCCT and the genetic basis of day-length adaptation underlying the postdomestication spread of maize.*

Jackson D. P., 1991 In situ hybridization in plants. In: *Molecular Plant Pathology: A Practical Approach*,, pp. 163–174.

Jackson D. P., Hake S., 1999 Control of phyllotaxy in maize by the abphyl1 gene. Development **126**: 315–23.

Johnston R., Leiboff S., Scanlon M. J., 2015 Ontogeny of the sheathing leaf base in maize (Zea mays). New Phytol. **205**: 306–15.

Jönsson H., Heisler M. G., Shapiro B. E., Meyerowitz E. M., Mjolsness E., 2006 An auxin-driven polarized transport model for phyllotaxis. Proc. Natl. Acad. Sci. U. S. A. **103**: 1633–8.

Kashiwagi T., Togawa E., Hirotsu N., Ishimaru K., 2008 Improvement of lodging resistance with QTLs for stem diameter in rice (Oryza sativa L.). Theor. Appl. Genet. **117**: 749–57.

Kasten F., 1958 Aditional Schiff-type reagents for use in cytochemistry. Stain Technol. **33**: 39 – 45.

Kerstetter R. a, Laudencia-Chingcuanco D., Smith L. G., Hake S., 1997 Loss-of-function mutations in the maize homeobox gene, knotted1, are defective in shoot meristem maintenance. Development **124**: 3045–54.

Klein R. J., Zeiss C., Chew E. Y., Tsai J.-Y., Sackler R. S., Haynes C., Henning A. K., SanGiovanni J. P., Mane S. M., Mayne S. T., Bracken M. B., Ferris F. L., Ott J., Barnstable C., Hoh J., 2005 Complement factor H polymorphism in age-related macular degeneration. Science **308**: 385–9.

Lawrence C. J., Harper L. C., Schaeffer M. L., Sen T. Z., Seigfried T. E., Campbell D. A., 2008 MaizeGDB: The maize model organism database for basic, translational, and applied research. Int. J. Plant Genomics **2008**: 496957.

Li D., Wang L., Wang M., Xu Y. Y., Luo W., Liu Y. J., Xu Z. H., Li J., Chong K., 2009 Engineering OsBAK1 gene as a molecular tool to improve rice architecture for high yield. Plant Biotechnol. J. **7**: 791–806.

Li X., Zhu C., Yeh C.-T., Wu W., Takacs E. M., Petsch K. A., Tian F., Bai G., Buckler E. S., Muehlbauer G. J., Timmermans M. C. P., Scanlon M. J., Schnable P. S., Yu J., 2012 Genic and nongenic contributions to natural variation of quantitative traits in maize. Genome Res. **22**: 2436–44.

Li L., Petsch K., Shimizu R., Liu S., Xu W. W., Ying K., Yu J., Scanlon M. J., Schnable P. S., Timmermans M. C. P., Springer N. M., Muehlbauer G. J., 2013 Mendelian and Non-Mendelian Regulation of Gene Expression in Maize. PLoS Genet. **9**.

Lipka A. E., Tian F., Wang Q., Peiffer J., Li M., Bradbury P. J., Gore M. A., Buckler E. S., Zhang Z., 2012 GAPIT: genome association and prediction integrated tool. Bioinformatics **28**: 2397–9.

Liu K., Goodman M. M., Muse S., Smith J. S., Buckler E., Doebley J., 2003 Genetic Structure and Diversity Among Maize Inbred Lines as Inferred From DNA Microsatellites. Genetics **165**: 2117–2128.

Meijón M., Satbhai S. B., Tsuchimatsu T., Busch W., 2014 Genome-wide association study using cellular traits identifies a new regulator of root development in Arabidopsis. Nat. Genet. **46**: 77–81.

Miller T. A., Muslin E. H., Dorweiler J. E., 2008 A maize CONSTANS-like gene, conz1, exhibits distinct diurnal expression patterns in varied photoperiods. Planta **227**: 1377–88.

Monaco M. K., Stein J., Naithani S., Wei S., Dharmawardhana P., Kumari S., Amarasinghe V., Youens-Clark K., Thomason J., Preece J., Pasternak S., Olson A.,

Jiao Y., Lu Z., Bolser D., Kerhornou A., Staines D., Walts B., Wu G., D'Eustachio P., Haw R., Croft D., Kersey P. J., Stein L., Jaiswal P., Ware D., 2014 Gramene 2013: comparative plant genomics resources. Nucleic Acids Res. **42**: D1193–9.

Niklas K. J., Mauseth J. D., 1980 Simulations of Cell Dimensions in Shoot Apical Meristems: Implications Concerning Zonate Apices. Am. J. Bot. **67**: 715.

Pautler M., Tanaka W., Hirano H.-Y., Jackson D., 2013 Grass meristems I: shoot apical meristem maintenance, axillary meristem determinacy and the floral transition. Plant Cell Physiol. **54**: 302–12.

Peiffer J. A., Romay M. C., Gore M. A., Flint-Garcia S. A., Zhang Z., Millard M. J., Gardner C. A. C., McMullen M. D., Holland J. B., Bradbury P. J., Buckler E. S., 2014 The genetic architecture of maize height. Genetics **196**: 1337–56.

Poethig R. S., Szymkowiak E. J., 1995 Clonal analysis of leaf development in maize. Maydica. **40**: 67.

Reinhardt D., Pesce E.-R., Stieger P., Mandel T., Baltensperger K., Bennett M., Traas J., Friml J., Kuhlemeier C., 2003 Regulation of phyllotaxis by polar auxin transport. Nature **426**: 255–60.

Romay M. C., Millard M. J., Glaubitz J. C., Peiffer J. a, Swarts K. L., Casstevens T. M., Elshire R. J., Acharya C. B., Mitchell S. E., Flint-Garcia S. A., McMullen M. D., Holland J. B., Buckler E. S., Gardner C. A. C., 2013 Comprehensive genotyping of the USA national maize inbred seed bank. Genome Biol. **14**: R55.

Ruzin S., 1999 *Plant microtechnique and microscopy*. Oxford University Press, New York.

Scanlon M. J., 2003 The polar auxin transport inhibitor N-1-naphthylphthalamic acid disrupts leaf initiation, KNOX protein regulation, and formation of leaf margins in maize. Plant Physiol. **133**: 597–605.

Schnable P. S., Ware D., Fulton R. S., Stein J. C., Wei F., Pasternak S., Liang C., Zhang J., Fulton L., Graves T. A., Minx P., Reily A. D., Courtney L., Kruchowski S. S., Tomlinson C., Strong C., Delehaunty K., Fronick C., Courtney B., Rock S. M., Belter E., Du F., Kim K., Abbott R. M., Cotton M., Levy A., Marchetto P., Ochoa K., Jackson S. M., Gillam B., Chen W., Yan L., Higginbotham J., Cardenas M., Waligorski J., Applebaum E., Phelps L., Falcone J., Kanchi K., Thane T., Scimone

A., Thane N., Henke J., Wang T., Ruppert J., Shah N., Rotter K., Hodges J., Ingenthron E., Cordes M., Kohlberg S., Sgro J., Delgado B., Mead K., Chinwalla A., Leonard S., Crouse K., Collura K., Kudrna D., Currie J., He R., Angelova A., Rajasekar S., Mueller T., Lomeli R., Scara G., Ko A., Delaney K., Wissotski M., Lopez G., Campos D., Braidotti M., Ashley E., Golser W., Kim H., Lee S., Lin J., Dujmic Z., Kim W., Talag J., Zuccolo A., Fan C., Sebastian A., Kramer M., Spiegel L., Nascimento L., Zutavern T., Miller B., Ambroise C., Muller S., Spooner W., Narechania A., Ren L., Wei S., Kumari S., Faga B., Levy M. J., McMahan L., Buren P. Van, Vaughn M. W., Ying K., Yeh C.-T., Emrich S. J., Jia Y., Kalyanaraman A., Hsia A.-P., Barbazuk W. B., Baucom R. S., Brutnell T. P., Carpita N. C., Chaparro C., Chia J.-M., Deragon J.-M., Estill J. C., Fu Y., Jeddeloh J. A., Han Y., Lee H., Li P., Lisch D. R., Liu S., Liu Z., Nagel D. H., McCann M. C., SanMiguel P., Myers A. M., Nettleton D., Nguyen J., Penning B. W., Ponnala L., Schneider K. L., Schwartz D. C., Sharma A., Soderlund C., Springer N. M., Sun Q., Wang H., Waterman M., Westerman R., Wolfgruber T. K., Yang L., Yu Y., Zhang L., Zhou S., Zhu Q., Bennetzen J. L., Dawe R. K., Jiang J., Jiang N., Presting G. G., Wessler S. R., Aluru S., Martienssen R. A., Clifton S. W., McCombie W. R., Wing R. A., Wilson R. K., 2009 The B73 maize genome: complexity, diversity, and dynamics. Science **326**: 1112–1115.

Schneider C. A., Rasband W. S., Eliceiri K. W., 2012 NIH Image to ImageJ: 25 years of image analysis. Nat. Methods **9**: 671–675.

Sétamou M., Schulthess F., Bosque-Pérez N. A., Thomas-Odjo A., 1995 The effect of stem and cob borers on maize subjected to different nitrogen treatments. Entomol. Exp. Appl. **77**: 205–210.

Shani E., Yanai O., Ori N., 2006 The role of hormones in shoot apical meristem function. Curr. Opin. Plant Biol. **9**: 484–9.

Sharman B. C., 1942 Developmental Anatomy of the Shoot of Zea mays L. Ann. Bot. **6**: 245–282.

Smith R. S., Guyomarc'h S., Mandel T., Reinhardt D., Kuhlemeier C., Prusinkiewicz P., 2006 A plausible model of phyllotaxis. Proc. Natl. Acad. Sci. U. S. A. **103**: 1301–6.

Steeves T. A., Sussex I. M., 1972 *Patterns in plant development*. Prentice-Hall, Englewood Cliffs, N.J.

Sussex I. M., Kerk N. M., 2001 The evolution of plant architecture. Curr. Opin. Plant Biol. **4**: 33–7.

Swarup R., Péret B., 2012 AUX/LAX family of auxin influx carriers-an overview. Front. Plant Sci. **3**: 225.

Taguchi-Shiobara F., Yuan Z., Hake S., Jackson D. P., 2001 The fasciated ear2 gene encodes a leucine-rich repeat receptor-like protein that regulates shoot meristem proliferation in maize. Genes Dev. **15**: 2755–66.

Thompson A. M., Crants J., Schnable P. S., Yu J., Timmermans M. C. P., Springer N. M., Scanlon M. J., Muehlbauer G. J., 2014 Genetic control of maize shoot apical meristem architecture. G3 (Bethesda). **4**: 1327–37.

Thompson A. M., Yu J., Timmermans M. C. P., Schnable P., Crants J. C., Scanlon M. J., Muehlbauer G. J., 2015 Diversity of Maize Shoot Apical Meristem Architecture and Its Relationship to Plant Morphology. G3!; Genes|Genomes|Genetics: 1–14.

Tian F., Bradbury P. J., Brown P. J., Hung H., Sun Q., Flint-Garcia S. A., Rocheford T. R., McMullen M. D., Holland J. B., Buckler E. S., 2011 Genome-wide association study of leaf architecture in the maize nested association mapping population. Nat. Genet. **43**: 159–62.

Vollbrecht E., Reiser L., Hake S., 2000 Shoot meristem size is dependent on inbred background and presence of the maize homeobox gene, knotted1. Development **127**: 3161–72.

Wallace J. G., Larsson S. J., Buckler E. S., 2014 Entering the second century of maize quantitative genetics. Heredity (Edinb). **112**: 30–8.

Yang Q., Li Z., Li W., Ku L., Wang C., Ye J., Li K., Yang N., Li Y., Zhong T., Li J., Chen Y., Yan J., Yang X., Xu M., 2013 CACTA-like transposable element in ZmCCT attenuated photoperiod sensitivity and accelerated the postdomestication spread of maize. Proc. Natl. Acad. Sci. U. S. A. **110**: 16969–74.

Yang F., Bui H. T., Pautler M., Llaca V., Johnston R., Lee B.-H., Kolbe A., Sakai H., Jackson D., 2015 A Maize Glutaredoxin Gene, Abphyl2, Regulates Shoot Meristem Size and Phyllotaxy. Plant Cell.

Yu J., Pressoir G., Briggs W. H., Vroh Bi I., Yamasaki M., Doebley J. F., McMullen M. D., Gaut B. S., Nielsen D. M., Holland J. B., Kresovich S., Buckler E. S., 2006 A unified mixed-model method for association mapping that accounts for multiple levels of relatedness. Nat. Genet. **38**: 203–8.

3 Modeling the morphometric evolution of the maize shoot apical meristem

3.1 Abstract

The maize (Zea mays subsp. mays L.) shoot apical meristem (SAM) is a self-replenishing pool of stem cells that produces the above-ground plant. Improvements in image acquisition and processing techniques have allowed high-throughput, quantitative genetic analyses of SAM morphology. As with other large-scale phenotyping efforts, meaningful descriptions of genetic architecture depend on the collection of relevant measures. In this study, we tested two quantitative image processing methods to describe SAM morphology within the genus Zea, represented by 33 wild relatives of maize and 841 lines from a domesticated maize by wild teosinte progenitor (MxT) backcross population, along with previously-reported data from several hundred diverse maize inbred lines. Approximating the MxT SAM as a paraboloid derived eight parabolic estimators of SAM morphology that identified highly-overlapping QTL on eight chromosomes, which implicated previously-identified SAM morphology candidate genes along with new QTL for SAM morphological variation. Using a Fourier-transform related method of comprehensive shape analysis, we detected cryptic SAM shape variation that identified QTL on six chromosomes. We found that Fourier transform shape descriptors and parabolic estimation measures are highly correlated and identified similar QTL. Analysis of shoot apex contours from 73 anciently-diverged plant taxa further suggested that parabolic shape may be a universal feature of plant SAMs, regardless of evolutionary clade. Future high-throughput examinations of SAM morphology may

benefit from the ease of acquisition and phenotypic fidelity of modeling the SAM as a paraboloid.

3.2 Introduction

The maize (*Zea mays* subsp. *mays* L.) shoot apical meristem (SAM) comprises a dome of pluripotent cells that generates the entire above-ground plant through regulated maintenance of stem cells and recruitment of initial cells for organogenesis (Steeves and Sussex 1972). Mutational studies have shown that the maize shoot meristem morphology is genetically regulated (Jackson and Hake 1999; Taguchi-Shiobara *et al.* 2001; Jia *et al.* 2009; Bommert *et al.* 2013b; Pautler *et al.* 2015; Yang *et al.* 2015). Although natural variation in shoot meristem morphology is associated with relatively few loci, natural variants of master regulatory genes do not appear to contribute to standing variation in SAM shape and size in domesticated maize (Thompson *et al.* 2014, 2015; Leiboff *et al.* 2015).

Recent investigations of maize meristem morphology as a quantitative trait incorporated small numbers of descriptive measurements approximating SAM shape and size for genome-wide association studies (GWAS) and quantitative trait locus (QTL) mapping (Thompson *et al.* 2014, 2015; Leiboff *et al.* 2015). Quantitative morphological analyses are highly biased by the measurement methodologies, the traits selected for analyses, and any corrections for correlations between measurements (Langlade *et al.* 2005). Our previous study of maize inbred varieties exploited similarities between observed SAM contours and parabolic functions to estimate several shape parameters describing meristem morphology (Leiboff *et al.* 2015), although other models for SAM morphometrics have not been tested in quantitative genetic analyses.

Progress toward the description of complex shapes utilizing Fourier transform methods has enabled unbiased interrogations of biological shape (Dommergues *et al.* 2007; Klingenberg 2010). By processing carefully-placed landmarks or object outlines, Fourier transform and related methods use multiple sinusoid harmonics to reproduce highly complex shapes (Claude 2008). High-dimensional matrices of Fourier model parameters can then be separated by principle component analysis to identify subtle, often cryptic, variations in complex plant shapes (Chitwood *et al.* 2014). Previous studies characterizing leaf morphology in *Antirrhinum* spp. and *Solanum* spp. have utilized Fourier shape descriptors as quantitative traits in QTL analyses of evolutionary novelty (Langlade *et al.* 2005; Chitwood *et al.* 2013, 2014).

Collectively known as teosintes, the wild members of the genus *Zea* provide a rich, highly-diverse genetic system for maize genomics (Doebley 2004; Hufford *et al.* 2012; Hake and Ross-Ibarra 2015). Crosses between *Zea mays* subsp. *mays* and its progenitor, *Zea mays* subsp. *parviglumis* have been used to understand the genetic basis for striking changes in plant morphology associated with the domestication of maize (Beadle 1980; Doebley 2004; Hung *et al.* 2012; Shannon 2013; Huang *et al.* 2016). Although general morphology and ontogeny of inflorescence meristem development have been reported in the genus *Zea* (Sundberg and Orr 1986, 1990, Orr and Sundberg 1994, 2004), little is known about variation in vegetative SAM morphology outside of domesticated maize. To date no comparative study has described the morphospace, or collection of shapes for vegetative meristems within the genus *Zea.* Indeed, no putative genetic factors underlying differences in maize and teosinte SAMs have been proposed.

This project utilizes a maize x teosinte (MxT) backcross population to examine the genetic architecture of SAM shape and size (Hung *et al.* 2012; Shannon 2013; Huang *et al.* 2016). We show that complex shape descriptors generated by Fourier methods detect previously undescribed, but genetically-attributable minor variations in meristem shape, although the majority of the genetic loci contributing to SAM shape that are identified by Fourier analyses overlap tightly with loci identified by modeling the SAM as a paraboloid. Testing this expectation with a broad sampling of plant taxa suggests that parabolic shape may be a universal feature of plant shoot apical meristems.

3.3 Materials and Methods

3.3.1 Plant growth

Germplasm for all experiments was grown in 10hr-day standard conditions in Percival A100 growth chambers (Percival Scientific, Perry, IA) with randomized planting positions within 98-well trays. All edge positions were filled with maize inbred B73. Soil media was a 1:1 mixture of Turface MVP (PROFILE Products LLC, Buffalo Grove, IL) and LM111 (Lambert Peat Moss, Qc, Canada). Wild teosintes (Supplementary Data 3.1) were grown in 4 repeated experiments. Maize x teosinte backcross lines (Supplementary Data 3.1) were grown in 2 repeated experiments. Plants were harvested 14 days after planting and quickly trimmed to small SAM-containing tissue cassettes and fixed in FAA (3.7% formalin, 5% acetic acid, 50% ethanol in water) on ice, overnight.

3.3.2 Histology and Image Acquisition

After overnight fixation in FAA, plant tissue was dehydrated through an ethanol dilution series, transferred to a 1:1 mix of ethanol and methyl salicylate, then transferred to methyl salicylate for clearing overnight. Fully cleared tissue was imaged by DIC with Nomarski optics on an Axio Imager.Z10 (Carl Zeiss Microscopy, LLC, Thornwood, NY) with an AxioCam MRc5 camera. We captured near-median longitudinal optical sections using SAM apex contours and primordia appearance as morphological cues. All MxT images were oriented so that the next primordium to initiate (P0) appeared on the left-hand side of the image.

Several of shoot apex images of anciently diverged plant taxa were collected from high quality publications (Supplementary Data 3.1). Figures from printed texts were scanned at 300 dpi, 16-bit greyscale using an Epson Perfection 3490 photo scanner (Epson America, Long Beach, CA).

A small number of shoot apex images from demonstrative plant taxa were collected from fresh tissues (Supplementary Data 3.1). Shoot apical regions were harvested by hand from growing tissue, fixed overnight in FAA, and stained with a modified Feulgen method (as described in 10). After a brief destain, samples were dehydrated, cleared with methyl salicylate and imaged with a Leica TCS-SP5 confocal laser scanning microscope (Leica Microsystems Exton, PA, USA) using an argon ion laser (488 nm).

3.3.3 Image processing: Parabolic estimation and Fourier transform

Near-median DIC images were processed by custom ImageJ macros to extract meristem contours and measures of SAM height and SAM radius (as reported in Leiboff

et *al.* 2015). Using a custom Python script SAM height and radius were used to calculate a table of 8 parabolic estimators: height, radius, height to radius ratio (H/R), volume (Vol.), surface area (Surf. Area), arc length (Arc Len.), parabolic coefficient (Para. Coeff.), and cross-sectional area (Area) (as reported in Leiboff et *al.* 2015).

SAM contours were digitized with an Intuos Draw Tablet (Wacom Technology Corporation, Portland, OR) and used for both linear model fitting with the lm() function and Fourier transform with the Momocs package for R. Traced SAM coordinates were imported as open contours (data type Opn), Procrustes-aligned, and Fourier transformed by the discrete cosine transform in the Momocs package for R.

3.3.4 QTL mapping

Using publically-available genotype information for the MxT population from panzea.org, genotype and phenotype information were processed via the R/qtl package for R. MxT genotypes were coded as BC2S3 and mapped using the Kosambi algorithm. Single QTL were detected using the scanone() function. We used a 95% confidence threshold generated from 10,000 permutations to determine significant QTL. Bayesian 95% confidence QTL intervals were called using the bayesint() function to estimate QTL location.

3.3.5 Statistical analysis and plotting

Descriptive statistical analysis, correlation analysis, Wilcoxon one-sided rank sum test, and two-way ANOVA were carried out using core R packages. Raw data were summarized according to replicate by BLUP + coefficient using the nmle package in R (Leiboff *et al.* 2015). All correlations report Pearson's product-moment, r and were

evaluated for statistical significance with the Fisher transformation. Maize inbred variety SAM shape and size data were collected from published datasets (Leiboff *et al.* 2015). Plots were produced using ggplot2 and R/qtl packages in R.

3.4 Results

3.4.1 Diversity of shoot meristems in the genus Zea

We utilized microscopic imaging of 14-day-old seedling vegetative SAMs (described in Methods) to construct a morphospace of SAM height and radius for the genus *Zea,* which included 33 wild teosinte isolates from 3 different species (*Z. diploperennis*, *Z. luxiurians*, and *Z. perennis*), 3 subspecies (*Z. mays* subsp. *huehuetenangensis*, *Z. mays* subsp. *mexicana*, and *Z. mays* subsp. *parviglumis*), 841 lines from a *Zea mays* subsp. *mays* W22 by *Zea mays* subsp. *parviglumis* backcross (Bc2S3) population (hereafter designated MxT) (Hung *et al.* 2012; Shannon 2013; Huang *et al.* 2016), and our previously reported data on 369 diverse maize inbred lines (Figure 3.1; Supplementary Data 3.2) (Leiboff *et al.* 2015). Although there is a small zone of overlap between teosinte and maize inbred SAM shapes, wild teosinte meristems are significantly narrower (est. 23μm between medians, Wilcoxon one-sided rank sum test, p-value < 2.2e-16) and shorter (est. 28μm between medians, Wilcoxon one-sided rank sum test, p-value = 1.257e-10) than meristems from domesticated maize inbred lines (Figure 3.1A). Measurements of MxT shoot meristems cluster around the recurrent maize parent, inbred W22 (Figure 3.1B), possibly reflecting the two generations of backcrosses to the maize parent that were incurred prior to analyses of SAM morphometric phenotypes (Hung *et al.* 2012). We detected quantitative variation in

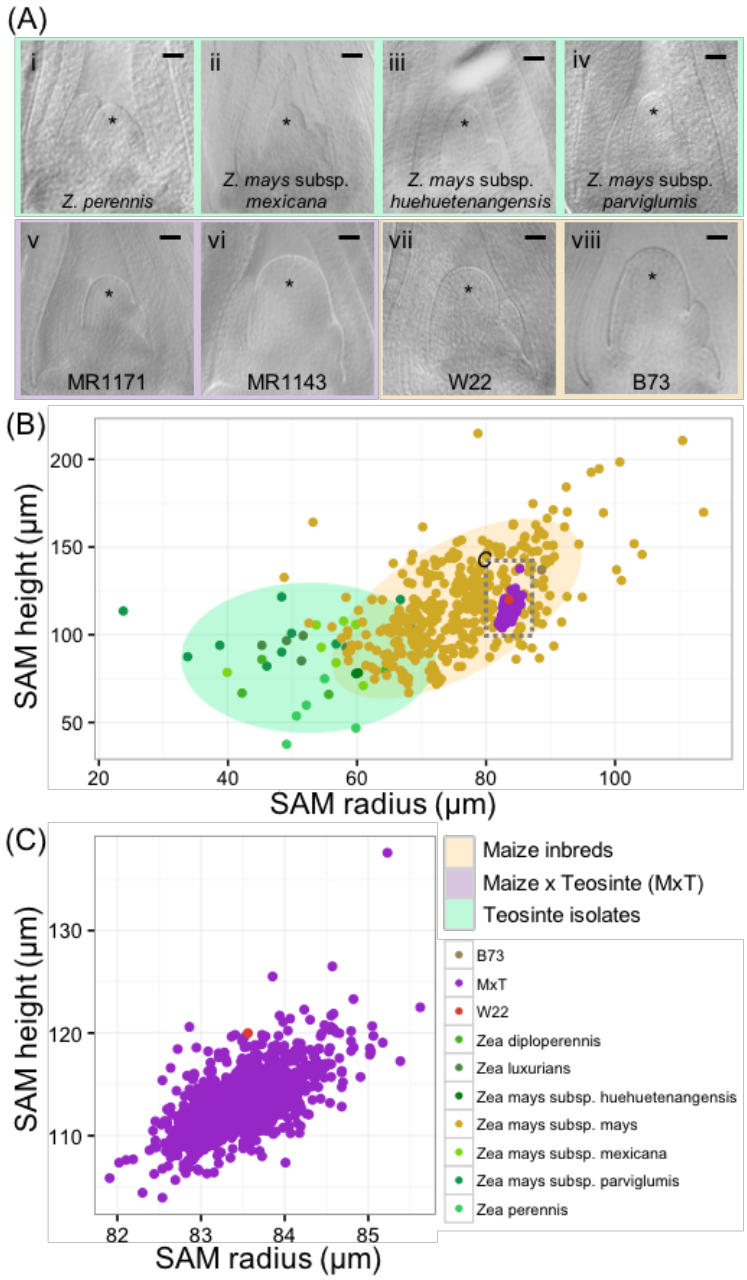

Figure 3.1 The maize and teosinte shoot apical meristem (SAM) morphospace. (A) Median longitudinal images of shoot meristems from wild teosinte isolates (i-iv), large and small SAMs from the maize x teosinte (MxT) intercross (BC2S3) lines (v-vi), and maize inbred varieties W22 (vii) and B73 (viii). * indicates SAM with flanking leaf primorida. Scale bar, 50 µm. (B) Quantification of meristem radius and height show that SAM morphology observed in teosinte varieties (greens) and maize inbred varieties (yellow) partially overlap but teosinte SAMs are generally smaller than maize inbred SAMs. Measures from MxT lines (purple) cluster closely around the recurrent maize parent, inbred W22 (pink). Grey dashed box, location of data in panel (C). Shaded ellipses, 90% density estimation of SAM shape data. (C) Variation in SAM shape and size in MxT lines (purple) around the W22 maize inbred parent (pink).

shoot meristem shape and size in SAMs isolated from MxT lines (Figure 3.1A,C) and focused our analysis on this population to understand the genetic architecture of maize/teosinte SAM morphometric variation.

3.4.2 Parabolic estimators of MxT variation identify new meristem morphology QTL

We used image-processing to collect two discrete measurements, SAM height and SAM radius and approximate the MxT shoot meristem as a paraboloid surface, the geometric shape yielded from revolving a parabolic curve around its central axis (additionally described in Leiboff et *al.* 2015). Exploiting the simple geometry of a paraboloid, we used two primary measures to derive eight total parabolic shape estimators: height, radius, height to radius ratio (H/R), volume (Vol.), surface area (Surf. Area), arc length (Arc Len.), parabolic coefficient (Para. Coeff.), and cross-sectional area (Area) (Supplementary Data 3.3) (Leiboff *et al.* 2015).

Our previous study analyzed SAM volume as a quantitative trait (Leiboff *et al.* 2015). In this analysis we identified QTL for MxT SAM volume on chromosomes 1, 4, and 7 (Figure 3.2B). Intervals detected on chromosomes 4 and 7 were not previously implicated in natural variation of SAM morphology in 369 domesticated maize inbred varieties (Supplementary Data 3.4) (Leiboff *et al.* 2015). The large QTL interval identified on chromosome 1 contains several previously identified candidate genes for shoot meristem morphology including *ZmLAX2*, a putative auxin import protein which exhibits haplotype-specific differences in transcript accumulation patterns in maize inbred varieties that correlate with differences in SAM size (Leiboff *et al.* 2015).

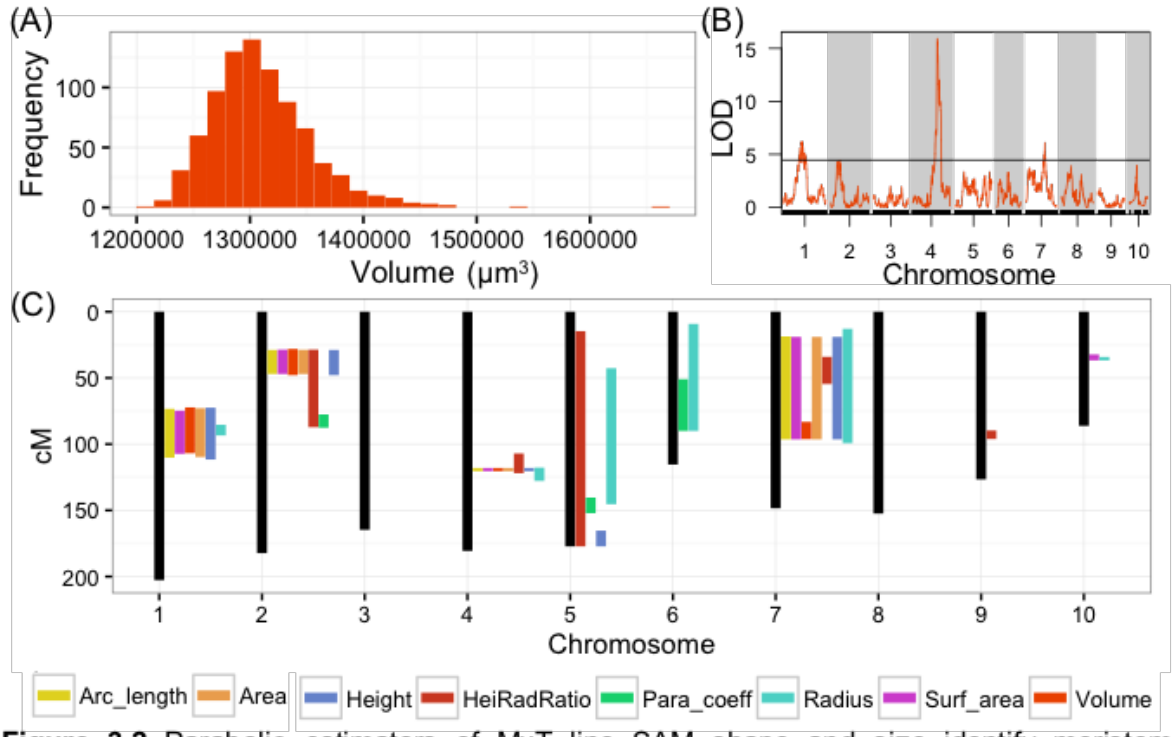

Figure 3.2 Parabolic estimators of MxT line SAM shape and size identify meristem morphology QTL. (A) Volume measures of SAMs harvested from 841 BC2S3 MxT lines. Measures are BLUP + coefficient values from 2 replicates. (B) Single QTL models detect significant loci for SAM volume on chromosome 1, 4, and 7. Black line, significance threshold α=0.05. (C) Additional significant SAM morphology QTL are detected for all 8 parabolic estimators genome-wide.

The remaining 7 parabolic estimators mapped QTL to several chromosomes (Figure 3.2C). Several parabolic estimators identified highly-overlapping QTL intervals. Chromosome 4, for example, contains a QTL that is coincidently associated with SAM height, radius, H/R, volume, surface area, arc length, and cross-sectional area (Figure 3.2C). All detected QTL were implicated by multiple parabolic estimators, except one QTL on chromosome 9 that is uniquely associated with SAM H/R. We find a high level of correlation between measures (Figure 3.3), as expected from their common derivation (Materials and Methods).

In total, QTL intervals recaptured 11 previously identified SAM-morphology candidate genes implicated by GWAS of maize inbred varieties (Supplementary Data 3.4) (Leiboff *et al.* 2015). Intriguingly, the QTL intervals mapped on chromosomes 4, 7, and 9 have not previously been associated with SAM shape and size.

3.4.3 Discrete cosine transform uncovers cryptic, genetically-attributable variation in MxT SAM shape variation

Using Fourier- related transform methods, we processed Procrustes-aligned and scaled MxT shoot meristem outlines (Figure 3.4) into Fourier shape principle components (PCs) to comprehensively describe SAM shape variation within this population (Supplementary Data 3.7). Three principle components describe more than 95% of the total observed shape variation, with PC1, PC2, and PC3, explaining 85.4%, 8.2%, and 2.3% respectively. Examining raw images of SAMs, and predicted shapes at the extremes of these principle components, revealed unexpected phenotypic variance (Figure 3.5). The majority of shape variation detected in the MxT population is attributed to PC1, identifying meristems that vary in appearance from ‘post-like’ to ‘dome-like’

	Arc Length	Surface Area	Volume	Area	H/R	Parabolic Coeff.	Height	Radius
Arc Length		0.97	0.95	0.99	0.66	*0.06*	0.98	0.78
Surface Area	0.97		0.99	0.99	0.48	-0.16	0.90	0.89
Volume	0.95	0.99		0.98	0.43	-0.19	0.87	0.89
Area	0.99	0.99	0.98		0.57	*-0.05*	0.95	0.83
H/R	0.66	0.48	0.43	0.57		0.78	0.80	*0.05*
Parabolic Coeff.	*0.06*	-0.16	-0.19	*-0.05*	0.78		0.26	-0.57
Height	0.98	0.90	0.87	0.95	0.80	0.26		0.63
Radius	0.78	0.89	0.89	0.83	*0.05*	-0.57	0.63	

Figure 3.3 Pearson correlation (r) between parabolic estimator phenotypes. Correlation value, red to blue. Non-significant correlation Fischer transformation P > 0.05, italics.

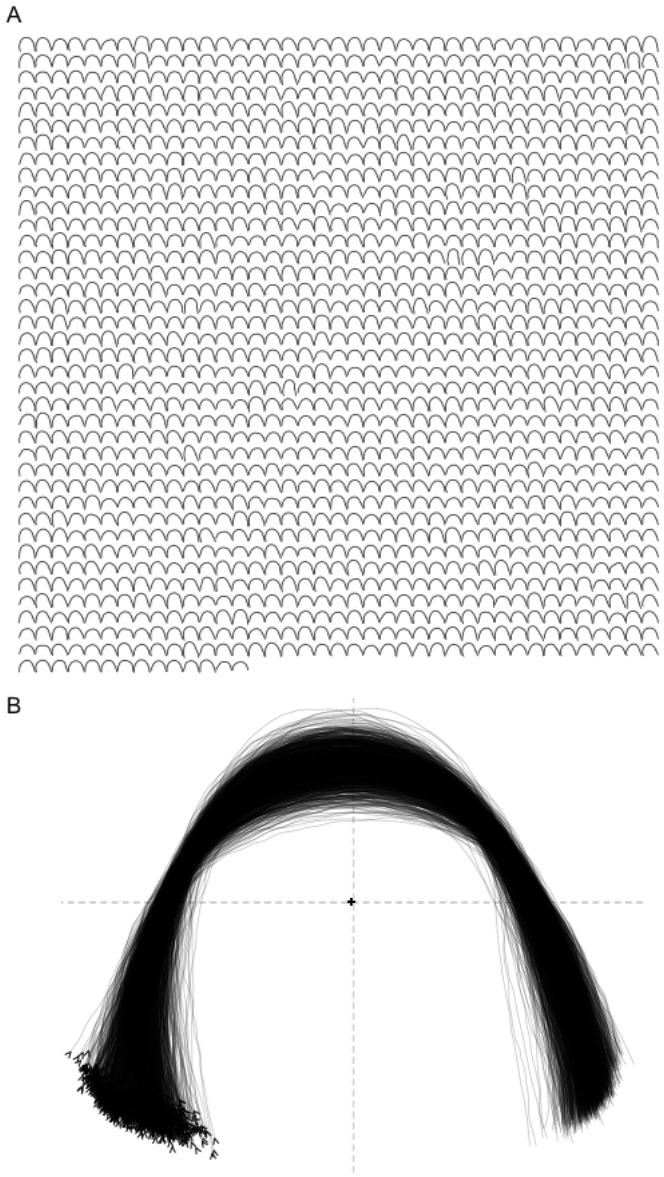

Figure 3.4 A. Unaligned MxT SAM traces. B. Contours superimposed after Procrustes alignment

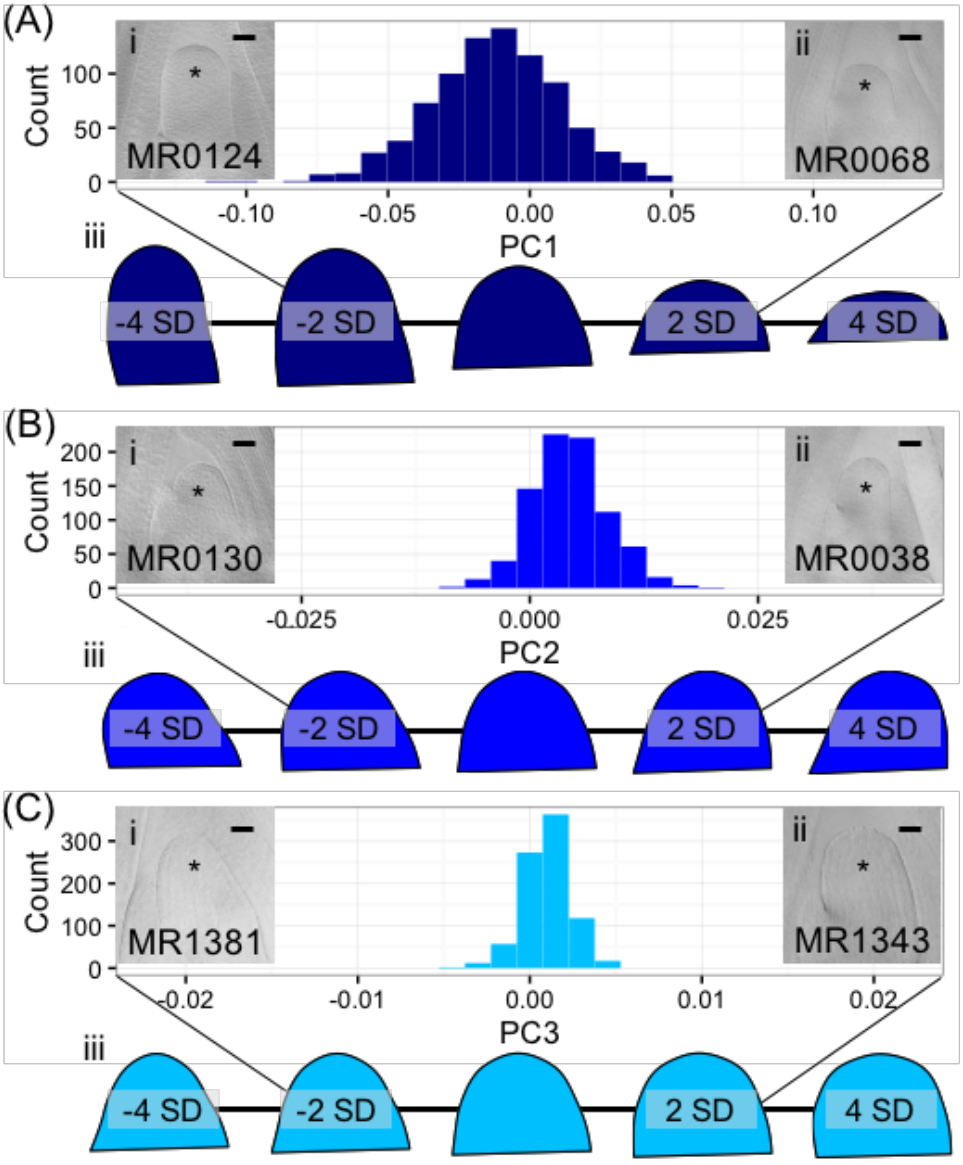

Figure 3.5 Discreet cosine transformation identifies three SAM-morphology principal components (PCs) describing MxT meristem shape and size. (A) PC1 identifies SAMs that vary from highly elongated, post-like to flattened, dome-like. (B) PC2 identifies asymmetrical SAMs that vary from left-leaning to right-leaning within the plane of histological sectioning. (C) PC3 identifies SAMs that vary from highly peaked to rounded. *i* and *ii*, median longitudinal images of meristems from MxT lines with low and high values for each PC, respectively. * indicates SAM with flanking leaf primorida. *iii*, renderings of expected SAM shapes with PC values of -4, -2, 0, 2, and 4 standard deviations from the average recorded SAM shape. Histogram x-axes, -2 to 2 standard dev. Scale bars, 50μm.

(Figure 3.5A). PC2 identifies meristems that vary in 2-dimensional asymmetry with respect to the plane of sample dissection, and describes variation from ‘left-leaning’ to ‘right-leaning’ SAMs (Figure 3.5B). PC3 identifies meristems that vary in slope from the SAM base to tip, and includes ‘peaked’ to ‘rounded’ shapes (Figure 3.5C).

Using PC1, PC2, and PC3 as quantitative phenotypes, we identified significant QTL for each trait: PC1 identified QTL on chromosomes 2, 4, 7, and 9 (Figure 3.6A), PC2 identified similar QTL intervals on chromosomes 2 and 4 (Figure 3.6B), whereas PC3 identified equivalent QTL intervals on chromosomes 2 and 4, in addition to different QTL on chromosomes 1 and 5 (Figure 3.6C). Despite differences in SAM measurement methods, the total QTL identified by all 8 parabolic estimators (Figure 3.2C) and 3 Fourier shape PCs overlap closely (Figure 3.6D). In a correlation analysis of parabolic estimators and Fourier shape PCs, we find a strong, significant correlation between PC1 and several parabolic estimators, especially SAM H/R (Pearson’s r = -0.67, Fisher transformation p-value < 2.2e-16) (Figure 3.7A). This close association is mirrored in the tight overlap of QTL identified by PC1 and H/R (Figure 3.7B). Because PC1 explains the majority of shape variation in the MxT population and is correlated in both numeric value and genetic architecture to parabolic estimators, we postulated that other populations of meristems might be likewise described by quantitative parabolic models.

3.4.4 Diverse meristems and their parabolic models

Despite their similar roles in stem cell maintenance and the production of lateral organs, the shoot apices of anciently diverged plant lineages have remarkable anatomical and transcriptomic differences (Figure 3.8A) (Bierhorst 1971; Evert 2006a; Frank and Scanlon 2015; Frank *et al.* 2015). In an analysis of 111 images from 73 plant taxa, we

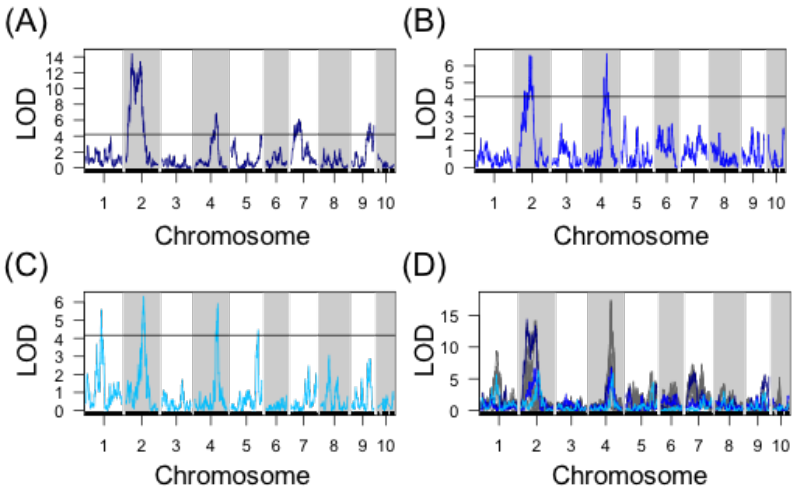

Figure 3.6 QTL identified for discreet cosine transform principal components. (A) QTL for PC1. (B) QTL for PC2. (C) QTL for PC3. (D) Superimposed QTL profiles for discreet cosine transform descriptors (blues) and parabolic estimator phenotypes (grey). Black line, significance threshold α = 0.05.

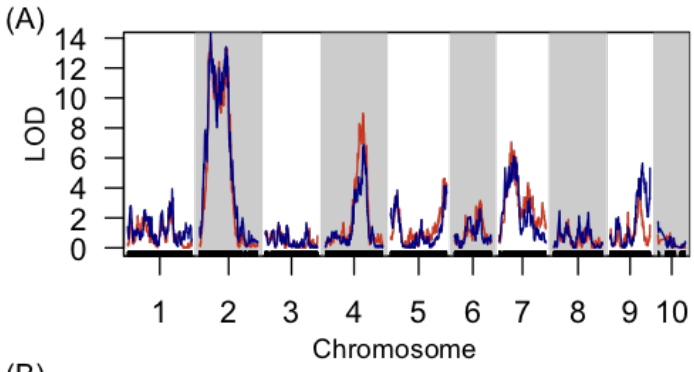

(B)

	PC1	PC2	PC3
Arc Len.	-0.54	0.22	0.14
Surf. Area	-0.43	0.12	0.16
Vol.	-0.40	0.09	0.16
Area	-0.49	0.17	0.16
H/R	**-0.67**	0.42	*0.04*
Para. Coeff.	-0.44	0.37	*-0.06*
Height	-0.61	0.29	0.13
Radius	-0.16	*-0.07*	0.16

Figure 3.7 Discreet cosine transform PC1 recaptures QTL and phenotypic variation identified by parabolic estimators. (A) Close overlap of QTL identified using PC1 (blue) and H/R (red). (B) Strong pearson correlation (r) between PC1 and several parabolic estimator phenotypes. Correlation value, red to blue. Non-significant correlation Fischer transformation P > 0.05, italics.

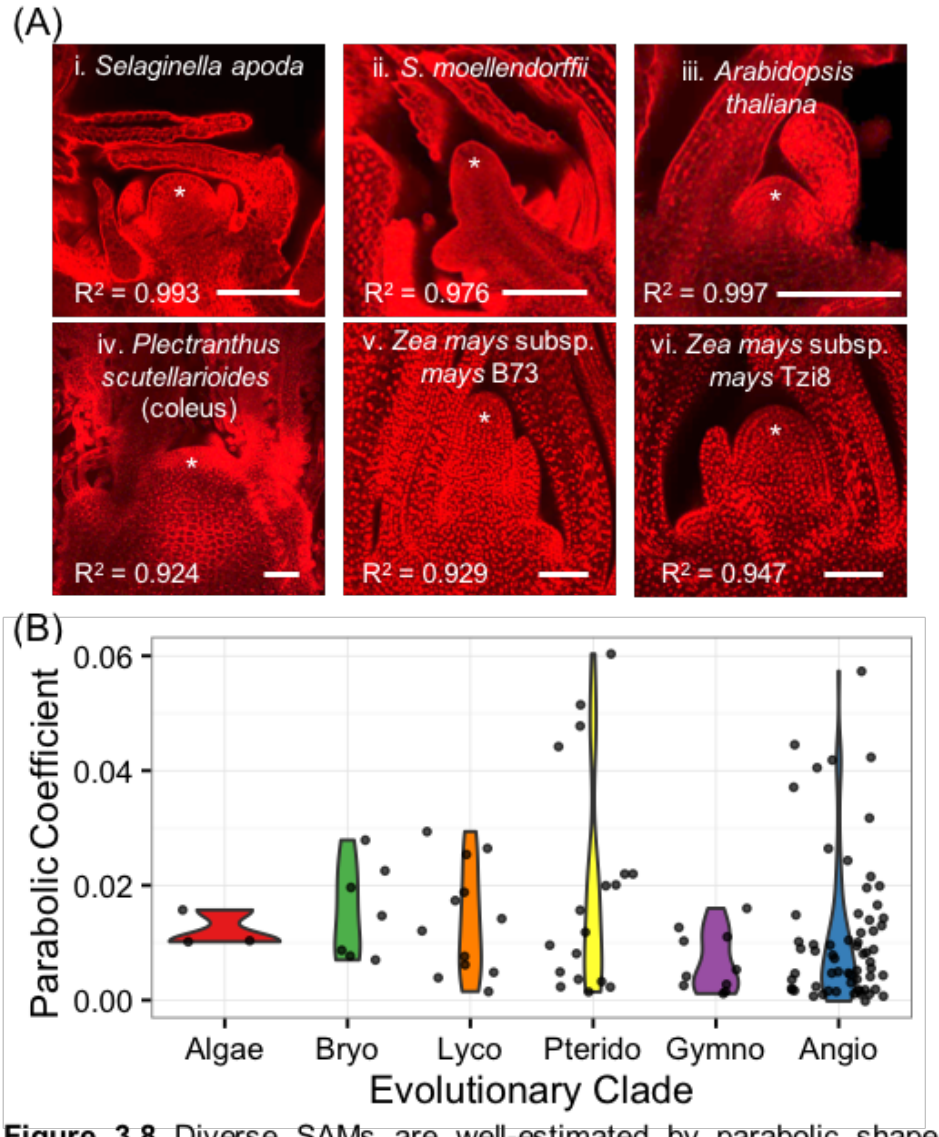

Figure 3.8 Diverse SAMs are well-estimated by parabolic shape models. (A) Median optical sections of the vegetative apex from example lycophytes with a shoot meristem dominated by an inverted pyramidal cell (i, ii) and angiosperms exhibiting a 'tunica-corpus' shoot meristem anatomy with at least one clonal 'tunica' layer (iii-vi). * indicates SAM and flanking leaf primorida. R^2, goodness-of-fit of parabolic model. Bar, 50um. (B) SAMs from broadly diverse evolutionary lineages exhibit a range of parabolic coefficients.

find that shoot apices are well fit by a parabolic model of meristem shape (Supplementary Data 3.1). Linear regression of shoot apex contours with a parabolic model yielded R^2 goodness-of-fit scores ranging from 0.838 to 0.997 with a mean of 0.963 and median of 0.975. Interestingly, SAM shape parameters do not significantly separate anciently diverged evolutionary clades (ANOVA, p-value = 0.158) (Figure 3.8B).

3.5 Discussion

We processed SAM images from 33 wild teosintes and 841 lines from a maize by teosinte (MxT) backcross population to generate a meristem morphospace for the genus *Zea*. In our SAM morphospace, we find that teosintes and maize inbred varieties occupy partially overlapping regions of the SAM shape, where SAMs in wild teosintes are diminutive compared to SAMs observed in domesticated maize varieties. We expect this SAM morphometric gradient to reflect the effect of domestication on the flowering time of Zea mays. The domestication and spread of maize outside its tropical Meso-American center of origin required adaptation to flowering during long summer days. Genetic studies of flowering time in maize, teosintes, and maize x teosinte backcross populations indicate that wild teosintes repress flowering during long days (Emerson 1924; Briggs *et al.* 2007; Hung *et al.* 2012). Allelic variants which have decreased activity of *ZmCCT* (an ortholog of rice flowering time gene, *Gdh7*) allow flowering during long days and were selected for during the domestication of maize (Briggs *et al.* 2007; Tsuji *et al.* 2011; Hung *et al.* 2012; Yang *et al.* 2013). Previous studies of natural variation in maize inbred variety SAM shape and size revealed correlations between large meristem size and short flowering time (Leiboff *et al.* 2015; Thompson *et al.* 2015),

reflected in GWAS candidate alleles at the *CONZ1* locus (Leiboff *et al.* 2015), proposed to act in a shared pathway with *ZmCCT* (Dong *et al.* 2012; Hung *et al.* 2012). QTL intervals for SAM surface area and radius on chromosome 10 include ZmCCT, which may contribute to differences in SAM size within the MxT population. Although the underlying mechanism that links flowering time and meristem size remains unresolved, our data agree with other reports of SAM natural variation and flowering time in maize.

Comprehensive analysis of SAM shape by Fourier methods yielded unexpected and interesting phenotypes for quantitative genetics. Prior implementations of Fourier methods for morphometrics have revealed genetically-attributable, cryptic shape phenotypes including quantitative tissue asymmetry as we observed in PC2 (Langlade *et al.* 2005; Chitwood *et al.* 2013, 2014). Yet, because QTL identified with Fourier transform PCs overlap strongly with QTL identified by estimating the maize SAM as a paraboloid, we expect that parabolic estimation methods are effective at representing heritable variation in SAM morphology.

Approximating SAM shape and size with a parabolic model has several advantages for quantitative genetics. Parabolic estimates of SAM morphology can be generated by collecting two simple measures, SAM height and radius, whereas Fourier methods requires the careful placement of pseudo-landmarks or outline information generated from laborious manual image tracing or automated image processing of high signal-to-noise SAM micrographs. Despite the increased sensitivity of Fourier methods, we expect that the throughput of approximating SAM morphology with a paraboloid is better suited to large-scale genetic analyses of SAM morphology in maize.

We furthermore demonstrated that shoot apical regions from diverse plant taxa are well fit by parabolic curves. Our observations suggest that parabolic meristem shape is found in all plant evolutionary clades and SAM anatomical organization types (ex. tunica-corpus, histological zonation, single apical cell, etc.), which generally correlate with evolutionary clade. Interestingly, we found that anciently diverged plant lineages have similar shoot meristem parabolic curvatures, despite rich diversity in anatomy, development, and whole-plant morphology. The universality of parabolic SAM shape in diverse lineages may, in part, be the result of biophysical forces incurred during the essential functions of the SAM. All shoot meristems maintain at least one undifferentiated stem cell initial, which divides to produce both stem cell initials and lateral organ initials (Steeves and Sussex 1972; Evert 2006a; b). Internal cellular division from the replication of initials places stress on epidermal cell walls, deforming the shoot apical domain into a parabolic shape (Niklas and Mauseth 1980; Green 1999; Kwiatkowska 2004). Within possible parabolic shapes, our broad sampling of plant shoot meristems suggests that evolutionary clade alone is not a significant determinant of specific SAM parabolic shape; plant taxa from disparate evolutionary clades may have similar parabolic shapes. As previous studies in maize have uncovered statistically significant correlations between SAM size and selected adult plant traits (Leiboff *et al.* 2015; Thompson *et al.* 2015), our analyses of SAM parabolic diversity within divergent plant taxa provide a framework for future investigations as to whether a fundamental correlation between SAM architecture and adult plant morphology may extend beyond phylogenetic boundaries.

3.6 Acknowledgements

We thank K. Niklas (Cornell) for strategic advice in modeling SAMs as paraboloids. Many thanks to the organizers and participants of the 2015 NIMBioS Investigative Workshop: Morphological Plant Models for advice on morphometric concepts and techniques. We thank N. Ronning (Cornell) for assistance with plant harvest and image acquisition. This work was funded by National Science Foundation (NSF) grant IOS-1238142.

3.7 Works Cited

Beadle G. W., 1980 The ancestry of corn. Sci. Am. **242**: 112–119.

Bierhorst D. W., 1971 *Morphology of vascular plants*. Macmillan.

Bommert P., Je B. Il, Goldshmidt A., Jackson D., 2013 The maize Gα gene COMPACT PLANT2 functions in CLAVATA signalling to control shoot meristem size. Nature **502**: 555–8.

Briggs W. H., McMullen M. D., Gaut B. S., Doebley J., 2007 Linkage mapping of domestication loci in a large maize teosinte backcross resource. Genetics **177**: 1915–28.

Chitwood D. H., Kumar R., Headland L. R., Ranjan A., Covington M. F., Ichihashi Y., Fulop D., Jiménez-Gómez J. M., Peng J., Maloof J. N., Sinha N. R., 2013 A quantitative genetic basis for leaf morphology in a set of precisely defined tomato introgression lines. Plant Cell **25**: 2465–81.

Chitwood D. H., Ranjan A., Kumar R., Ichihashi Y., Zumstein K., Headland L. R., Ostria-Gallardo E., Aguilar-Martínez J. a., Bush S., Carriedo L., Fulop D., Martinez C. C., Peng J., Maloof J. N., Sinha N. R., 2014 Resolving Distinct Genetic Regulators of Tomato Leaf Shape within a Heteroblastic and Ontogenetic Context. Plant Cell **26**: 3616–3629.

Claude J., 2008 Morphometrics with R.

Doebley J., 2004 The genetics of maize evolution. Annu. Rev. Genet. **38**: 37–59.

Dommergues C. H., Dommergues J. L., Verrecchia E. P., 2007 The discrete cosine transform, a Fourier-related method for morphometric analysis of open contours. Math. Geol. **39**: 749–763.

Dong Z., Danilevskaya O., Abadie T., Messina C., Coles N., Cooper M., 2012 A gene regulatory network model for Floral transition of the shoot apex in maize and its dynamic modeling. PLoS One **7**.

Emerson R. A., 1924 Control of Flowering in Teosinte: Short-Day Treatment Brings Early Flowers. J. Hered.: 41–48.

Evert R. F., 2006a Apical Meristems. In: *Esau's Plant Anatomy*, John Wiley & Sons, Inc., pp. 133–174.

Evert R. F., 2006b Meristems and Differentiation. In: *Esau's Plant Anatomy*, John Wiley & Sons, Inc., pp. 103–131.

Frank M. H., Scanlon M. J., 2015 Transcriptomic evidence for the evolution of shoot meristem function in sporophyte-dominant land plants through concerted selection of ancestral gametophytic and sporophytic genetic programs. Mol. Biol. Evol. **32**: 355–367.

Frank M. H., Edwards M. B., Schultz E. R., McKain M. R., Fei Z., Sørensen I., Rose J. K. C., Scanlon M. J., 2015 Dissecting the molecular signatures of apical cell-type shoot meristems from two ancient land plant lineages. New Phytol. **207**: 893–904.

Green P., 1999 Expression of pattern in plants: combining molecular and calculus-based biophysical paradigms. Am. J. Bot. **86**: 1059–1076.

Hake S., Ross-Ibarra J., 2015 Genetic, evolutionary and plant breeding insights from the domestication of maize. Elife **2015**: 1–8.

Huang C., Chen Q., Xu G., Xu D., Tian J., Tian F., 2016 Identification and fine mapping of quantitative trait loci for the number of vascular bundle in maize stem. J. Integr. Plant Biol. **58**: 81–90.

Hufford M. B., Bilinski P., Pyhäjärvi T., Ross-Ibarra J., 2012 Teosinte as a model system for population and ecological genomics. Trends Genet. **28**: 606–615.

Hung H.-Y., Shannon L. M., Tian F., Bradbury P. J., Chen C., Flint-Garcia S. A., McMullen M. D., Ware D., Buckler E. S., Doebley J. F., Holland J. B., 2012 *ZmCCT and the genetic basis of day-length adaptation underlying the postdomestication spread of maize.*

Jackson D. P., Hake S., 1999 Control of phyllotaxy in maize by the abphyl1 gene. Development **126**: 315–23.

Jia Y., Lisch D. R., Ohtsu K., Scanlon M. J., Nettleton D., Schnable P. S., 2009 Loss of RNA-dependent RNA polymerase 2 (RDR2) function causes widespread and unexpected changes in the expression of transposons, genes, and 24-nt small RNAs. PLoS Genet. **5**: e1000737.

Klingenberg C. P., 2010 Evolution and development of shape: integrating quantitative approaches. Nat. Rev. Genet. **11**: 623–635.

Kwiatkowska D., 2004 Structural integration at the shoot apical meristem: Models, measurements, and experiments. Am. J. Bot. **91**: 1277–1293.

Langlade N. B., Feng X., Dransfield T., Copsey L., Hanna A. I., Thébaud C., Bangham A., Hudson A., Coen E., 2005 Evolution through genetically controlled allometry space. Proc. Natl. Acad. Sci. U. S. A. **102**: 10221–6.

Leiboff S., Li X., Hu H.-C., Todt N., Yang J., Li X., Yu X., Muehlbauer G. J., Timmermans M. C. P., Yu J., Schnable P. S., Scanlon M. J., 2015 Genetic control of morphometric diversity in the maize shoot apical meristem. Nat. Commun. **6**: 8974.

Niklas K. J., Mauseth J. D., 1980 Simulations of Cell Dimensions in Shoot Apical Meristems: Implications Concerning Zonate Apices. Am. J. Bot. **67**: 715.

Orr A. R., Sundberg M. D., 1994 Inflorescence Development in a Perennial Teosinte: Zea perennis (Poaceae). Am. J. Bot. **81**: 598–608.

Orr A. R., Sundberg M. D., 2004 Inflorescence Development in a New Teosinte: Zea nicaraguensis (Poaceae). Am. J. Bot. **91**: 165–173.

Pautler M., Eveland A. L., LaRue T., Yang F., Weeks R., Lunde C., Je B. Il, Meeley R. B., Komatsu M., Vollbrecht E., Sakai H., Jackson D., 2015 FASCIATED EAR4 Encodes a bZIP Transcription Factor That Regulates Shoot Meristem Size in Maize. Plant Cell Online **27**: tpc.114.132506.

Shannon L. M., 2013 *The Genetic Architecture of Maize Domestication and Range Expansion*.

Steeves T. A., Sussex I. M., 1972 *Patterns in plant development*. Prentice-Hall, Englewood Cliffs, N.J.

Sundberg M. D., Orr A. R., 1986 Early Inflorescence and Floral Development in Zea diploperennis, Diploperennial Teosinte. Am. J. Bot. **73**: 1699–1712.

Sundberg M. D., Orr A. R., 1990 Inflorescence Development in Two Annual Teosintes: Zea mays subsp. Mexicana and Z. mays subsp. Parviglumis. Am. J. Bot. **77**: 141–152.

Taguchi-Shiobara F., Yuan Z., Hake S., Jackson D. P., 2001 The fasciated ear2 gene encodes a leucine-rich repeat receptor-like protein that regulates shoot meristem proliferation in maize. Genes Dev. **15**: 2755–66.

Thompson A. M., Crants J., Schnable P. S., Yu J., Timmermans M. C. P., Springer N. M., Scanlon M. J., Muehlbauer G. J., 2014 Genetic control of maize shoot apical meristem architecture. G3 (Bethesda). **4**: 1327–37.

Thompson A. M., Yu J., Timmermans M. C. P., Schnable P., Crants J. C., Scanlon M. J., Muehlbauer G. J., 2015 Diversity of Maize Shoot Apical Meristem Architecture and Its Relationship to Plant Morphology. G3!; Genes|Genomes|Genetics: 1–14.

Tsuji H., Taoka K. I., Shimamoto K., 2011 Regulation of flowering in rice: Two florigen genes, a complex gene network, and natural variation. Curr. Opin. Plant Biol. **14**: 45–52.

Yang Q., Li Z., Li W., Ku L., Wang C., Ye J., Li K., Yang N., Li Y., Zhong T., Li J., Chen Y., Yan J., Yang X., Xu M., 2013 CACTA-like transposable element in ZmCCT attenuated photoperiod sensitivity and accelerated the postdomestication spread of maize. Proc. Natl. Acad. Sci. U. S. A. **110**: 16969–74.

Yang F., Bui H. T., Pautler M., Llaca V., Johnston R., Lee B.-H., Kolbe A., Sakai H., Jackson D., 2015 A Maize Glutaredoxin Gene, Abphyl2, Regulates Shoot Meristem Size and Phyllotaxy. Plant Cell.

4 Summary

In this dissertation we investigated natural variation in the shoot apical meristem (SAM) including a novel diversity panel of 369 maize inbred varieties, 33 wild teosinte isolates, 841 lines derived from a domesticated maize x wild progenitor teosinte cross, as well as 72 plant species from anciently-diverged evolutionary lineages. By developing image processing and morphometric modeling techniques, which we coupled to GWAS and QTL mapping studies, we identified candidate genes and loci underlying natural variation in maize SAM morphology. We found that meristems from diverse lineages can universally be represented by parabolic shapes, and that parabolic estimation is efficient and effective for large scale quantitative genetics. In correlations between SAM morphometric parameters and candidate loci, we found that SAM morphology is related to, but not uniquely controlled by plant flowering time.

While quantitative genetics can indeed be applied to understand the genetic regulation of microscopic plant tissues such as the SAM, the underlying genetic architecture of the maize SAM suggests that plant stem cell master regulators discovered by mutagenesis may not participate in natural variation of the maize SAM. High-density genotyping suggests, however, that many essential plant stem cell regulator genes are highly polymorphic in diverse inbred lines. We are therefore confident in our finding that SAM master regulatory genes do not play a primary role in natural variation in SAM morphology.

The candidate genes that we have correlated with SAM morphological variation, are likely to comprise peripheral components of stem cell function. Perhaps these genes

function as minor modulators of maize SAM function, and may therefore be mutable without adverse effect to the total organism. We explored the regulation of a putative plant hormone transporter and saw that spatial patterns of *ZmLAX2* transcript accumulation correlate with differences in SAM size. With such a central role in development and cellular growth (Jönsson *et al.* 2006; Sablowski 2011; Swarup and Péret 2012), it is very possible that even subtle changes to auxin dynamics may influence both plant stem cell activity and SAM morphology. We also confirmed correlations between natural variants of candidate genes with putative influence over cell number (ZmSDA1) and cell size (ZmBAK1-like) and maize SAM morphology. Many details about the molecular mechanisms that underlie this observation have not yet been elucidated in maize.

4.1 Research outcomes

Candidate loci, phenotype and genotype matrices, as well as morphometric modelling techniques may guide future research on the modulation of SAM morphology and maize stem cell activity. Few discoveries from mutagenesis of plant stem cell regulators have yielded agronomically-valuable information (Bommert *et al.* 2013a; Je *et al.* 2016). This may be due, in part, to the severe deleterious nature of many known mutants in plant stem cell regulatory pathways (Weigel and Nordborg 2005). The candidate loci listed here already exist as natural variants in the US maize germplasm and may therefore be more suited for selection in breeding experiments (Tanksley 1993). Collaborators at Iowa State University are currently exploiting the maize SAM measures reported here to conduct genomic selection (GS) for SAM size.

Additional high-throughput investigations of SAM morphology, in maize and in other species, may benefit from the morphometric models established here. Parabolic estimation of SAM shape has been efficient for analysis of hundreds of inbred lines in replicated experiments, representing thousands of total samples. The near universal applicability of parabolic models of SAM shape to diverse species suggests that SAM image processing pipelines in many plants may take advantage of the models presented here to dissect the genetic architecture of SAM shape and size.

4.2 Recommendations for future research

The research presented here provides a detailed exploration of natural variation in SAM morphology in maize. However, many questions about the genetic underpinning of SAM shape in size remain. Our studies have associated candidate genes and broader genomic regions with changes in SAM shape and size. The link between these natural sequence variants and observed phenotypic changes remains unexplored. Conducting RNA sequencing on shoot meristem tissue from the diverse lines reported here would reveal if transcriptional regulation (combined synthesis and turnover) of naturally-varying candidate genes is related to differences in SAM morphology. If no changes in transcript expression are detected, we may expect that natural variants of candidate genes have different post-transcriptional activities, in either protein activity or translational activity. In that case, additional developmental genetic studies of the reported candidate loci and their putative genetic pathways may especially yield novel insight into the regulation of plant stem cells.

Studying the developmental impact of transposition knock-out resources in maize (UniformMu, Ac/Ds, etc) with putative insertions into candidate loci may reveal their

exact mode of function. Candidate genes with many paralogous family members may be ideal targets for mutagenesis via CRISPR/Cas9, where several genes may be targeted for mutation at once (Bortesi and Fischer 2015). Studying the impact of knock-out mutations on SAM morphology as well as adult plant morphology may reveal additional relationships between the microscopic SAM and the whole plant it produces.

4.3 Conclusion

The maize SAM is a microscopic parabolic structure that exhibits rich variation within maize inbred varieties, the broader genus *Zea*, and many other species within the plant kingdom. The genetic regulation of maize SAM morphology involves several loci genome-wide and implicates gene candidates of uncertain function which have not previously been tied to maize stem cell regulation. Through the work presented here, and subsequent research which may follow, it is inevitable that the already complex regulatory network of interacting factors that manages plant stem cells will continue to grow and yield insight to how plants generate their varied and magnificent forms.

4.4 Works Cited

Bommert P., Nagasawa N. S., Jackson D., 2013 Quantitative variation in maize kernel row number is controlled by the FASCIATED EAR2 locus. Nat. Genet. **45**: 334–7.

Bortesi L., Fischer R., 2015 The CRISPR/Cas9 system for plant genome editing and beyond. Biotechnol. Adv. **33**: 41–52.

Jönsson H., Heisler M. G., Shapiro B. E., Meyerowitz E. M., Mjolsness E., 2006 An auxin-driven polarized transport model for phyllotaxis. Proc. Natl. Acad. Sci. U. S. A. **103**: 1633–8.

Sablowski R., 2011 Plant stem cell niches: from signalling to execution. Curr. Opin. Plant Biol. **14**: 4–9.

Swarup R., Péret B., 2012 AUX/LAX family of auxin influx carriers-an overview. Front. Plant Sci. **3**: 225.

Tanksley S. D., 1993 Mapping Polygenes. Annu. Rev. Genet. **27**: 205–233.

Weigel D., Nordborg M., 2005 Natural variation in Arabidopsis. How do we find the causal genes? Plant Physiol. **138**: 567–8.

5 Appendix A: Nano-scale Computed Tomography (CT) to understand the ontogeny of the sheathing leaf base in maize (*Zea mays*)

5.1 Introduction

Natural variation in leaf morphology is one of the most striking characteristics of different taxa from across the plant kingdom. Leaves are generated at the shoot apical meristem (SAM) as part of an iterative unit that includes leaf, node, and internode, together called the phytomer (reviewed in Roberts 2007). In angiosperms, leaves typically resemble one of two types: 1) the eudicot leaf consists of a distinct lamina with reticulate, or net-like venation atop an elongated petiole, 2) the monocot leaf consists of a long strap-like lamina with parallel veins that run along the length of the leaf and into the sheathing leaf base, with overlapping margins that originate from the leaf node and encircle the stem (Kaplan 1973). The ontogeny of most eudicot and monocot leaves appears distinct as well: eudicot leaf primordia form a peg-like outgrowth around the central midvein and initiate an expansive lamina sometime after initial stem cell recruitment, whereas monocot primordia originate from a disk of insertion (DOI) of recruited stem cells that forms the lamina as a hooded structure with its peak at the central midvein (Sharman 1942; Kaplan 1973, 2001). Although the initial and final morphologies of these distinct leaf types have been known for several years, the ontogenic steps between states in maize have, to date, been limited to inference by analysis of clonal sectors and tissue culture experiments (Poethig 1984; Poethig and

Szymkowiak 1995; Scanlon and Freeling 1997; Scanlon 2003). The leaf primordia that surround the SAM in maize and other monocots wrap tightly around the shoot apex, prohibiting direct observation of intact structures (Pautler *et al.* 2013).

Here we present the first application of nanometer-scale computed tomography (NanoCT) to analyze the morphology of initiating and developing leaf primordia in maize. Computed tomography methods use tissue-penetrating x-ray absorption profiles to generate 3-dimensional (3-D) image datasets which may reveal internal structures without destructive dissection (Gamisch *et al.* 2013). We find that throughout successive stages of early leaf primordia development, the DOI gives rise to the primordia lamina in a wave of outgrowth that progresses from leaf midvein to margin along two advancing fronts. These fronts give rise to the overlapping sheath margins without ever intersecting, thus demonstrating that the sheathing base of the maize leaf is patterned to encircle the stem without requiring post-primordial lateral outgrowth, which forms the majority of the leaf margins.

5.2 Methods

Computed tomography (CT) imaging was performed on maize seedlings harvested 14 days after planting. Hand-trimmed apices were fixed overnight in FAA then dehydrated to 100% ethanol as in Ruzin (1999). Apices were stained for four days in 1% crystalline iodine dissolved in 100% ethanol. After a brief series of rinses in 100% ethanol, apices were transferred to 100% xylene and then to liquid paraffin as described (Ruzin 1999). Paraffin-embedded samples were utilized for CT imaging.

Tomographic datasets were acquired using the Xradia (Pleasanton, CA) Versa XRM-500 at one of the following settings: (1) 80keV, 7W, 2 second exposures with 2400 projections, 4x binned at 2000nm pixel resolution; (2) 60keV, 5W, 5 second exposures with 1800 projections through the LE1 filter, 4x binned at 1533nm or 1496nm pixel resolution. Data were exported as TIFF-stacks to the image processing software OsiriX (Rosset *et al.* 2004). Using the 3-D MPR and 3-D volume-rendering tools in OsiriX v.5.8.1 64-bit, the shoot apex and leaf primordia were examined from longitudinal, lateral, transverse, and paramarginal vantage points. Final micrographs were compiled by volumetric rendering of between 5 - 45 µm of optical data, depending upon the thickness of the plant microstructure that was imaged.

5.3 Results and Discussion

5.3.1 Computed Tomographic imaging of the emerging maize leaf base

Computed Tomography (CT) permits X-ray imaging of intact biological samples. Optical sections are collated to form 3-dimensional (3-D) images of biological structures that can be viewed from any planar orientation. We used CT imaging of fixed, iodine-stained 14-day-old seedlings to observe the successive stages of morphological development during maize leaf ontogeny. CT enables the simultaneous observation of different plastochron (P) stages of leaf margin development, from all possible vantage points and orientations (Figure 5.1*A*-*C*), in a single study. A plastochron comprises the time period between successive leaf initiations from the vegetative SAM; significant developmental changes occur within each leaf primordium during the length of a single plastochron. Although CT imaging captures a morphological ‘still shot’ of multiple leaf primordia in a single seedling, any given P3 primordium (for example) may be at a

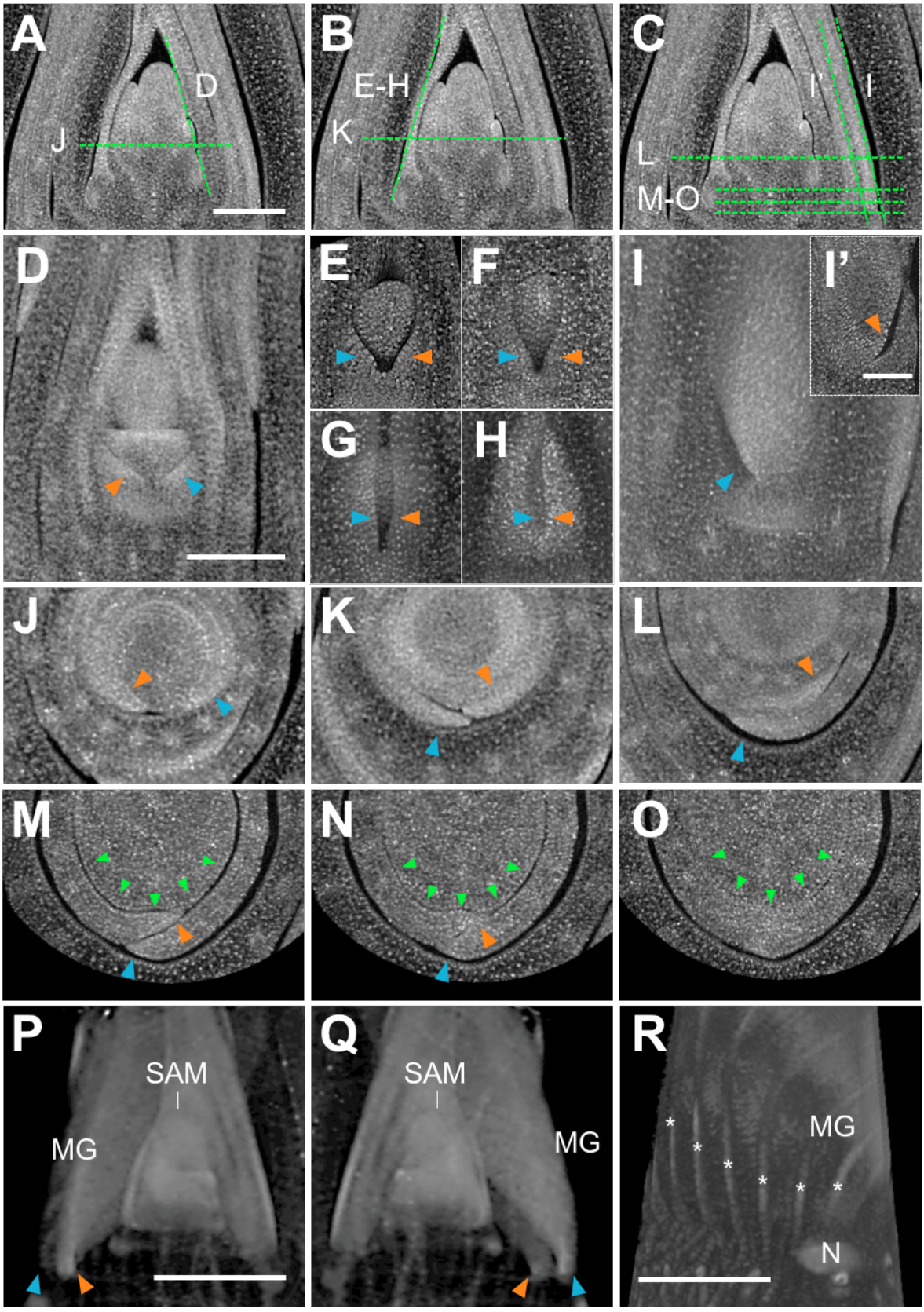
A
D
J
B
E-H
K
C
I'
I
L
M-O
D
E
F
G
H
I
I'
J
K
L
M
N
O
P
SAM
MG
Q
SAM
MG
R
MG
N

Figure 5.1 Computed tomography analysis of the ontogeny of the maize sheathing leaf base. (A–C) Median, longitudinal views of maize shoot apical meristems (SAMs). Dotted lines designate the plane of optical sections in succeeding panels. (D) Paramarginal view of the maize shoot apex focusing on the P2 primordium. Distinct, nonoverlapping marginal outgrowths (arrows) from the disc of insertion (DOI) of the P2 primordium reveal that, at this stage of development, all of the as yet emerged leaf primordium comprises blade tissue in which the margins do not overlap the shoot apex. (J) Transverse view of the P2 primordium shown in (D). (E–H) Paramarginal views of four individual P3 primordia show progressive stages of leaf development. In early P3 (E), the margins of the leaf primordium emerge as separate, nonoverlapping tissue (arrows), presumably fated to form blade in the mature leaf. As development continues (F, G), sheath margins emerge from the DOI with overlapping edges (H). (K) Transverse view of the P3 primordium shown in (H) reveals that margins are 'pre-wrapped' before their emergence from the DOI, such that one margin emerges on the outside of the other forming unfused, overlapping leaf edges. (I, I') Paramarginal views of the outer margin (blue arrow in (I)) and inner margin (orange arrow in (I')) of the P4 leaf. By P4, margins form tightly overlapped, unfused tissue fated to form the sheath in the mature leaf. (L) Transverse view of the primordium shown in (I). (M–O) Transverse, acropetal optical sections of a P4 primordium base reveal that the outer (blue arrow) and inner (orange arrow) margins emerge as pre-wrapped, overlapping outgrowths from the tubular DOI. Note that the DOI shown in (M) forms a ring of tissue that is separate from the outer edge of the stem (highlighted by green arrows). (P, Q) Rotational views of a 3D rendering of a maize seedling shoot apex show that the highly overlapped P5 margins insert at separate outer (blue arrow) and inner (orange arrow) regions along the perimeter of the DOI. SAM, shoot apical meristem; MG, marginal axis. (R) 3D rendering of P6 leaf tissue shows the arrangement of parallel leaf veins (asterisks) in the young leaf primordium. N, node; MG, marginal axis. Bars, 50 μm; serial sections in (M–O) are vertically spaced by 5 μm.

slightly different developmental stage than another P3-staged sample within the same plastochron.

As shown in Figure. 5.1*D-G,* and *J*, the left and right edges of P2 and early-staged P3 leaf primordia insert into the tubular DOI at the leaf base without overlapping. When considered alongside the data from numerous fate maps of maize leaf development (Poethig 1984; Poethig and Szymkowiak 1995; Scanlon and Freeling 1997), these observations suggest that the entirety of the as yet elaborated leaf primordium observed during these early stages of maize leaf development comprises blade tissue, the margins of which do not overlap the shoot apex. Moreover, the data further suggest that the sheath components of these P2 and early P3 primordia comprise as yet unelaborated initials within the DOI.

Beginning in late-P3 (Figure 5.1*H* and *K)* and early-P4 (Figure 5.1*I,I*',*M-O*), the inner and outer sheath margins emerge from the DOI as two separate fronts of tissue growth. In this way, a sheathing leaf base is formed in which the right and left margins overlap from their very inception, not simply as a result of post-primordial, lateral growth. Figure 5.1*I*,*I'* shows paramarginal views of the outer and inner edges of P4 sheath margins, respectively. Supplementary Movie 5.1 shows paramarginal views of the P4 leaf base, revealing the edges of the outer (time point 00:02) and inner (time point 00:06) P4 sheath margins. As shown in serial transverse, serial optical sections (Figure 5.1*M-O*) and at time point 00:07 in Supplementary Movie 5.2, the DOI below the emerging P4 sheath margins forms an uninterrupted “tube” of tissue that is distinct from and surrounds the stem. By contrast, serial sections distal to the DOI reveal the P4 sheath margins emerge as separate, but *already-overlapping*, sheets of primordial

tissue. These multidimensional CT data provide support to the interpretations of previous cell fate analyses (Poethig and Szymkowiak 1995; Scanlon and Freeling 1997; Scanlon 2000), which suggested that the maize sheathing leaf base does not arise as a result of the extended, differential growth of primordial sheath margins. By contrast, the primordial sheath margins overlap the shoot apex from their very inception, thereby forming a sheathing leaf base. Whole mount 3-D reconstructions clearly illustrate the separate insertion points of the overlapping P5 sheath margins (Figure 5.1*P* and *Q*), as does time point 00:11 in Supplementary Movie 5.3. Lastly, the parallel arrangement of the primordial leaf vasculature is clearly seen in the CT scans of P6 leaf primordia shown in Figure 5.1*R.*

5.4 Works Cited

Gamisch A., Staedler Y. M., Schönenberger J., Fischer G. A., Comes H. P., 2013 Histological and micro-CT evidence of stigmatic rostellum receptivity promoting auto-pollination in the madagascan orchid Bulbophyllum bicoloratum. PLoS One **8**: e72688.

Kaplan D. R., 1973 THE PROBLEM OF LEAF MORPHOLOGY AND EVOLUTION IN THE MONOCOTYLEDONS. Q. Rev. Biol. **48**: 437–457.

Kaplan D. R., 2001 Fundamental Concepts of Leaf Morphology and Morphogenesis: A Contribution to the Interpretation of Molecular Genetic Mutants. Int. J. Plant Sci. **162**: 465–474.

Pautler M., Tanaka W., Hirano H.-Y., Jackson D., 2013 Grass meristems I: shoot apical meristem maintenance, axillary meristem determinacy and the floral transition. Plant Cell Physiol. **54**: 302–12.

Poethig R., 1984 Cellular parameters of leaf morphogenesis in maize and tobacco. In: White RA, Dickison WC (Eds.), *Contemporary problems in plant anatomy*, Academic Press, New York, pp. 235–238.

Poethig R. S., Szymkowiak E. J., 1995 Clonal analysis of leaf development in maize. Maydica.

40: 67.

Roberts K., 2007 *Handbook of plant science*. Wiley, Chichester, West Sussex, England; Hoboken, NJ, USA.

Rosset A., Spadola L., Ratib O., 2004 OsiriX: An open-source software for navigating in multidimensional DICOM images. J. Digit. Imaging **17**: 205–216.

Ruzin S., 1999 *Plant microtechnique and microscopy*. Oxford University Press, New York.

Scanlon M. J., Freeling M., 1997 Clonal sectors reveal that a specific meristematic domain is not utilized in the maize mutant narrow sheath. Dev. Biol. **182**: 52–66.

Scanlon M. J., 2000 NARROW SHEATH1 functions from two meristematic foci during founder-cell recruitment in maize leaf development. Development **127**: 4573–85.

Scanlon M. J., 2003 The polar auxin transport inhibitor N-1-naphthylphthalamic acid disrupts leaf initiation, KNOX protein regulation, and formation of leaf margins in maize. Plant Physiol. **133**: 597–605.

Sharman B. C., 1942 Developmental Anatomy of the Shoot of Zea mays L. Ann. Bot. **6**: 245–282.

6 Bibliography

Abbe E. C., Phinney B. O., Baer D. F., 1951 The Growth of the Shoot Apex in Maize: Internal Features. Am. J. Bot. **38**: 744.

Bainbridge K., Guyomarc'h S., Bayer E., Swarup R., Bennett M., Mandel T., Kuhlemeier C., 2008 Auxin influx carriers stabilize phyllotactic patterning. Genes Dev. **22**: 810–23.

Barbazuk W. B., Emrich S. J., Chen H. D., Li L., Schnable P. S., 2007 SNP discovery via 454 transcriptome sequencing. Plant J. **51**: 910–918.

Barkoulas M., Hay A., Kougioumoutzi E., Tsiantis M., 2008 A developmental framework for dissected leaf formation in the Arabidopsis relative Cardamine hirsuta. Nat. Genet. **40**: 1136–1141.

Bassiri a, Irish E., Poethig R., 1992 Heterochronic Effects of Teopod 2 on the Growth and Photosensitivity of the Maize Shoot. Plant Cell **4**: 497–504.

Bauchet G., Munos S., Sauvage C., Bonnet J., Grivet L., Causse M., 2014 Genes involved in floral meristem in tomato exhibit drastically reduced genetic diversity and signature of selection. BMC Plant Biol. **14**: 279.

Bayer E. M., Smith R. S., Mandel T., Nakayama N., Sauer M., Prusinkiewicz P., Kuhlemeier C., 2009 Integration of transport-based models for phyllotaxis and midvein formation. Genes Dev. **23**: 373–84.

Beadle G. W., 1980 The ancestry of corn. Sci. Am. **242**: 112–119.

Bharathan G., Goliber T. E., Moore C., Kessler S., Pham T., Sinha N. R., 2002 Homologies in leaf form inferred from KNOXI gene expression during development. Science **296**: 1858–1860.

Bierhorst D. W., 1971 *Morphology of vascular plants*. Macmillan.

Blein T., Pulido A., Vialette-Guiraud A., Nikovics K., Morin H., Hay A., Johansen I. E., Tsiantis M., Laufs P., 2008 A conserved molecular framework for compound leaf development. Science **322**: 1835–1839.

Bolduc N., Hake S., 2009 The maize transcription factor KNOTTED1 directly regulates the gibberellin catabolism gene ga2ox1. Plant Cell **21**: 1647–58.

Bolduc N., Yilmaz A., Mejia-Guerra M. K., Morohashi K., O'Connor D., Grotewold E., Hake S., 2012 Unraveling the KNOTTED1 regulatory network in maize meristems. Genes Dev. **26**: 1685–90.

Bommert P., Lunde C., Nardmann J., Vollbrecht E., Running M., Jackson D., Hake S., Werr W., 2005 thick tassel dwarf1 encodes a putative maize ortholog of the Arabidopsis CLAVATA1 leucine-rich repeat receptor-like kinase. Development **132**: 1235–45.

Bommert P., Nagasawa N. S., Jackson D., 2013a Quantitative variation in maize kernel row number is controlled by the FASCIATED EAR2 locus. Nat. Genet. **45**: 334–7.

Bommert P., Je B. Il, Goldshmidt A., Jackson D., 2013b The maize Gα gene COMPACT PLANT2 functions in CLAVATA signalling to control shoot meristem size. Nature **502**: 555–8.

Bonnett O. T., 1953 *Developmental morphology of the vegetative and floral shoots of maize*. University of Illinois Agricultural Experiment Station, Urbana, Ill.

Bortesi L., Fischer R., 2015 The CRISPR/Cas9 system for plant genome editing and beyond. Biotechnol. Adv. **33**: 41–52.

Brand U., 2000 Dependence of Stem Cell Fate in Arabidopsis on a Feedback Loop Regulated by CLV3 Activity. Science **289**: 617–619.

Bray M.-A., Vokes M. S., Carpenter A. E., 2015 Using CellProfiler for Automatic Identification and Measurement of Biological Objects in Images. Curr. Protoc. Mol. Biol. **109**: 14.17.1-14.17.13.

Briggs W. H., McMullen M. D., Gaut B. S., Doebley J., 2007 Linkage mapping of domestication loci in a large maize teosinte backcross resource. Genetics **177**: 1915–28.

Broman K. W., Wu H., Sen ??aunak, Churchill G. A., 2003 R/qtl: QTL mapping in experimental crosses. Bioinformatics **19**: 889–890.

Buckler E. S., Holland J. B., Bradbury P. J., Acharya C. B., Brown P. J., Browne C., Ersoz E., Flint-Garcia S. A., Garcia A., Glaubitz J. C., Goodman M. M., Harjes C., Guill K., Kroon D. E., Larsson S., Lepak N. K., Li H., Mitchell S. E., Pressoir G., Peiffer J. a, Rosas M. O., Rocheford T. R., Romay M. C., Romero S., Salvo S., Sanchez Villeda H., Silva H. S. da, Sun Q., Tian F., Upadyayula N., Ware D., Yates H., Yu J., Zhang Z., Kresovich S., McMullen M. D., 2009 The genetic architecture of maize flowering time. Science **325**: 714–8.

Buscemi G., Saracino F., Masnada D., Carbone M., 2000 The Saccharomyces cerevisiae SDA1 gene is required for actin cytoskeleton organization and cell cycle progression. J. Cell Sci. **113**: 1199–1211.

Busch W., Miotk A., Ariel F. D., Zhao Z., Forner J., Daum G., Suzaki T., Schuster C., Schultheiss S. J., Leibfried A., Haubeiss S., Ha N., Chan R. L., Lohmann J. U., 2010 Transcriptional control of a plant stem cell niche. Dev. Cell **18**: 849–61.

Carraro N., Peaucelle A., Laufs P., Traas J., 2006 Cell differentiation and organ initiation at the shoot apical meristem. Plant Mol. Biol. **60**: 811–26.

Carroll S. B., 2000 Endless Forms: The Evolution of Gene Regulation and Morphological Diversity. Cell **101**: 577–580.

Carroll S. B., 2008 Evo-devo and an expanding evolutionary synthesis: a genetic theory of morphological evolution. Cell **134**: 25–36.

Chan R. L., Gago G. M., Palena C. M., Gonzalez D. H., 1998 Homeoboxes in plant development. Biochim. Biophys. Acta **1442**: 1–19.

Chickarmane V. S., Gordon S. P., Tarr P. T., Heisler M. G., Meyerowitz E. M., 2012 Cytokinin signaling as a positional cue for patterning the apical-basal axis of the growing Arabidopsis shoot meristem. Proc. Natl. Acad. Sci. **109**: 4002–4007.

Chitwood D. H., Kumar R., Headland L. R., Ranjan A., Covington M. F., Ichihashi Y., Fulop D., Jiménez-Gómez J. M., Peng J., Maloof J. N., Sinha N. R., 2013 A quantitative genetic basis for leaf morphology in a set of precisely defined tomato introgression lines. Plant Cell **25**: 2465–81.

Chitwood D. H., Ranjan A., Kumar R., Ichihashi Y., Zumstein K., Headland L. R., Ostria-Gallardo E., Aguilar-Martínez J. a., Bush S., Carriedo L., Fulop D., Martinez C. C., Peng J., Maloof J. N., Sinha N. R., 2014 Resolving Distinct Genetic Regulators of Tomato Leaf Shape within a Heteroblastic and Ontogenetic Context. Plant Cell **26**: 3616–3629.

Chuck G., Lincoln C., Hake S., 1996 KNAT1 induces lobed leaves with ectopic meristems when overexpressed in Arabidopsis. Plant Cell **8**: 1277–89.

Clark S. E., Jacobsen S. E., Levin J. Z., Meyerowitz E. M., 1996 The CLAVATA and SHOOT MERISTEMLESS loci competitively regulate meristem activity in Arabidopsis. Development **122**: 1567–75.

Claude J., 2008 Morphometrics with R.

Cook J. P., McMullen M. D., Holland J. B., Tian F., Bradbury P., Ross-Ibarra J., Buckler E. S., Flint-Garcia S. A., 2012 Genetic architecture of maize kernel composition in the nested association mapping and inbred association panels. Plant Physiol. **158**: 824–34.

Cronk Q. C., 2001 Plant evolution and development in a post-genomic context. Nat. Rev. Genet. **2**: 607–619.

Daum G., Medzihradszky A., Suzaki T., Lohmann J. U., 2014 A mechanistic framework for noncell autonomous stem cell induction in Arabidopsis. Proc. Natl. Acad. Sci. **111**: 14619–14624.

Deb Y., Marti D., Frenz M., Kuhlemeier C., Reinhardt D., 2015 Phyllotaxis involves auxin drainage through leaf primordia. Development: 1–10.

Deyoung B. J., Clark S. E., 2008 BAM receptors regulate stem cell specification and organ development through complex interactions with CLAVATA signaling. Genetics **180**: 895–904.

Doebley J., 2004 The genetics of maize evolution. Annu. Rev. Genet. **38**: 37–59.

Dommergues C. H., Dommergues J. L., Verrecchia E. P., 2007 The discrete cosine transform, a Fourier-related method for morphometric analysis of open contours. Math. Geol. **39**: 749–763.

Dong Z., Danilevskaya O., Abadie T., Messina C., Coles N., Cooper M., 2012 A gene regulatory network model for Floral transition of the shoot apex in maize and its dynamic modeling. PLoS One **7**.

Doonan J. H., Sablowski R., 2010 Walls around tumours - why plants do not develop cancer. Nat. Rev. Cancer **10**: 794–802.

Durbak A. R., Tax F. E., 2011 CLAVATA signaling pathway receptors of Arabidopsis regulate cell proliferation in fruit organ formation as well as in meristems. Genetics **189**: 177–94.

Emerson R. A., 1924 Control of Flowering in Teosinte: Short-Day Treatment Brings Early Flowers. J. Hered.: 41–48.

Engstrom E. M., Andersen C. M., Gumulak-Smith J., Hu J., Orlova E., Sozzani R., Bowman J. L., 2011 Arabidopsis homologs of the petunia hairy meristem gene are required for maintenance of shoot and root indeterminacy. Plant Physiol. **155**: 735–50.

Evert R. F., 2006a Apical Meristems. In: *Esau's Plant Anatomy*, John Wiley & Sons, Inc., pp. 133–174.

Evert R. F., 2006b Meristems and Differentiation. In: *Esau's Plant Anatomy*, John Wiley & Sons, Inc., pp. 103–131.

Fletcher J. C., Meyerowitz E. M., 2000 Cell signaling within the shoot meristem. Curr. Opin. Plant Biol. **3**: 23–30.

Flint-Garcia S. A., Thuillet A.-C., Yu J., Pressoir G., Romero S. M., Mitchell S. E., Doebley J., Kresovich S., Goodman M. M., Buckler E. S., 2005 Maize association population: a high-resolution platform for quantitative trait locus dissection. Plant J. **44**: 1054–64.

Forster B. P., Franckowiak J. D., Lundqvist U., Lyon J., Pitkethly I., Thomas W. T. B., 2007 The barley phytomer. Ann. Bot. **100**: 725–733.

Francis D., Halford N. G., 2006 Nutrient sensing in plant meristems. Plant Mol. Biol. **60**: 981–93.

Frank M. H., Scanlon M. J., 2015 Transcriptomic evidence for the evolution of shoot meristem function in sporophyte-dominant land plants through concerted selection of ancestral gametophytic and sporophytic genetic programs. Mol. Biol. Evol. **32**: 355–367.

Frank M. H., Edwards M. B., Schultz E. R., McKain M. R., Fei Z., Sørensen I., Rose J. K. C., Scanlon M. J., 2015 Dissecting the molecular signatures of apical cell-type shoot meristems from two ancient land plant lineages. New Phytol. **207**: 893–904.

Fujita H., Kawaguchi M., 2011 Strategy for shoot meristem proliferation in plants. Plant Signal. Behav.: 1851–1854.

Furumizu C., Alvarez J. P., Sakakibara K., Bowman J. L., 2015 Antagonistic Roles for KNOX1 and KNOX2 Genes in Patterning the Land Plant Body Plan Following an Ancient Gene Duplication. PLOS Genet. **11**: e1004980.

Gamisch A., Staedler Y. M., Schönenberger J., Fischer G. A., Comes H. P., 2013 Histological and micro-CT evidence of stigmatic rostellum receptivity promoting auto-pollination in the madagascan orchid Bulbophyllum bicoloratum. PLoS One **8**: e72688.

Gordon S. P., Chickarmane V. S., Ohno C., Meyerowitz E. M., 2009 Multiple feedback loops through cytokinin signaling control stem cell number within the Arabidopsis shoot meristem. Proc. Natl. Acad. Sci. U. S. A. **106**: 16529–16534.

Graaff E. van der, Laux T., Rensing S. a, 2009 The WUS homeobox-containing (WOX) protein family. Genome Biol. **10**: 248.

Green P., 1999 Expression of pattern in plants: combining molecular and calculus-based biophysical paradigms. Am. J. Bot. **86**: 1059–1076.

Ha C. M., Jun J. H., Fletcher J. C., 2010 Shoot apical meristem form and function. Curr. Top. Dev. Biol. **91**: 103–40.

Hake S., Vollbrecht E., Freeling M., 1989 Cloning Knotted, the dominant morphological mutant in maize using Ds2 as a transposon tag. EMBO J. **8**: 15–22.

Hake S., Char B. R., Chuck G., Foster T., Long J. A., Jackson D. P., 1995 Homeobox genes in the functioning of plant meristems. Philos. Trans. R. Soc. Lond. B. Biol.

Sci. **350**: 45–51.

Hake S., Ross-Ibarra J., 2015 Genetic, evolutionary and plant breeding insights from the domestication of maize. Elife **2015**: 1–8.

Hamant O., 2013 Widespread mechanosensing controls the structure behind the architecture in plants. Curr. Opin. Plant Biol. **16**: 654–60.

Hay A., Kaur H., Phillips A., Hedden P., Hake S., Tsiantis M., 2002 The gibberellin pathway mediates KNOTTED1-type homeobox function in plants with different body plans. Curr. Biol. **12**: 1557–65.

Hay A., Barkoulas M., Tsiantis M., 2006 ASYMMETRIC LEAVES1 and auxin activities converge to repress BREVIPEDICELLUS expression and promote leaf development in Arabidopsis. Development **133**: 3955–3961.

Hay A., Tsiantis M., 2010 KNOX genes: versatile regulators of plant development and diversity. Development **137**: 3153–65.

Heisler M. G., Ohno C., Das P., Sieber P., Reddy G. V, Long J. a, Meyerowitz E. M., 2005 Patterns of auxin transport and gene expression during primordium development revealed by live imaging of the Arabidopsis inflorescence meristem. Curr. Biol. **15**: 1899–911.

Hill W. G., 2010 Understanding and using quantitative genetic variation. Philos. Trans. R. Soc. Lond. B. Biol. Sci. **365**: 73–85.

Hochholdinger F., Wulff D., Reuter K., Park W. J., Feix G., 2000 Tissue-specific expression of AUX1 in maize roots. J. Plant Physiol. **157**: 315–319.

Hoekstra H. E., Coyne J. A., 2007 The locus of evolution: evo devo and the genetics of adaptation. Evolution **61**: 995–1016.

Holland P. W. H., 2013 Evolution of homeobox genes. Wiley Interdiscip. Rev. Dev. Biol. **2**: 31–45.

Huang C., Chen Q., Xu G., Xu D., Tian J., Tian F., 2016 Identification and fine mapping of quantitative trait loci for the number of vascular bundle in maize stem. J. Integr.

Plant Biol. **58**: 81–90.

Hufford M. B., Bilinski P., Pyhäjärvi T., Ross-Ibarra J., 2012 Teosinte as a model system for population and ecological genomics. Trends Genet. **28**: 606–615.

Hung H.-Y., Shannon L. M., Tian F., Bradbury P. J., Chen C., Flint-Garcia S. A., McMullen M. D., Ware D., Buckler E. S., Doebley J. F., Holland J. B., 2012 *ZmCCT and the genetic basis of day-length adaptation underlying the postdomestication spread of maize.*

Jackson D. P., 1991 In situ hybridization in plants. In: *Molecular Plant Pathology: A Practical Approach*,, pp. 163–174.

Jackson D. P., Veit B., Hake S., 1994 Expression of maize KNOTTED1 related homeobox genes in the shoot apical meristem predicts patterns of morphogenesis in the vegetative shoot. Development **413**: 405–413.

Jackson D. P., Hake S., 1999 Control of phyllotaxy in maize by the abphyl1 gene. Development **126**: 315–23.

Jackson D. P., 2001 The long and the short of it: signaling development through plasmodesmata. Plant Cell **13**: 2569–2572.

Jackson D. P., 2002 Double labeling of KNOTTED1 mRNA and protein reveals multiple potential sites of protein trafficking in the shoot apex. Plant Physiol. **129**: 1423–1429.

Jasinski S., Piazza P., Craft J., Hay A., Woolley L., Rieu I., Phillips A., Hedden P., Tsiantis M., 2005 KNOX action in Arabidopsis is mediated by coordinate regulation of cytokinin and gibberellin activities. Curr. Biol. **15**: 1560–5.

Je B. Il, Gruel J., Lee Y. K., Bommert P., Arevalo E. D., Eveland A. L., Wu Q., Goldshmidt A., Meeley R., Bartlett M., Komatsu M., Sakai H., Jonsson H., Jackson D., 2016 Signaling from maize organ primordial via FASCIATED EAR3 regulates stem cell proliferation and yield traits. Nat. Genet. **48**: 785–791.

Jia Y., Lisch D. R., Ohtsu K., Scanlon M. J., Nettleton D., Schnable P. S., 2009 Loss of RNA-dependent RNA polymerase 2 (RDR2) function causes widespread and unexpected changes in the expression of transposons, genes, and 24-nt small

RNAs. PLoS Genet. **5**: e1000737.

Johnston R., Wang M., Sun Q., Sylvester A. W., Hake S., Scanlon M. J., 2014 Transcriptomic Analyses Indicate That Maize Ligule Development Recapitulates Gene Expression Patterns That Occur during Lateral Organ Initiation. Plant Cell Online **26**: 4718–4732.

Johnston R., Leiboff S., Scanlon M. J., 2015 Ontogeny of the sheathing leaf base in maize (Zea mays). New Phytol. **205**: 306–15.

Jönsson H., Heisler M. G., Shapiro B. E., Meyerowitz E. M., Mjolsness E., 2006 An auxin-driven polarized transport model for phyllotaxis. Proc. Natl. Acad. Sci. U. S. A. **103**: 1633–8.

Jun J., Fiume E., Roeder A. H. K., Meng L., Sharma V. K., Osmont K. S., Baker C., Ha C. M., Meyerowitz E. M., Feldman L. J., Fletcher J. C., 2010 Comprehensive analysis of CLE polypeptide signaling gene expression and overexpression activity in Arabidopsis. Plant Physiol. **154**: 1721–1736.

Kaplan D. R., 1973 THE PROBLEM OF LEAF MORPHOLOGY AND EVOLUTION IN THE MONOCOTYLEDONS. Q. Rev. Biol. **48**: 437–457.

Kaplan D. R., 2001 Fundamental Concepts of Leaf Morphology and Morphogenesis: A Contribution to the Interpretation of Molecular Genetic Mutants. Int. J. Plant Sci. **162**: 465–474.

Kashiwagi T., Togawa E., Hirotsu N., Ishimaru K., 2008 Improvement of lodging resistance with QTLs for stem diameter in rice (Oryza sativa L.). Theor. Appl. Genet. **117**: 749–57.

Kasten F., 1958 Aditional Schiff-type reagents for use in cytochemistry. Stain Technol. **33**: 39–45.

Kerstetter R. a, Laudencia-Chingcuanco D., Smith L. G., Hake S., 1997 Loss-of-function mutations in the maize homeobox gene, knotted1, are defective in shoot meristem maintenance. Development **124**: 3045–54.

Kim J. Y., Yuan Z., Cilia M., Khalfan-Jagani Z., Jackson D., 2002 Intercellular trafficking of a KNOTTED1 green fluorescent protein fusion in the leaf and shoot meristem of

Arabidopsis. Proc. Natl. Acad. Sci. U. S. A. **99**: 4103–8.

Kim J. Y., Yuan Z., Jackson D., 2003 Developmental regulation and significance of KNOX protein trafficking in Arabidopsis. Development **130**: 4351–4362.

Kimura S., Koenig D., Kang J., Yoong F. Y., Sinha N. R., 2008 Natural Variation in Leaf Morphology Results from Mutation of a Novel KNOX Gene. Curr. Biol. **18**: 672–677.

Klein R. J., Zeiss C., Chew E. Y., Tsai J.-Y., Sackler R. S., Haynes C., Henning A. K., SanGiovanni J. P., Mane S. M., Mayne S. T., Bracken M. B., Ferris F. L., Ott J., Barnstable C., Hoh J., 2005 Complement factor H polymorphism in age-related macular degeneration. Science **308**: 385–9.

Klingenberg C. P., 2010 Evolution and development of shape: integrating quantitative approaches. Nat. Rev. Genet. **11**: 623–635.

Koenig D., Bayer E., Kang J., Kuhlemeier C., Sinha N. R., 2009 Auxin patterns Solanum lycopersicum leaf morphogenesis. Development **136**: 2997–3006.

Korte A., Farlow A., 2013 The advantages and limitations of trait analysis with GWAS: a review. Plant Methods **9**: 29.

Kwiatkowska D., 2004 Structural integration at the shoot apical meristem: Models, measurements, and experiments. Am. J. Bot. **91**: 1277–1293.

Langlade N. B., Feng X., Dransfield T., Copsey L., Hanna A. I., Thébaud C., Bangham A., Hudson A., Coen E., 2005 Evolution through genetically controlled allometry space. Proc. Natl. Acad. Sci. U. S. A. **102**: 10221–6.

Laux T., Mayer K. F., Berger J., Jürgens G., 1996 The WUSCHEL gene is required for shoot and floral meristem integrity in Arabidopsis. Development **122**: 87–96.

Lawrence C. J., Harper L. C., Schaeffer M. L., Sen T. Z., Seigfried T. E., Campbell D. A., 2008 MaizeGDB: The maize model organism database for basic, translational, and applied research. Int. J. Plant Genomics **2008**: 496957.

Leibfried A., To J. P. C., Busch W., Stehling S., Kehle A., Demar M., Kieber J. J., Lohmann J. U., 2005 WUSCHEL controls meristem function by direct regulation of

cytokinin-inducible response regulators. Nature **438**: 1172–5.

Leiboff S., Li X., Hu H.-C., Todt N., Yang J., Li X., Yu X., Muehlbauer G. J., Timmermans M. C. P., Yu J., Schnable P. S., Scanlon M. J., 2015 Genetic control of morphometric diversity in the maize shoot apical meristem. Nat. Commun. **6**: 8974.

Lenhard M., Bohnert A., Jürgens G., Laux T., 2001 Termination of stem cell maintenance in Arabidopsis floral meristems by interactions between WUSCHEL and AGAMOUS. Cell **105**: 805–14.

Lenhard M., Jürgens G., Laux T., 2002 The WUSCHEL and SHOOTMERISTEMLESS genes fulfil complementary roles in Arabidopsis shoot meristem regulation. Development **129**: 3195–3206.

Li D., Wang L., Wang M., Xu Y. Y., Luo W., Liu Y. J., Xu Z. H., Li J., Chong K., 2009 Engineering OsBAK1 gene as a molecular tool to improve rice architecture for high yield. Plant Biotechnol. J. **7**: 791–806.

Li X., Zhu C., Yeh C.-T., Wu W., Takacs E. M., Petsch K. A., Tian F., Bai G., Buckler E. S., Muehlbauer G. J., Timmermans M. C. P., Scanlon M. J., Schnable P. S., Yu J., 2012 Genic and nongenic contributions to natural variation of quantitative traits in maize. Genome Res. **22**: 2436–44.

Li L., Petsch K., Shimizu R., Liu S., Xu W. W., Ying K., Yu J., Scanlon M. J., Schnable P. S., Timmermans M. C. P., Springer N. M., Muehlbauer G. J., 2013 Mendelian and Non-Mendelian Regulation of Gene Expression in Maize. PLoS Genet. **9**.

Lin H., Niu L., McHale N. a, Ohme-Takagi M., Mysore K. S., Tadege M., 2013 Evolutionarily conserved repressive activity of WOX proteins mediates leaf blade outgrowth and floral organ development in plants. Proc. Natl. Acad. Sci. U. S. A. **110**: 366–71.

Lincoln C., Long J. A., Yamaguchi J., Serikawa K., Hake S., 1994 A knotted1-like homeobox gene in Arabidopsis is expressed in the vegetative meristem and dramatically alters leaf morphology when overexpressed in transgenic plants. Plant Cell **6**: 1859–76.

Lipka A. E., Tian F., Wang Q., Peiffer J., Li M., Bradbury P. J., Gore M. A., Buckler E. S., Zhang Z., 2012 GAPIT: genome association and prediction integrated tool.

Bioinformatics **28**: 2397–9.

Liu K., Goodman M. M., Muse S., Smith J. S., Buckler E., Doebley J., 2003 Genetic Structure and Diversity Among Maize Inbred Lines as Inferred From DNA Microsatellites. Genetics **165**: 2117–2128.

Lohmann J. U., Hong R. L., Hobe M., Busch M. a, Parcy F., Simon R., Weigel D., 2001 A molecular link between stem cell regulation and floral patterning in Arabidopsis. Cell **105**: 793–803.

Long J. A., Moan E., Medford J., Barton M., 1996 A member of the KNOTTED class of homeodomain proteins encoded by the STM gene of Arabidopsis. Nature **379**: 66–69.

Long J. A., Woody S., Poethig S., Meyerowitz E. M., Barton M. K., 2002 Transformation of shoots into roots in Arabidopsis embryos mutant at the TOPLESS locus. Development **129**: 2797–806.

Long J. A., Ohno C., Smith Z. R., Meyerowitz E. M., 2006 TOPLESS Regulates Apical Embryonic Fate in Arabidopsis. Science **312**: 1520–1522.

Lucas W. J., Bouché-Pillon S., Jackson D. P., Nguyen L., Baker L., Ding B., Hake S., 1995 Selective trafficking of KNOTTED1 homeodomain protein and its mRNA through plasmodesmata. Science **270**: 1980–1983.

Lunde C., Hake S., 2009 The interaction of knotted1 and thick tassel dwarf1 in vegetative and reproductive meristems of maize. Genetics **181**: 1693–7.

Magnani E., Hake S., 2008 KNOX lost the OX: the Arabidopsis KNATM gene defines a novel class of KNOX transcriptional regulators missing the homeodomain. Plant Cell **20**: 875–887.

Matsumoto N., Okada K., 2001 A homeobox gene, PRESSED FLOWER, regulates lateral axis-dependent development of Arabidopsis flowers. Genes Dev. **15**: 3355–3364.

Mayer K. F., Schoof H., Haecker A., Lenhard M., Jürgens G., Laux T., 1998 Role of WUSCHEL in regulating stem cell fate in the Arabidopsis shoot meristem. Cell **95**: 805–15.

Meijón M., Satbhai S. B., Tsuchimatsu T., Busch W., 2014 Genome-wide association study using cellular traits identifies a new regulator of root development in Arabidopsis. Nat. Genet. **46**: 77–81.

Miller T. A., Muslin E. H., Dorweiler J. E., 2008 A maize CONSTANS-like gene, conz1, exhibits distinct diurnal expression patterns in varied photoperiods. Planta **227**: 1377–88.

Miyawaki K., Tabata R., Sawa S., 2013 Evolutionarily conserved CLE peptide signaling in plant development, symbiosis, and parasitism. Curr. Opin. Plant Biol. **16**: 598–606.

Monaco M. K., Stein J., Naithani S., Wei S., Dharmawardhana P., Kumari S., Amarasinghe V., Youens-Clark K., Thomason J., Preece J., Pasternak S., Olson A., Jiao Y., Lu Z., Bolser D., Kerhornou A., Staines D., Walts B., Wu G., D'Eustachio P., Haw R., Croft D., Kersey P. J., Stein L., Jaiswal P., Ware D., 2014 Gramene 2013: comparative plant genomics resources. Nucleic Acids Res. **42**: D1193-9.

Mukherjee K., Brocchieri L., Bürglin T. R., 2009 A comprehensive classification and evolutionary analysis of plant homeobox genes. Mol. Biol. Evol. **26**: 2775–2794.

Müller R., Borghi L., Kwiatkowska D., Laufs P., Simon R., 2006 Dynamic and compensatory responses of Arabidopsis shoot and floral meristems to CLV3 signaling. Plant Cell **18**: 1188–98.

Nardmann J., Werr W., 2013 Symplesiomorphies in the WUSCHEL clade suggest that the last common ancestor of seed plants contained at least four independent stem cell niches. New Phytol. **199**: 1081–92.

Niklas K. J., Mauseth J. D., 1980 Simulations of Cell Dimensions in Shoot Apical Meristems: Implications Concerning Zonate Apices. Am. J. Bot. **67**: 715.

Nimchuk Z. L., Tarr P. T., Ohno C., Qu X., Meyerowitz E. M., 2011 Plant stem cell signaling involves ligand-dependent trafficking of the CLAVATA1 receptor kinase. Curr. Biol. **21**: 345–52.

Nordborg M., Weigel D., 2008 Next-generation genetics in plants. Nature **456**: 720–723.

Orr A. R., Sundberg M. D., 1994 Inflorescence Development in a Perennial Teosinte: Zea perennis (Poaceae). Am. J. Bot. **81**: 598–608.

Orr A. R., Sundberg M. D., 2004 Inflorescence Development in a New Teosinte: Zea nicaraguensis (Poaceae). Am. J. Bot. **91**: 165–173.

Pautler M., Tanaka W., Hirano H.-Y., Jackson D., 2013 Grass meristems I: shoot apical meristem maintenance, axillary meristem determinacy and the floral transition. Plant Cell Physiol. **54**: 302–12.

Pautler M., Eveland A. L., LaRue T., Yang F., Weeks R., Lunde C., Je B. Il, Meeley R. B., Komatsu M., Vollbrecht E., Sakai H., Jackson D., 2015 FASCIATED EAR4 Encodes a bZIP Transcription Factor That Regulates Shoot Meristem Size in Maize. Plant Cell Online **27**: tpc.114.132506.

Peiffer J. A., Romay M. C., Gore M. A., Flint-Garcia S. A., Zhang Z., Millard M. J., Gardner C. A. C., McMullen M. D., Holland J. B., Bradbury P. J., Buckler E. S., 2014 The genetic architecture of maize height. Genetics **196**: 1337–56.

Phelps-Durr T. L., Thomas J., Vahab P., Timmermans M. C. P., 2005 Maize rough sheath2 and its Arabidopsis orthologue ASYMMETRIC LEAVES1 interact with HIRA, a predicted histone chaperone, to maintain knox gene silencing and determinacy during organogenesis. Plant Cell **17**: 2886–2898.

Poethig R., 1984 Cellular parameters of leaf morphogenesis in maize and tobacco. In: White RA, Dickison WC (Eds.), *Contemporary problems in plant anatomy*, Academic Press, New York, pp. 235–238.

Poethig R. S., Szymkowiak E. J., 1995 Clonal analysis of leaf development in maize. Maydica. **40**: 67.

Ragni L., Belles-Boix E., Günl M., Pautot V., 2008 Interaction of KNAT6 and KNAT2 with BREVIPEDICELLUS and PENNYWISE in Arabidopsis inflorescences. Plant Cell **20**: 888–900.

Reddy G. V., Meyerowitz E. M., 2005 Stem-cell homeostasis and growth dynamics can be uncoupled in the Arabidopsis shoot apex. Science **310**: 663–7.

Reinhardt D., 2000 Auxin Regulates the Initiation and Radial Position of Plant Lateral

Organs. Plant Cell Online **12**: 507–518.

Reinhardt D., Pesce E.-R., Stieger P., Mandel T., Baltensperger K., Bennett M., Traas J., Friml J., Kuhlemeier C., 2003 Regulation of phyllotaxis by polar auxin transport. Nature **426**: 255–60.

Roberts K., 2007 *Handbook of plant science*. Wiley, Chichester, West Sussex, England; Hoboken, NJ, USA.

Rojo E., 2002 CLV3 Is Localized to the Extracellular Space, Where It Activates the Arabidopsis CLAVATA Stem Cell Signaling Pathway. Plant Cell Online **14**: 969–977.

Romay M. C., Millard M. J., Glaubitz J. C., Peiffer J. a, Swarts K. L., Casstevens T. M., Elshire R. J., Acharya C. B., Mitchell S. E., Flint-Garcia S. A., McMullen M. D., Holland J. B., Buckler E. S., Gardner C. A. C., 2013 Comprehensive genotyping of the USA national maize inbred seed bank. Genome Biol. **14**: R55.

Rosset A., Spadola L., Ratib O., 2004 OsiriX: An open-source software for navigating in multidimensional DICOM images. J. Digit. Imaging **17**: 205–216.

Rupp H. M., Frank M., Werner T., Strnad M., Schmülling T., 1999 Increased steady state mRNA levels of the STM and KNAT1 homeobox genes in cytokinin overproducing Arabidopsis thaliana indicate a role for cytokinins in the shoot apical meristem. Plant J. **18**: 557–63.

Ruzin S., 1999 *Plant microtechnique and microscopy*. Oxford University Press, New York.

Sablowski R., 2011 Plant stem cell niches: from signalling to execution. Curr. Opin. Plant Biol. **14**: 4–9.

Sakakibara K., Ando S., Yip H. K., Tamada Y., Hiwatashi Y., Murata T., Deguchi H., Hasebe M., Bowman J. L., 2013 KNOX2 genes regulate the haploid-to-diploid morphological transition in land plants. Science **339**: 1067–70.

Sakamoto T., Kamiya N., Ueguchi-Tanaka M., Iwahori S., Matsuoka M., 2001 KNOX homeodomain protein directly suppresses the expression of a gibberellin biosynthetic gene in the tobacco shoot apical meristem. Genes Dev. **15**: 581–90.

Sarkar A. K., Luijten M., Miyashima S., Lenhard M., Hashimoto T., Nakajima K., Scheres B., Heidstra R., Laux T., 2007 Conserved factors regulate signalling in Arabidopsis thaliana shoot and root stem cell organizers. Nature **446**: 811–814.

Scanlon M. J., Freeling M., 1997 Clonal sectors reveal that a specific meristematic domain is not utilized in the maize mutant narrow sheath. Dev. Biol. **182**: 52–66.

Scanlon M. J., 2000 NARROW SHEATH1 functions from two meristematic foci during founder-cell recruitment in maize leaf development. Development **127**: 4573–85.

Scanlon M. J., 2003 The polar auxin transport inhibitor N-1-naphthylphthalamic acid disrupts leaf initiation, KNOX protein regulation, and formation of leaf margins in maize. Plant Physiol. **133**: 597–605.

Schnable P. S., Ware D., Fulton R. S., Stein J. C., Wei F., Pasternak S., Liang C., Zhang J., Fulton L., Graves T. A., Minx P., Reily A. D., Courtney L., Kruchowski S. S., Tomlinson C., Strong C., Delehaunty K., Fronick C., Courtney B., Rock S. M., Belter E., Du F., Kim K., Abbott R. M., Cotton M., Levy A., Marchetto P., Ochoa K., Jackson S. M., Gillam B., Chen W., Yan L., Higginbotham J., Cardenas M., Waligorski J., Applebaum E., Phelps L., Falcone J., Kanchi K., Thane T., Scimone A., Thane N., Henke J., Wang T., Ruppert J., Shah N., Rotter K., Hodges J., Ingenthron E., Cordes M., Kohlberg S., Sgro J., Delgado B., Mead K., Chinwalla A., Leonard S., Crouse K., Collura K., Kudrna D., Currie J., He R., Angelova A., Rajasekar S., Mueller T., Lomeli R., Scara G., Ko A., Delaney K., Wissotski M., Lopez G., Campos D., Braidotti M., Ashley E., Golser W., Kim H., Lee S., Lin J., Dujmic Z., Kim W., Talag J., Zuccolo A., Fan C., Sebastian A., Kramer M., Spiegel L., Nascimento L., Zutavern T., Miller B., Ambroise C., Muller S., Spooner W., Narechania A., Ren L., Wei S., Kumari S., Faga B., Levy M. J., McMahan L., Buren P. Van, Vaughn M. W., Ying K., Yeh C.-T., Emrich S. J., Jia Y., Kalyanaraman A., Hsia A.-P., Barbazuk W. B., Baucom R. S., Brutnell T. P., Carpita N. C., Chaparro C., Chia J.-M., Deragon J.-M., Estill J. C., Fu Y., Jeddeloh J. A., Han Y., Lee H., Li P., Lisch D. R., Liu S., Liu Z., Nagel D. H., McCann M. C., SanMiguel P., Myers A. M., Nettleton D., Nguyen J., Penning B. W., Ponnala L., Schneider K. L., Schwartz D. C., Sharma A., Soderlund C., Springer N. M., Sun Q., Wang H., Waterman M., Westerman R., Wolfgruber T. K., Yang L., Yu Y., Zhang L., Zhou S., Zhu Q., Bennetzen J. L., Dawe R. K., Jiang J., Jiang N., Presting G. G., Wessler S. R., Aluru S., Martienssen R. A., Clifton S. W., McCombie W. R., Wing R. A., Wilson R. K., 2009 The B73 maize genome: complexity, diversity, and dynamics. Science **326**: 1112–1115.

Schneider C. A., Rasband W. S., Eliceiri K. W., 2012 NIH Image to ImageJ: 25 years of image analysis. Nat. Methods **9**: 671–675.

Schoof H., Lenhard M., Haecker A., Mayer K. F., Jürgens G., Laux T., 2000 The stem cell population of Arabidopsis shoot meristems in maintained by a regulatory loop between the CLAVATA and WUSCHEL genes. Cell **100**: 635–44.

Scofield S., Dewitte W., Nieuwland J., Murray J. a H., 2013 The Arabidopsis homeobox gene SHOOT MERISTEMLESS has cellular and meristem-organisational roles with differential requirements for cytokinin and CYCD3 activity. Plant J. **75**: 53–66.

Sétamou M., Schulthess F., Bosque-Pérez N. A., Thomas-Odjo A., 1995 The effect of stem and cob borers on maize subjected to different nitrogen treatments. Entomol. Exp. Appl. **77**: 205–210.

Shah N., Sukumar S., 2010 The Hox genes and their roles in oncogenesis. Nat. Rev. Cancer **10**: 361–371.

Shani E., Yanai O., Ori N., 2006 The role of hormones in shoot apical meristem function. Curr. Opin. Plant Biol. **9**: 484–9.

Shannon L. M., 2013 The Genetic Architecture of Maize Domestication and Range Expansion.

Sharman B. C., 1942 Developmental Anatomy of the Shoot of Zea mays L. Ann. Bot. **6**: 245–282.

Shimizu R., Ji J., Kelsey E., Ohtsu K., Schnable P. S., Scanlon M. J., 2009 Tissue specificity and evolution of meristematic WOX3 function. Plant Physiol. **149**: 841–850.

Smith E. F., Brown N. A., McCulloch L., 1912 *The structure and development of crown gall: A plant cancer*. US Government Printing Office.

Smith L. G., Greene B., Veit B., Hake S., 1992 A dominant mutation in the maize homeobox gene, Knotted-1, causes its ectopic expression in leaf cells with altered fates. Development **116**: 21–30.

Smith H. M. S., Boschke I., Hake S., 2002 Selective interaction of plant homeodomain proteins mediates high DNA-binding affinity. Proc. Natl. Acad. Sci. U. S. A. **99**: 9579–84.

Smith R. S., Guyomarc'h S., Mandel T., Reinhardt D., Kuhlemeier C., Prusinkiewicz P., 2006 A plausible model of phyllotaxis. Proc. Natl. Acad. Sci. U. S. A. **103**: 1301–6.

Steeves T. A., Sussex I. M., 1972 *Patterns in plant development*. Prentice-Hall, Englewood Cliffs, N.J.

Sultan S. E., 2000 Phenotypic plasticity for plant development, function and life history. Trends Plant Sci. **5**: 537–542.

Sundberg M. D., Orr A. R., 1986 Early Inflorescence and Floral Development in Zea diploperennis, Diploperennial Teosinte. Am. J. Bot. **73**: 1699–1712.

Sundberg M. D., Orr A. R., 1990 Inflorescence Development in Two Annual Teosintes: Zea mays subsp. Mexicana and Z. mays subsp. Parviglumis. Am. J. Bot. **77**: 141–152.

Sussex I. M., Kerk N. M., 2001 The evolution of plant architecture. Curr. Opin. Plant Biol. **4**: 33–7.

Swarup R., Péret B., 2012 AUX/LAX family of auxin influx carriers-an overview. Front. Plant Sci. **3**: 225.

Taguchi-Shiobara F., Yuan Z., Hake S., Jackson D. P., 2001 The fasciated ear2 gene encodes a leucine-rich repeat receptor-like protein that regulates shoot meristem proliferation in maize. Genes Dev. **15**: 2755–66.

Tanksley S. D., 1993 Mapping Polygenes. Annu. Rev. Genet. **27**: 205–233.

Theodoris G., Inada N., Freeling M., 2003 Conservation and molecular dissection of ROUGH SHEATH2 and ASYMMETRIC LEAVES1 function in leaf development. Proc. Natl. Acad. Sci. U. S. A. **100**: 6837–6842.

Thompson A. M., Crants J., Schnable P. S., Yu J., Timmermans M. C. P., Springer N. M., Scanlon M. J., Muehlbauer G. J., 2014 Genetic control of maize shoot apical meristem architecture. G3 (Bethesda). **4**: 1327–37.

Thompson A. M., Yu J., Timmermans M. C. P., Schnable P., Crants J. C., Scanlon M. J., Muehlbauer G. J., 2015 Diversity of Maize Shoot Apical Meristem Architecture

and Its Relationship to Plant Morphology. G3!; Genes|Genomes|Genetics: 1–14.

Tian F., Bradbury P. J., Brown P. J., Hung H., Sun Q., Flint-Garcia S. A., Rocheford T. R., McMullen M. D., Holland J. B., Buckler E. S., 2011 Genome-wide association study of leaf architecture in the maize nested association mapping population. Nat. Genet. **43**: 159–62.

Timmermans M. C. P., Hudson A., Becraft P. W., Nelson T., 1999 ROUGH SHEATH2: A Myb Protein That Represses knox Homeobox Genes in Maize Lateral Organ Primordia. Science **284**: 151–153.

Tsiantis M., Schneeberger R., Golz J. F., Freeling M., Langdale J. a, 1999 The maize rough sheath2 gene and leaf development programs in monocot and dicot plants. Science **284**: 154–6.

Tsuji H., Taoka K. I., Shimamoto K., 2011 Regulation of flowering in rice: Two florigen genes, a complex gene network, and natural variation. Curr. Opin. Plant Biol. **14**: 45–52.

Vandenbussche M., Horstman A., Zethof J., Koes R., Rijpkema A. S., Gerats T., 2009 Differential recruitment of WOX transcription factors for lateral development and organ fusion in Petunia and Arabidopsis. Plant Cell **21**: 2269–2283.

Vollbrecht E., Veit B., Sinha N. R., Hake S., 1991 The developmental gene Knotted-1 is a member of a maize homeobox gene family. Nature **350**: 241–243.

Vollbrecht E., Reiser L., Hake S., 2000 Shoot meristem size is dependent on inbred background and presence of the maize homeobox gene, knotted1. Development **127**: 3161–72.

Walbot V., 1985 On the life strategies of plants and animals. Trends Genet. **1**: 165–169.

Wallace J. G., Larsson S. J., Buckler E. S., 2014 Entering the second century of maize quantitative genetics. Heredity (Edinb). **112**: 30–8.

Weigel D., Nordborg M., 2005 Natural variation in Arabidopsis. How do we find the causal genes? Plant Physiol. **138**: 567–8.

Wong C. E., Singh M. B., Bhalla P. L., 2013 Spatial expression of CLAVATA3 in the shoot apical meristem suggests it is not a stem cell marker in soybean. J. Exp. Bot.

Wu X., Chory J., Weigel D., 2007 Combinations of WOX activities regulate tissue proliferation during Arabidopsis embryonic development. Dev. Biol. **309**: 306–316.

Xu L., Shen W.-H., 2008 Polycomb silencing of KNOX genes confines shoot stem cell niches in Arabidopsis. Curr. Biol. **18**: 1966–71.

Xu X. M., Wang J., Xuan Z., Goldshmidt A., Borrill P. G. M., Hariharan N., Kim J. Y., Jackson D., 2011 Chaperonins facilitate KNOTTED1 cell-to-cell trafficking and stem cell function. Science **333**: 1141–1144.

Xu C., Liberatore K. L., MacAlister C. a, Huang Z., Chu Y.-H., Jiang K., Brooks C., Ogawa-Ohnishi M., Xiong G., Pauly M., Eck J. Van, Matsubayashi Y., Knaap E. van der, Lippman Z. B., 2015 A cascade of arabinosyltransferases controls shoot meristem size in tomato. Nat. Genet.

Yadav R. K., Tavakkoli M., Reddy G. V., 2010 WUSCHEL mediates stem cell homeostasis by regulating stem cell number and patterns of cell division and differentiation of stem cell progenitors. Development **137**: 3581–9.

Yadav R. K., Perales M., Gruel J., Girke T., Jönsson H., Reddy G. V., 2011 WUSCHEL protein movement mediates stem cell homeostasis in the Arabidopsis shoot apex. Genes Dev. **25**: 2025–30.

Yadav R. K., Perales M., Gruel J., Ohno C., Heisler M. G., Girke T., Jönsson H., Reddy G. V., 2013 Plant stem cell maintenance involves direct transcriptional repression of differentiation program. Mol. Syst. Biol. **9**: 654.

Yang Q., Li Z., Li W., Ku L., Wang C., Ye J., Li K., Yang N., Li Y., Zhong T., Li J., Chen Y., Yan J., Yang X., Xu M., 2013 CACTA-like transposable element in ZmCCT attenuated photoperiod sensitivity and accelerated the postdomestication spread of maize. Proc. Natl. Acad. Sci. U. S. A. **110**: 16969–74.

Yang F., Bui H. T., Pautler M., Llaca V., Johnston R., Lee B.-H., Kolbe A., Sakai H., Jackson D., 2015 A Maize Glutaredoxin Gene, Abphyl2, Regulates Shoot Meristem Size and Phyllotaxy. Plant Cell.

Yu J., Pressoir G., Briggs W. H., Vroh Bi I., Yamasaki M., Doebley J. F., McMullen M. D., Gaut B. S., Nielsen D. M., Holland J. B., Kresovich S., Buckler E. S., 2006 A unified mixed-model method for association mapping that accounts for multiple levels of relatedness. Nat. Genet. **38**: 203–8.

Zhang Z., Ersoz E., Lai C.-Q., Todhunter R. J., Tiwari H. K., Gore M. a, Bradbury P. J., Yu J., Arnett D. K., Ordovas J. M., Buckler E. S., 2010 Mixed linear model approach adapted for genome-wide association studies. Nat. Genet. **42**: 355–60.

Zhang W., Swarup R., Bennett M., Schaller G. E., Kieber J. J., 2013 Cytokinin induces cell division in the quiescent center of the Arabidopsis root apical meristem. Curr. Biol. **23**: 1979–89.

Zhou Y., Liu X., Engstrom E. M., Nimchuk Z. L., Pruneda-Paz J. L., Tarr P. T., Yan A., Kay S. a., Meyerowitz E. M., 2014 Control of plant stem cell function by conserved interacting transcriptional regulators. Nature **517**: 377–380.